

eISSN 2037-0164

International Journal of

plant biology

Environmental effect on the leaf morphology and anatomy of *Berberis microphylla* G. Forst

Silvia Radice,¹ Miriam E. Arena²

¹Laboratorio de Fisiología Vegetal, CONICET-Facultad de Agronomía y Ciencias Agroalimentarias, Universidad de Morón, Buenos Aires; ²Laboratorio de Recursos Agroforestales, Centro Austral de Investigaciones Científicas, Ushuaia, Argentina

Abstract

Berberis microphylla G. Forst is a fruit shrub native from Patagonia, considered as a non-timber forest product. In recent years, there has been an increased demand for its fruits, both for fresh and industrialized consumption, being the establishment of commercial orchards in different sites a need to meet this demand. *B. microphylla* cloned plants have been introduced from Ushuaia, Tierra del Fuego to Buenos Aires province in order to evaluate its phenotypic plasticity and the possibility of fruit production. At the same time, a comparative study on the morphology and anatomy of the mature leaves of *B. microphylla* grown in two different environmental conditions was carried out. Moreno leaves were significantly larger than Ushuaia leaves in all the morphological parameters registered, while Ushuaia leaves were more circular than Moreno leaves with the highest roundness and elongation indexes. Nevertheless, histological sections showed that Ushuaia leaves have one more layer of palisade cells respect to Moreno leaves. Ushuaia leaves showed higher palisade cells, larger abaxial epidermal cells and thicker cuticles than Moreno leaves. The stomatal density was superior on Moreno leaves. Scanning Electron Microscope of abaxial epidermis showed a surface with numerous ridges of different forms that prevent the layout of epidermal cells on Moreno leaves. Appearance of this surface is glossy and oily. On the contrary, epidermal cells are well recognized on Ushuaia leaves. Stomata of anomocytic type were observed and surface looks waxy. Auto-fluorescence on leaf cross sections were observed on the vascular bundles and partially on the epidermis cells. *B. microphylla* leaves showed a high phenotypic plasticity between the two sites of cultivation. The changes in the leaf morphology and structure observed in Moreno leaves could indicate that the plants are trying to adjust its morphology to the new culture conditions *i.e.* higher temperatures and lower irradiance.

Introduction

Berberis microphylla G. Forst (in the past *Berberis buxifolia* Lam.) is an evergreen shrub that may be semi-evergreen where winters are particularly cold and harsh, as it occurs in Tierra del Fuego. It is a spiny and erect shrub up to 4 m high, often growing in the magellanic subpolar forest Eco region,¹ in coastal scrub, *Nothofagus* forest margins and clearings, moister areas in grass steppes, and along streams and rivers.² It is one of the understory species in timber quality and associated non-timber quality stands of *Nothofagus* forests in Tierra del Fuego,³ being considered as a non-timber forest product. In recent years, there has been an increased demand for the fruits of these shrubs and particularly for *B. microphylla*, both for fresh consumption and for the production of various products such as candies and jellies, pulps for making ice cream, beverages without alcohol and they are used in cosmetic products too. Also, in *B. microphylla* as in most of the species of the genus are assigned medicinal properties due to the presence of the alkaloids called berberine and berbamine.⁴⁻⁸ Moreover, phenolics like as anthocyanins in the fruits,⁹⁻¹³ in the leaves¹⁴ and in the roots^{15,16} were found, which give a medicinal and tinctorial application.

Floral biology, fruit development and quality, and the assessment of morphological variability were studied in natural populations of *B. microphylla*,^{12,17-20} as well as the phenological stages and the annual cycle of growth and development.^{21,22} However, nothing has been yet said about the leaf morphology and structure of *B. microphylla*. The leaf can be considered as a micro copy of the plant,²³ and the variations of leaf morphology can reflect the plant capacity to acquire, use and conserve resources. Under abiotic stress, plants alter their physiology, morphology and development in response to environmental changes.²⁴

Some studies have been performed in the genus *Berberis* on this subject. Arambarri *et al.*,²⁵ studied the leaf anatomy of *B. ruscifolia*. Histological description related to the pharmacological property was noticed on *B. aristata*, *B. lyceum* and *B. asiatica*.^{26,27} Other antecedents have given greater importance to the study of the leaf compounds produced for their therapeutic action.^{14,28-32}

In the last two years, a plot of *B. microphylla* cloned plants has been introduced to the Buenos Aires province in order to carry out experimental studies, *i.e.* evaluate its phenotypic plasticity and the possibility of fruit production. These plants have shown a good vegetative growth; flower differentiation was observed but until now fruits have not been formed. Leaves are photosynthetic organs thus their shapes, sizes and structure are important

Correspondence: Miriam E. Arena, Laboratorio de Recursos Agroforestales, Centro Austral de Investigaciones Científicas (CADIC - CONICET), Bernardo Houssay 200, 9410 Ushuaia, Tierra del Fuego, Argentina.
Tel.: +54.2901.422310/4 - Fax: +54.2901.430644.
E-mail: arena@cadic-conicet.gob.ar

Key words: barberry, leaf morphology, leaf anatomy, auto-fluorescence.

Acknowledgments: the authors thank to Isabel Fariás for her technical assistance. They would also thank Eng Agr Marta Alonso, Mr S.E. Agüero, A. O. Medina and J. Peralta.

Contributions: the authors contributed equally.

Conflict of interest: the authors declare no conflict of interest.

Finding: This work received funds from CONICET (PIP 0263 y 0223).

Received for publication: 22 October 2015.

Revision received: 21 January 2015.

Accepted for publication: 21 January 2015.

This work is licensed under a Creative Commons Attribution NonCommercial 3.0 License (CC BY-NC 3.0).

©Copyright S. Radic and M.E. Arena, 2015

Licensee PAGEPress srl, Italy

International Journal of Plant Biology 2015; 6:5677

doi:10.4081/pb.2015.5677

factors influencing the success of the plants. Therefore the aim of this work was to study the morphology and anatomy of the mature leaves of *B. microphylla* plants grown in two different environmental conditions, on the origin site where they grow spontaneously and in a site where it is interesting to introduce them.

Materials and Methods

Plant material and growing conditions

Berberis microphylla plants were obtained through clonal propagation from a natural population and cultivated in pots (n=40) in the experimental field of the Centro Austral de Investigaciones Científicas, Ushuaia, Tierra del Fuego, Argentina (54°48' SL, 68°19' WL, 30 m a.s.l.) for five years. At the beginning of 2013, twenty plants were taken to Moreno (Buenos Aires) and cultivated in the experimental field of the Faculty of Agriculture, University of Morón (34° 39' SL, 58° 47' WL, 19 m a.s.l.).

Moreno climate is temperate sub humid with 1200 mm rainfalls per year and extreme temperatures are 40 and -1°C. On the other hand, Ushuaia climate is classified as sub polar oceanic with mild temperatures, *i.e.* not

Table 1. *Berberis microphylla* morphological characteristics and measures according to the cultivation site.

Cultivation site	Area, mm ²	Perimeter, mm	Leaf length, mm	Leaf width, mm			Petiole length
				Middle fraction	Bottom fraction	Top fraction	
Moreno	123.46 ^a	60.86 ^a	23.66 ^a	9.63 ^a	7.92 ^a	8.32 ^a	3.18 ^a
Ushuaia	46.64 ^b	30.94 ^b	12.06 ^b	5.73 ^b	4.71 ^b	4.51 ^b	2.27 ^b

Means in the same column followed by different letters are significantly different at $P \leq 0.01$ (Tukey's test).

extreme and abundant rainfalls throughout the year like the English weather and the extreme temperatures are 15 and -5°C . Climatic data were collected for mean, maxima and minima air daily temperatures ($^{\circ}\text{C}$), and rainfall (mm) by the Meteorological Station located at the Centro Austral de Investigaciones Científicas, and the Meteorological Station located at the Moreno experimental field, from January 2013 to February 2014 (Figure 1).

Leaf morphology and anatomy

One year after their establishment (February 2014), mature leaves ($n=20$) were taken from the plants of the two sites of culture and immediately they were scanned. The leaf area, leaf perimeter, leaf major and minor axis were registered. Then, the index of elongation (leaf major axis/leaf minor axis), roundness [$(4 \times \pi \times \text{area}) / \text{perimeter}^2$] and compactness [$\sqrt{4 \times \text{area} / \pi} / \text{major axis length}$] were calculated. Then, the leaves were fixed on FAA solution. Some of them were employed for histological section using Spurr's resin technique and the others were studied by SEM (Scanning Electron Microscope).

Light microscopy: leaves were dehydrated in an ethanol series and embedded in Spurr's resin. Thin sections (75-90 nm thick) were stained with uranyl acetate and lead citrate. Histological sections were used to study the mesophyll structure. Cells of each tissue were measured in height and width and the volume was calculated. Leaf cross sections without stain were observed by UV filter BP 340-380.

Scanning electron microscopy: leaves were dehydrated in an ethanol series and critical point drying technique was employed. Samples were sputter coated with 20 nm gold and observed with a SEM (Philips XL-30; Philips, Amsterdam, The Netherlands). Stomata of abaxial epidermis were measured and then density (stomata number/mm²) was calculated.

Results

Leaf morphology

Berberis microphylla leaf morphology was significantly different between the cultivation sites. In effect, Moreno leaves were signifi-

Table 2. Elongation, roundness and compactness indexes of *B. microphylla* leaf according to the cultivation site.

Cultivation site	Elongation	Roundness	Compactness
Moreno	0.43 ^b	0.43 ^b	0.54 ^b
Ushuaia	0.48 ^a	0.61 ^a	0.64 ^a

Means in the same column followed by different letters are significantly different at $P \leq 0.01$ (Tukey's test).

cantly larger than Ushuaia leaves in all the parameters registered (Table 1). Leaf length, leaf width and leaf perimeter of Moreno site were about twice than those of Ushuaia leaves, while leaf area was three times higher than Ushuaia leaves. Petiole length of Moreno leaves was significantly larger than Ushuaia leaves too (Table 1). Conversely, values of index calculated were higher for Ushuaia leaves (Table 2). Ushuaia leaves were more circular than Moreno leaves with the highest roundness and elongation indexes.

Light microscopy

Leaves of *B. microphylla* are exhibited dorsiventrality. Leaves are formed by a mesophyll differentiated into a palisade and a spongy mesophyll. Palisade cells are arranged on the adaxial surface. Cells of the palisade are elongated in the transverse plane of the leaf, with many chloroplasts (Figure 2A,B) and they are densely packed together into two layers on Moreno leaves (Figure 2A) and into three layers on Ushuaia leaves (Figure 2B). Sclerenchyma cells are present in adaxial sub epidermal position only on Ushuaia leaves (Figure 2B). The spongy mesophyll is present with irregular branching cells containing chloroplasts and separated by large air spaces. The spongy mesophyll is arranged on the abaxial side (Figure 2A,B,G,H). Vascular bundles which are part of the venation can be observed into the mesophyll. Phloem and xylem tissues are in abaxial and adaxial positions, respectively (Figure 2A). Parenchyma cells and some sclerenchyma cells are present surrounded the vascular bundle on Ushuaia leaves (Figure 2B). Nevertheless, parenchyma cells dominate Moreno leaves. Auto-fluorescence on leaf cross sections was observed. In effect, on the vascular bundles there was possible to detect cells with fluorescence (Figure 3A,B). Some parts of the epidermis present fluorescence too (Figure 3C). This confirms that there are laticifer-idioblast cells.

All the mesophyll is surrounded by the epidermis and cover by the cuticle (Figure 2E,I,J). The adaxial epidermis has larger cells than abaxial epidermis (Figure 2C-F). No significant differences were observed between the cell measures of adaxial epidermis of the two cultivation sites (Table 3). However, the height and volume of the abaxial epidermis cells and the cuticle was larger on the Ushuaia leaves. In effect, the cuticle of Moreno leaves were 2 μm wide while Ushuaia leaves were 5-6 μm wide (Figure 2E,F). On the other hand, the same differences were observed on the abaxial epidermis. Cuticle of Ushuaia leaves were 2.5 - 3 μm width, while Moreno leaves were 1-1.5 μm width, (Figure 2I,J). The abaxial epidermis cells on Ushuaia leaves were significant higher than those of Moreno leaves (Table 3). Finally, Moreno leaves were thinner than Ushuaia leaves, being the leaf thickness of 350 μm and 470 μm , respectively (Figure 2A,B).

Scanning electron microscopy

The abaxial epidermis appearance is different depending on the cultivation site. In effect, the leaves taken from Moreno site show an irregular surface due to the molecular architecture of the films of the epi-cuticle wax. The surface presents numerous ridges of different forms and closely placed near to the stomata that don't allow the differentiation of the arrangement of epidermal cells (Figure 3E,F). The appearance of this surface is glossy and oily. Numerous particles coating the surface of the guard cells flow from the stomatal pore (Figure 3G). On the other hand, epidermal cells are well recognized on abaxial epidermis from Ushuaia leaves (Figure 3H,I). Stomata of anomocytic type are observed, being the pair of guard cells surrounded by 5-6 unspecialized epidermal cells, and surface looks waxy (Figure 3G,I). Venation with its ramification is well recognized on diaphanized leaves (Figure 3K-M). Adaxial epidermal cell arrangement is isodiametric (Figure 3L) and

the stomata surrounded by generic format of epidermal cells are noticed on the abaxial epidermis (Figure 3M). Stomatal density for leaves collected on Moreno site varied between 330 and 450 per mm^2 , while in leaves from Ushuaia site the values recorded were 210-330 stomata/ mm^2 (data not shown).

Discussion

Leaves are important organs for photosynthesis and play a crucial role in survival and growth of a plant. The leaf can be considered as a microcopy of the plant, and the variations of leaf morphology can reflect the plant capacity to acquire, use and conserve resources.³³ Leaf morphology like as specific leaf area changes with the plant growth conditions *i.e.* temperature.³⁴ Light availability can modify leaf anatomy and therefore affect plant growth.³⁵ Climatic conditions of the two selected sites for this study are quite different so it is expected to be one of the causes of morphological differences. Furthermore, many species have acquired plasticity for the leaf shape giving responses to changes in the environmental conditions. Plants were grown in Moreno site surrounded by trees to reduce high temperatures, so that the presence of neighboring vegetation could have modified the light environment. It has been demonstrated in *Arabidopsis thaliana* that changes in environmental light generate signals that are perceived by phytochromes and cryptochromes.³⁶ In consequence, an elongation of the petiole and an increase of the leaf blade area is a typical example of leaf shape plasticity called shade-avoidance syndrome. Ushuaia leaves have a higher roundness and elongation indexes. A correlation between leaf roundness and irradiance was found in *Nothofagus solandri*, decreasing with increasing irradiance; however, a non-significant correlation was found in *N. fusca*.³⁷

As well knows on others species, external changes in *B. microphylla* were reflected in an increase in the volume of each cell when a decrease in cell proliferation was observed as a compensation phenomenon.³⁸ Another differ-

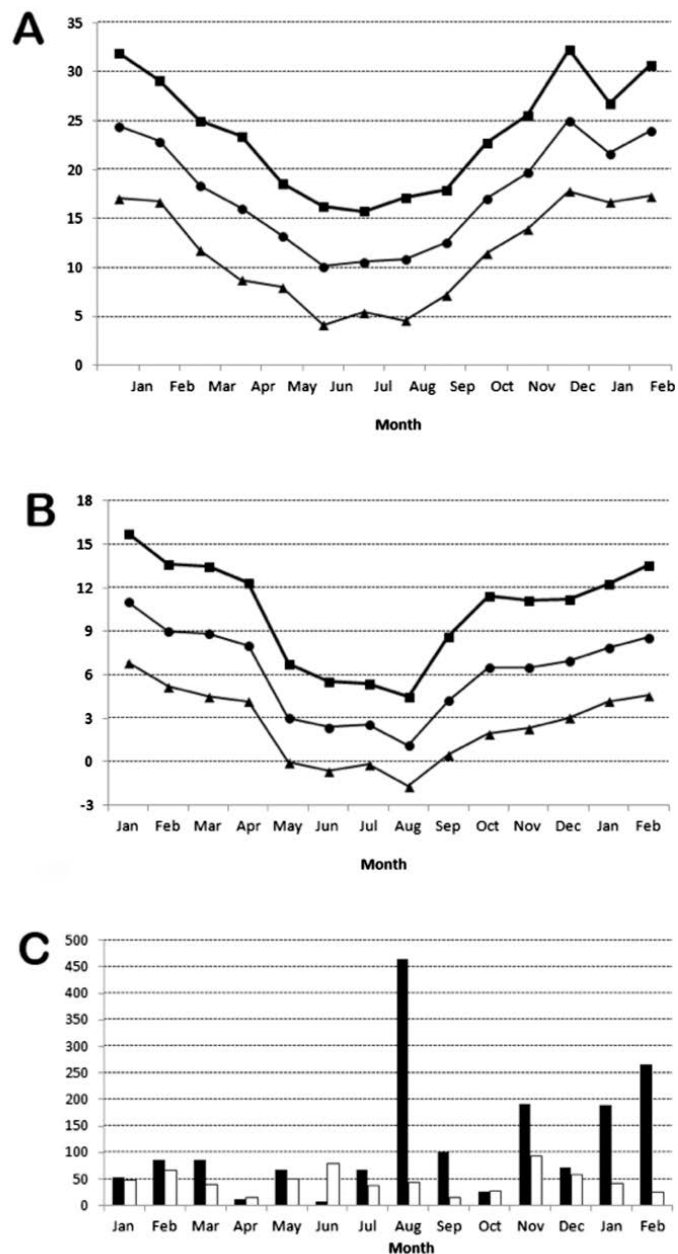


Figure 1. Temperature (A-B) and rainfall (C) registered by the Meteorological Station located at the Centro Austral de Investigaciones Científicas (Ushuaia, Tierra del Fuego, Argentina; B-C) and the Meteorological Station located at the Moreno experimental field (Buenos Aires, Argentina; A-C) from January 2013 to February 2014. A-B) Mean (circle), maxima (square) and minima (triangle) air daily temperatures ($^{\circ}\text{C}$); C, rainfall (mm), Moreno (black), Ushuaia (white).

Table 3. *Berberis microphylla* leaf cell measures studied by light microscopy according to the place of cultivation.

Tissue	Height μm		Width μm		Volume μm^3	
	Moreno	Ushuaia	Moreno	Ushuaia	Moreno	Ushuaia
Palisade cells	47.33 ^b	72.17 ^a	19.10 ^a	19.80 ^a	912.00 ^b	1435.00 ^a
Spongy cells	19.40 ^a	21.25 ^a	25.00 ^b	30.35 ^a	512.00 ^b	635.00 ^a
Adaxial epidermis cells	19.04 ^a	18.5 ^a	38.50 ^a	37.80 ^a	746.15 ^a	702.50 ^a
Abaxial epidermis cells	11.20 ^b	14.75 ^a	21.80 ^a	23.30 ^a	248.00 ^b	340.00 ^a
Stomata	3.24 ^a	2.10 ^b	3.53 ^a	2.07 ^b	-	-

Means in the same line and for each variable followed by different letters are significantly different at $P \leq 0.01$ (Tukey's test).

ence found between these leaves was the thickness of the cuticle. The cuticle has two main components: cutin and waxes. Cutin is a tough, cross-linked polyester matrix primarily composed of C16 and C18 oxygenated fatty acids and glycerol. Wax is a heterogenous mixture, primarily composed of very-long-chain fatty acid derivatives.³⁹ The cuticular wax in *Berberis* is crystalloid usually as clustered tubuli, chemically dominated by nonacosane-10-ol.⁴⁰ Little is known about how waxes are trafficked within the cell from their site of synthesis at the endoplasmic reticulum to the plasma membrane.⁴¹ Many authors considered that wax extruded from epidermal cells.⁴¹⁻⁴³ Epicuticular waxes are modified by changes in plant growth conditions such as temperature, relative humidity, irradiance, and wind, or acid rain.⁴⁰ Climatic conditions of the two selected sites for this study are quite different so it is expected to be one of the causes of morphological differences. Ushuaia leaves had thicker cuticle probably for the most extreme weather conditions that plants undergo. On the other hand, Ushuaia site has a greater intensity of visible and UV light and this factor is positively correlated with the enlargement of cuticle thickness to create a lotus effect to reflect UV radiation and integration of protective flavonoid compounds in the cuticle. These results are in agreement with Davi *et al.*²³ who determined that plants grown in high light generally have thick leaves caused by extra layers of palisade mesophyll or longer palisade cells to protect them from high-light damage.

Different appearance between the abaxial epidermis could be due to Moreno leaves were still growing while Ushuaia leaves growth had ceased. In effect, surface wax appears to be deposited only on young leaves, and essentially only during or shortly after the period of leaf expansion. Wax deposition is probably related to the development and solidification of the cuticular layer.⁴⁴

The structural basis of cuticle is a combination of surface roughness in the micrometer range combined with a strong hydrophobicity caused by superimposed wax sculptures (epicuticular waxes) in the nanometer range.⁴⁵ Epicuticular waxes strongly influence the wet ability, self-cleaning behavior and the light reflection at the cuticle interface.⁴⁶ It is remarkable that particularly secondary alcohols as nonacosane-10-ol among others induce non-planar structures such as tubules and other irregular forms.⁴⁵ Waxes are solid, but their structures reveal analogies to those of liquid crystals. The formation of a layer structure may be inhibited by a strong variation in the chain length of the molecules or by a missing positional order, causing a nematic structure with a two-dimensional order. For the other hand, wax synthesis and extraction stopped when cell expansion ceased.⁴⁷

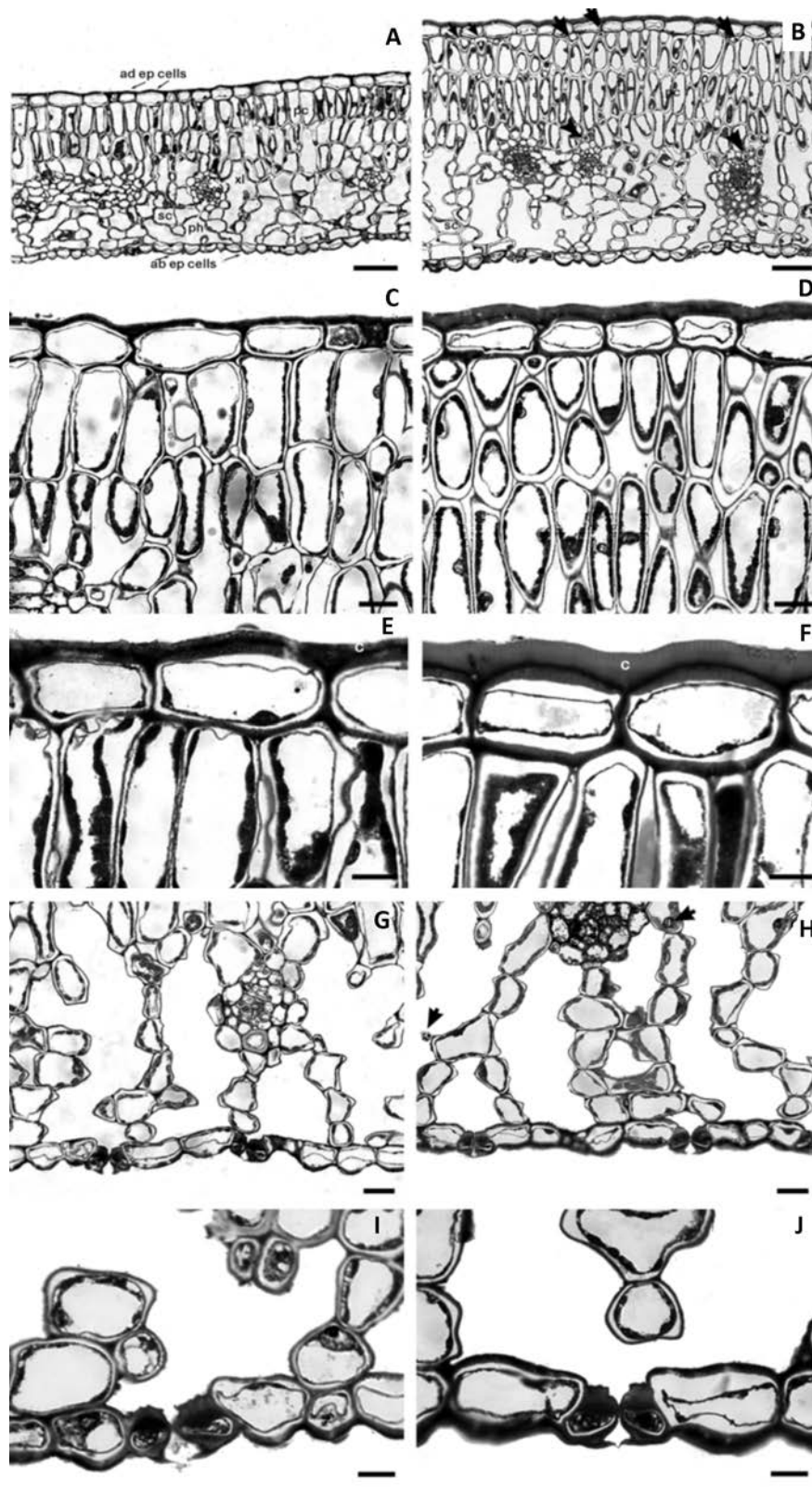


Figure 2. Micrograph of cross-section of *Berberis microphylla* leaves collected on Moreno (A,C,E) and Ushuaia sites (B, D, F). A-B, view of total cross-section leaf with adaxial epidermal cells (ad ep cells), abaxial epidermal cells (ab ep cells), palisade mesophyll cells (pc), spongy mesophyll cells (sc), phloem cells (ph), xylem cells (xl) and sclerenchyma cells (arrowhead); C-D, Detail of adaxial epidermal and palisade mesophyll tissues; E-F, Detail of abaxial epidermal cells and cuticle (c). Bars: A-B, 100 μ m; C-D, 25 μ m; E-F, 10 μ m. G-J) Detail of the palisade mesophyll tissue and the stomata of abaxial epidermal of *Berberis microphylla* leaves collected on Moreno (G,I) and Ushuaia sites (H,J). Bars: G-I, 25 μ m; H-J, 10 μ m.

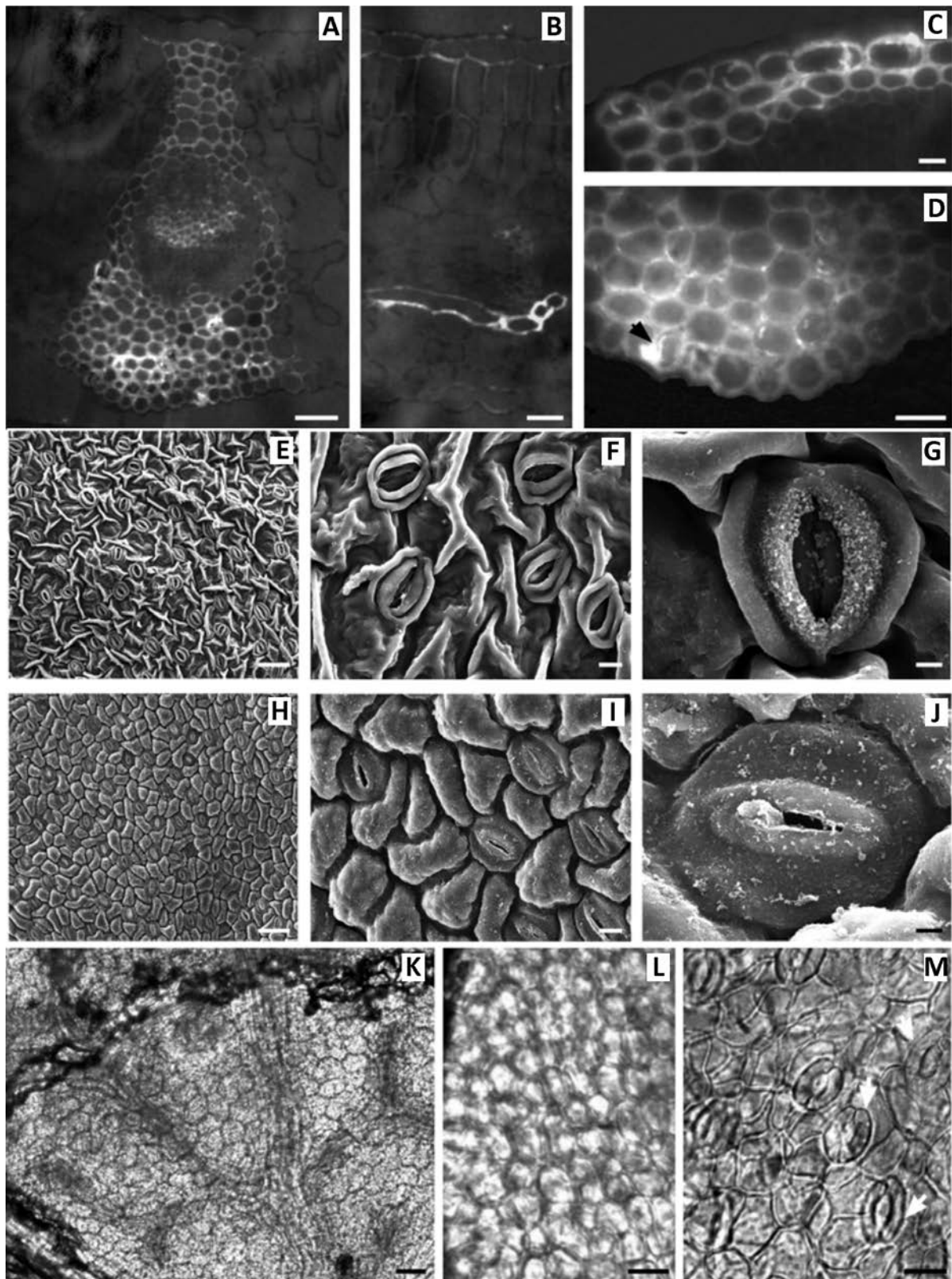


Figure 3. A-D) Micrograph of cross-section of *Berberis microphylla* leaves observed by UV filter BP 340-380. A) View of central vascular bundle and parenchyma cells with fluorescence; B) transverse vascular bundle with fluorescence; C) epidermal and sclerenchyma cells on the leaf apex with fluorescence; D) detail of stomata (arrowhead) and laticifer-idioblast cells. Bars: A-B, 10 μ m; C, 25 μ m; D, 5 μ m. E-J) SEM micrograph of abaxial epidermis of *Berberis microphylla* leaves collected on Moreno (E-G) and Ushuaia site (H-J). E,H) General view; F,I) detail of surface of abaxial epidermis tissue; G,J) stomata detail. Bars: E,H, 50 μ m; F,I, 10 μ m; G,J, 5000 nm. K-M) Micrograph of diaphanized *Berberis microphylla* leaves. K, leaf venation; L, Detail of adaxial epidermal cells; L, Detail of abaxial epidermal cells with stomata (arrows). Bars: 2 μ m.

Flavonoid compounds usually accumulate in the central vacuoles of guard cells and epidermal cells as well as subepidermal cells of leaves.⁴⁸ Several classes of phenolic compounds are strongly autofluorescent when irradiated with UV or blue light. Therefore, fluorescence microscopy is a powerful tool for studying tissue localization of these metabolites.⁴⁹ Berberine is a quaternary ammonium salt from the protoberberine group of isoquinoline alkaloids that possess low fluorescence emission in an aqueous solution⁵⁰ and it is well known that berberine stain a bright yellow.⁶ This property would explain the intense yellow color of diaphanized leaves (data not shown).

Conclusions

Plant plasticity is an advantageous strategy for survival in changing environmental conditions, being leaves photosynthetic organs thus their shapes, sizes and structure are important factors influencing the success of the plants. *B. microphylla* leaves showed a high phenotypic plasticity between the two sites of cultivation. The changes in the leaf morphology and structure observed in Moreno leaves could indicate that the plants are trying to adjust its morphology to the new culture conditions *i.e.* higher temperatures and lower irradiance. The correlation of the observed changes together with the plasticity on the leaf physiology, the nutrient and pigment contents will be of interest to study, as well as with the reproductive performance to apply on future genetic improvement.

References

- Hogan CM, WWF. Magellanic subpolar forests. 2014. Available from: <http://www.earth.org/view/article/154355/>
- Moore DM. Flora of Tierra del Fuego. Oswestry: Anthony Nelson & Missouri Botanical Garden; 1983.
- Lencinas MV, Martínez Pastur G, Rivero P, Busso C. Conservation value of timber quality versus associated non-timber quality stands for understory diversity in *Nothofagus* forests. *Biodivers Conserv* 2008;17:2579-97.
- Shaffer JE. Inotropic and chronotropic activity of berberine on isolated Guinea pig Atria. *J Cardiovasc Pharmacol* 1985;7:307-15.
- Orsi MC. Berberidaceae. In: Correa MN, ed. Flora Patagónica. Buenos Aires: INTA; 1984. pp 325-48.
- Fajardo Morales V, Podestá F, Urzúa A. Reseña de los alcaloides encontrados en el género *Berberis* de Chile. *Rev Latinoamer Quím* 1986;16:141-56.
- Fajardo Morales V. Estudio químico de las especies chilenas del género *Berberis*. *Rev Latinoamer Quím* 1987;18:46-50.
- Mokhber-Dezfuli N, Saeidnia S, Reza Gohari A, Kurepaz-Mahmoodabadi M. Phytochemistry and pharmacology of berberis species. *Pharmacogn Rev* 2014;8:8-15.
- Pomilio AB. Anthocyanins in fruits of *Berberis buxifolia*. *Phytochem* 1973;12: 218-20.
- Medrano MA, Tomas MA, Frontera MA. Isolation and identification of anthocyanins in fruits from Chubut Province (Argentina). *Fruits of Ribes aureum Pursh, R. magellanicum Poir and Berberis darwinii Hook*. *Rev Latinoamer Quím* 1985;16 84-6.
- Motalleb G, Hanachi P, Kua SH, et al. Evaluation of phenolic content and total antioxidant activity in *Berberis vulgaris* fruit extract. *J Biol Sci* 2005;5:648-53.
- Arena ME, Curvetto N. *Berberis buxifolia* fruiting: kinetic growth behavior and evolution of chemical properties during the fruiting period and different growing seasons. *Sci Hortic* 2008;11:120-7.
- Ruiz A, Hermosin-Gutierrez I, Mardones C, et al. Polyphenols and antioxidant activity of calafate (*Berberis microphylla*) fruits and other native berries from southern Chile. *J Agric Food Chem* 2010;58:6081-9.
- Koncic MZ, Kremer D, Karlovic K, Kosalec I. Evaluation of antioxidant activities and phenolic content of *Berberis vulgaris* L. and *Berberis croatica* Horvat. *Food Chem Toxic* 2010;48:2176-80.
- Surveswaran D, Cai YZ, Corke H, Sun M. Systematic evaluation of natural phenolic antioxidants from 133 Indian medicinal plants. *Food Chem* 2007;102:938-53.
- Tomosaka H, Chin YW, Salim AA, et al. Antioxidant and cytoprotective compounds from *Berberis vulgaris* (barberry). *Phytother Res* 2008;22:979-81.
- Arena ME, Vater G, Peri P. Fruit production of *Berberis buxifolia* Lam in Tierra del Fuego. *Hort Sci* 2003;38:200-2.
- Arena ME, Giordani E, Radice S. Phenological growth and development stages of the native Patagonian fruit species *Berberis buxifolia* Lam. *JFAE* 2013;11:1323-7.
- Arena ME, Postemsky P, Curvetto NR. Accumulation patterns of phenolic compounds during fruit growth and ripening of *Berberis buxifolia*, a native Patagonian species. *New Zeal J Bot* 2012;50:15-28.
- Arena ME, Zuleta A, Dynner L, et al. *Berberis buxifolia* fruit growth and ripening: evolution in carbohydrate and organic acid contents. *Sci Hortic* 2013;158:52-8.
- Arena ME, Giordani E, Radice S. Flowering, fruiting and leaf and seed variability in *Berberis buxifolia*, a native Patagonian fruit species. In: Marin L, Kovac D. Native species: identification, conservation and restoration. New York: Nova Sciences Publishers; 2011.
- Arena ME, Radice S. Shoot growth and development of *Berberis buxifolia* Lam. in Tierra del Fuego (Patagonia). *Sci Hortic* 2014;165:5-12.
- Davi H, Barbaroux C, Dufrière E, et al. Modelling leaf mass per area in forest canopy as affected by prevailing radiation conditions. *Ecol Model* 2008;211:339-49.
- Guo WH, Li B, Zhang XS, Wang R. Architectural plasticity and growth responses of *Hippophaerhamnoides* and *Caragana intermedia* seedlings to simulated water stress. *J Arid Environ* 2007;69:385-99.
- Arambarri AM, Freire SE, Colares MN, et al. Leaf anatomy of Medicinal Shrubs and Trees from Gallery Forests of the Paranaense Province (Argentina). Part 1. *Bol Soc Argent Bot* 2006;41:233-68.
- Tamiselvi S, Balasubramani SP, Venkatasubramanian P, Vasanthi NS. A review of the pharmacognosy and pharmacology of the herbals traded as Daruharidra. *Int J Pharm Biol Sci* 2014;5:556-70.
- Upadhyay GC, Bhatkoti M, Bhatt NN, et al. A comparative study of *Berberis aristata* D.C. and *Berberis asiatica* Roxb.ex. D.C. (Daruharidra) W.S.R to Madhumehahara Karma. *Int J Pharm Biol Arch* 2012;3:472-7.
- Henderson GA, Hay GW. The carbohydrates of the leaves of common barberry (*Berberis vulgaris*). The extraction, fractionation and structural studies of selected non-cellulosic polysaccharides. *Carbohydr Res* 1972;23:379-98.
- Freire SE, Arambarri AM, Bayón ND, et al. Epidermal characteristics of toxic plants for cattle from the Salado River Basin (Buenos Aires, Argentina). *Bol Soc Argent Bot* 2005;40:241-81.
- Komal S, Ranjan B, Neelan C, et al. *Berberis aristata*. A review. *IJRAP* 2011;2:383-8.
- Rathi B, Sahu J, Koul S, Khosa RL. Salient features of *Berberis aristata* and *Berberis asiatica*: A comparative pharmacognostical study. *Der Pharmacia Lettre* 2013;5:40-2.
- Sabir S, Tahir K, Rashid N, et al. Phytochemical and antioxidant studies of *Berberis lycium*. *Pak J Pharm Sci* 2013;26:1165-72.
- Wu H, Zhang L, Du L. Ionic liquid sensitized fluorescence determination of four isoquinoline alkaloids. *Talanta*

- 2011;85:787-93.
34. Atkin OK, Loveys BR, Atkinson LJ, Pons TL. Phenotypic plasticity and growth temperature: understanding interspecific variability. *J Exp Bot* 2006;57:267-81.
 35. Tognetti R, Minotta G, Pinzauti S, et al. Acclimation to changing light conditions of long-term shade-grown beech (*Fagus sylvatica*) seedlings of different geographic origins. *Trees* 1998;12:326-33.
 36. Casal JJ. Shade avoidance. *The Arabidopsis Book* 2012;10:e0157.
 37. Niinemets Ü, Cescatti A, Christian R. Constraints on light interception efficiency due to shoot architecture in broad-leaved *Nothofagus* species. *Tree Physiol* 2004;24:617-30.
 38. Tsukaya H. Leaf shape: genetic controls and environmental factors. *Int J Dev Biol* 2005;49:547-55.
 39. Pollard M, Beisson F, Li Y, Ohlrogge JB. Building lipid barriers: biosynthesis of cutin and suberin. *Trends Plant Sci* 2008;13:236-46.
 40. Barthlott W, Neinhuis C, Cutler D, et al. Classification and terminology of plant epicuticular waxes. *Bot J Linnean Soc* 1998;126:237-60.
 41. McFarlane HE, Watanabe Y, Yang W, et al. Golgi- and trans-golgi network-mediated vesicle trafficking is required for wax secretion from epidermal cells. *Plant Physiol* 2014;164:1250-60.
 42. Buschhaus C, Jetter R. Composition differences between epicuticular and intracuticular wax substructures: how do plants seal their epidermal surfaces? *J Exp Bot* 2011;62:841-53.
 43. De Bono A, Yeats TH, Rose JKC, et al. *Arabidopsis* LTPG is a glycosyl phosphatidylinositol-anchored lipid transfer protein required for export of lipids to the plant surface. *Plant Cell* 2009;21:1230-8.
 44. Schieferstein RH, Loomis WE. Development of the cuticular layer in angiosperm leaves. *Amer J Bot* 1959;46:625-35.
 45. Koch K, Ensikat HJ. The hydrophobic coatings of plant surfaces: epicuticular wax crystals and their morphologies, crystallinity and molecular self-assembly. *Micron* 2008;39:759-72.
 46. Bargel H, Koch K, Cerman Z, Neinhuis C. Structure-function relationships of the plant cuticle and cuticular waxes: a smart material? *Funct Plant Biol* 2006;3:893-910.
 47. Giese BN. Effects of light and temperature on the composition of epicuticular wax of barley leaves. *Phytochem* 1975;14:921-8.
 48. Weissenböck G, Hedrich R, Sachs H. Secondary phenolic products in isolated guard cell, epidermal cell and mesophyll cell protoplasts: distribution and determination. *Protoplasma* 1986;134:141-8.
 49. Hutzler P, Fischbach R, Heller W, et al. Tissue localisation of phenolic compounds in plants by confocal laser scanning microscopy. *J Exp Bot* 1998;49:953-65.
 50. Xu F, Gou W, Xu W, et al. Leaf morphology correlates with water and light availability: what consequences for simple and compound leaves? *Prog Nat Sci* 2009;19:1789-98.

A new species of *Freycinetia* Gaudich (*Pandanaceae*) from West Kalimantan, Indonesia

Fitri Sri Rizki,¹ Tatik Chikmawati,¹ T. Rugayah²

¹Department of Biology, Faculty of Mathematics and Natural Sciences, Bogor Agricultural University; ²Herbarium Bogoriense, Botany Division, Research Center For Biology, Indonesian Institute of Sciences, Bogor, Indonesia

Abstract

A new species *Freycinetia sessiliflora* Rizki & Rugayah is described and illustrated based on specimen character from Mount Nyiut-Sambas, West Kalimantan (Indonesia). The species is differed from others by having sessile pedicellus, concave cylindrical of inner bracts and bright red bracts.

Introduction

Freycinetia Gaudich (*Pandanaceae*) is mostly distributed in the region of Malesia, particularly in Borneo, Celebes, Papua and Sumatra. The genus comprises approximately 200-300 species all over the world; about 150 species found in Indonesia.¹ *Freycinetia* was first described by the French botanist Gaudichaud in 1824. Along with *Pandanus*, *Sararanga*, *Martelidendron*, and *Benstoniana* were classified into *Pandanaceae* family.^{2,3}

Bornean *Freycinetia* has seen thoroughly studied by Stone in 1970.⁴ He described 24 species, and 11 species of them were reported as endemic to Borneo. Those species account mostly from N. Borneo (Sabah and Sarawak), only 13 species occur in Kalimantan. It is indicated that, Kalimantan is still under collected for *Pandanaceae*.

In 2006, several field studies have conducted in Kalimantan (Bukit-Baka-Bukit Raya National Park and Sebangau National Park). Three new species of *Freycinetia* have discovered by Keim (2009), namely *F. kartawinatae* Keim, *F. runcingensis* Keim, and *F. subracemosa* Keim in Kalimantan based on the recent collection and the herbarium specimens deposited in Herbarium Bogoriense.^{5,6}

In 2013, there were conducted exploration of *Pandanaceae* in Mount Nyiut-Sambas, West Kalimantan. The Mt. Nyiut has wet tropical forest with moderate to steep topography and the highest area is 1701 m asl. From the exploration, 7 species *Freycinetia* were found, one of them is suspected as a new species namely *Freycinetia sessiliflora* Rizki & Rugayah. It has pectinate spinulose auricle similar to *F. rigidifolia* and *F. pectinata*, but it differs in its auricle apex, leaf and other generative characters. After comparing to the herbarium specimens deposited in Herbarium Bogoriense and a loan specimen from Rijksherbarium Leiden, we concluded this taxon as a new species.

Results

Freycinetia sessiliflora Rizki & Rugayah Sp. nov.

Freycinetia sessiliflora similar to *F. rigidifolia* and *F. pectinata* in its pectinate spinulose auricle. But differ in its leaf size and floral characters. The leaf size 47-55 cm x 0.7-1.6 cm. Pedicellus sessile, inner bract concave cylindrical (Figures 1 and 2).

Typus: Indonesia, Borneo, West Kalimantan, Mt. Nyiut Sambas, 108°59' - 109°07'40" east longitude and 0°48'30" - 0°52'20" north latitude. 20 August 2013, Rizki 03 (Holo-BO!).

Description: Climber, climbing up to 10 meters, internodes 3.5-12 cm long, 0.5-1 cm in diameter. *Leaves* imbricate, linear-lanceolate, 47-55x0.7-1.6 cm, stiff, longitudinal veins visible on the adaxial and abaxial surfaces; apex acuminate, sometimes revolute when dry; margins and midrib on the abaxial surfaces armed

Correspondence: Tatik Chikmawati, Department of Biology, Faculty of Mathematics and Natural Sciences, Bogor Agricultural University, Raya Darmaga Kampus IPB Darmaga Bogor 16680, West Java, Indonesia.
Tel.: +62.251.8622642.
E-mail: tchikmawati@yahoo.com

Key words: *Freycinetia sessiliflora*; Mount Nyiut; sessile.

Acknowledgements: the authors would like to thank to the Bogor Agricultural University (IPB), thanks also to Herbarium Bogoriense and Rijksherbarium, Leiden for the opportunity using the specimens. Thank also to Dr. Ary P. Keim and Prof. Mien A. Rifai for their opinion in the scientific writing and comments to the manuscript.

Contributions: the authors contributed equally.

Conflict of interest: the authors declare no potential conflict of interest.

Funding: this study was supported by Directorate General of Higher Education (DIKTI), Kemendikbud RI, Government of Indonesia.

Received for publication: 5 November 2014.
Revision received: 18 November 2014.
Accepted for publication: 18 December 2014.

This work is licensed under a Creative Commons Attribution NonCommercial 3.0 License (CC BY-NC 3.0).

©Copyright F.S. Rizki et al., 2015
Licensee PAGEPress srl, Italy
International Journal of Plant Biology 2015; 6:5701
doi:10.4081/pb.2015.5701

from the base to the apex; spine triangle 0.2x0.1 cm, gradually smaller and fewer to the apex, the smaller ones 0.1 mm. *Auricles* pectinate spinulose, lobed at the apex, 3.5-4x0.3-0.8 cm. *Staminate inflorescence* not known.

Pistillate inflorescence terminal, umbellate with 3 cephalia; peduncles cylindrical, glabrous, 5-6 cm long, 0.4 cm in diameter; bracts 9 (3x3), concave cylindrical spoon-like,

Table 1. Morphological differences between *Freycinetia sessiliflora*, *Freycinetia rigidifolia*, and *Freycinetia pectinata*.

Characters	<i>Freycinetia sessiliflora</i>	<i>Freycinetia rigidifolia</i>	<i>Freycinetia pectinata</i>
Size of leaf, cm	47-55 x 0.7-1.6	25-33 x 0.7-1.6	15-20 x 0.9
Auricles	Pectinate spinulose, apex lobed	Pectinate spinulose, apex rounded	Pectinate spinulose, apex rounded
Pedicellus	Sessile	1.5-3 x 0.3-0.4 cm	0.3-0.5 x 0.5-0.7 cm
Shape of bracts	Concave cylindrical	Oblong-cylindrical	Oblong-cylindrical
Number of bract	3-9	3-7	3-6
Number of cephalia per inflorescences	2-3	2-3	4-5
Number of stigma	2-4	2-3	4-6 (-12)

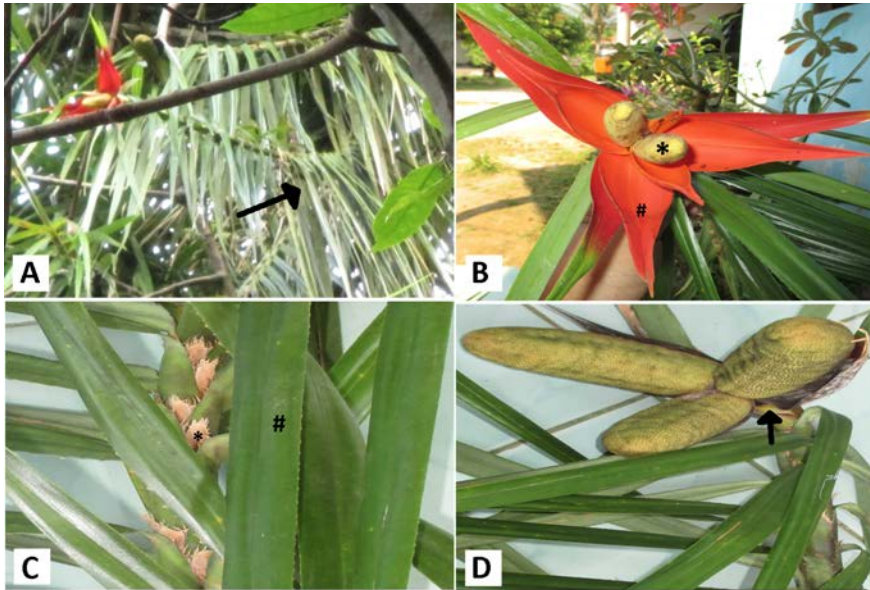


Figure 1. A) *Freycinetia sessiliflora* habit (see arrow); B) *F. sessiliflora* bractea and inflorescence: *cephalia, #bract concave cylindrical; C) *F. sessiliflora* auricle pectinate spinulose, apex lobed: *auricles pectinate spinulose, #leaves; *F. sessiliflora* cephalium and pedicellus sessile (arrow).

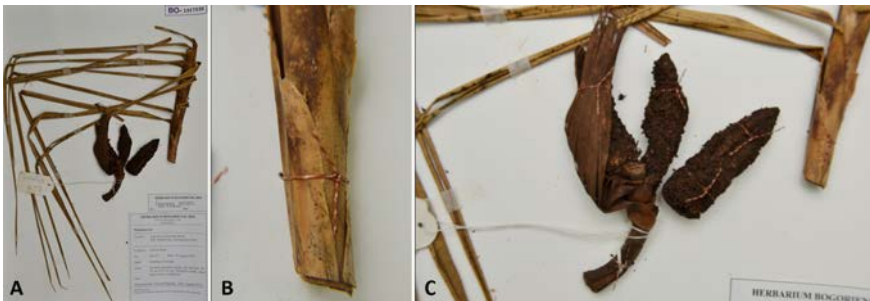


Figure 2. Holotype specimen of *Freycinetia sessiliflora* Rizki & Rugayah: A) *F. sessiliflora*; B) auricle of *F. sessiliflora*; C) inflorescent of *Freycinetia sessiliflora* Rizki & Rugayah.

outer 15-20×6-8 cm, inner 1.4-2×6-10 cm, red-orange, margins armed from the base to the apex. *Cephalia* 2-3, sessile, cylindrical, 6.5-8×2-2.5 cm long, berry pentagonal, 0.2- 0.5 mm in diameter; stigma remains mostly 2-4, areola stigma with rings, seeds ellipsoid.

Distribution: West Kalimantan, Mount

Nyiut-Sambas.

Etymology: The epithet name is given for its obvious depressed pedicellus characteristic.

Habitat: *Freycinetia sessiliflora* located in lowland bush and secondary forest area from 90 to 750 m above sea level. Fruiting in August and February.

Discussion

The naming of new species refers to the main character of this species i.e. sessile or sitting cephalium. This species closely related with *F. rigidifolia* and *F. pectinata* and included in section *Hemsleya* because it has a pectinate spinulose auricle. The differences of *Freycinetia sessiliflora* with *F. rigidifolia* and *F. pectinata* are the size of leaves, tip of auricle, shape of bractea, number of stigma and presence of pedicellus (Table 1).

References

1. Stone BC. Malayan climbing pandans. The genus *Freycinetia* in Malaya. *Malayan Nat J* 1970;23:44-91.
2. Callmender MW, Chassot P, Kupfer P, Lowry P. Recognition of *Martellidendron*, a new genus of Pandanaceae, and its biogeographic implications. *Taxon* 2003;52:747-62.
3. Callmender MW, Lowry P, Forest F, et al. *Benstonea* Callm. & Buerki (Pandanaceae): characterization, circumscription, and distribution of a new genus of screw-pines, with a synopsis of accepted species. *Candollea* 2012;67:323-45.
4. Stone BC. Materials for a monograph of *Freycinetia* Gaud. (Pandanaceae) VI. Species of Borneo. *Gard Bull Sing* 1970;25:209-33.
5. Keim AP, Rugayah, Rustiami H. The Pandanaceae of the Bukit Baka Bukit Raya National Park and adjacent areas, West and Central Kalimantan, Indonesia, with notes on their nomenclature and the rediscovery of *Pandanus aristatus* and several new records. *Gard Bull Sing* 2006;63: 31-62.
6. Keim AP. Three new species of *Freycinetia* (Pandanaceae) from Kalimantan, Indonesia. *Reinwardtia* 2009;13:15-20.

Effect of petrol and spent oil on the growth of Guinea Corn (*Sorghum bicolor* L.)

Ronke Justina Komolafe,¹ Olatunde M. Akinola,² Oludare James Agbolade¹

¹Department of Plant Science and Biotechnology, Federal University, Oye Ekiti; ²Department of Cell Biology and Genetics, University of Lagos, Nigeria

Abstract

This study assessed the effect of petrol and spent lubricating oil on the major growth traits (such as root length, stem length, leaf area, and biomass), and the changes in epidermal layer of leaf and its mitotic index in Guinea Corn (*Sorghum bicolor* L.) exposed to 0% (control), 5%, 10%, 15% and 20% concentrations of petrol and spent lubricating oil. Each concentration was mixed with 3 kg of soil in a plastic pot and each treatment was carried out in three replicates. Forty days after planting, the leaf areas of guinea corn plant were 95.83 cm², 89.67 cm², 89.47 cm², and 77.80 cm² in control, 5%, 10%, 15%, and 20% respectively of petrol pollutant. The means of stem length were 32.50±0.5 cm, 22.60±0.65 cm, 21.27±0.75 cm, 20.83±0.28 cm and 20.33±0.28 cm in control, 5%, 10%, 15% and 20% respectively. Both leaf area and stem length of treated seedlings reduced with increased concentration of the pollutants. Additionally, reduction in the dry weight of the seedlings increased with increasing concentration of both petrol and spent oil. The micrograph of the internal anatomy of the upper epidermal layers of the leaf revealed broken and scattered epidermal cells and smaller sizes of the stomata, and were increased with the increasing concentration of the treatment. Statistical analysis of the treatment shows that there was a significant reduction ($P < 0.05$) in the stem length and leaf area of the seedlings. This study revealed that petroleum pollutant adversely affected germination, growth and development of guinea corn but petroleum products like spent oil can provide nutrition necessary for growth and yield of plant at low concentration.

Introduction

Crude oil pollutants are highly stable compounds persisting in the environment for a long time before they can be broken down.¹ They accumulate in tissues of most fauna and flora life, poisoning and causing a wide range of toxic effect on them. Oil pollutants include

aviation fuel, engine oil, petrol, spent oil and diesel. The extent to which the environment is polluted by these oils depend on the frequency and severity of the spills in a given area.² Oil pollution is associated with highly toxic heavy metals such as cadmium, zinc, lead, chromium, nickel and manganese with great negative effects on plants.³ Different heavy metals at optimal concentrations have been shown to inhibit various metabolic processes in plants resulting in their reduced growth and development.⁴ Plants may be killed by oil pollution or suffer reduced growth and reproductive rates due to combination of physical coating, altered soil chemistry and toxic effects of crude oil components.⁵ Noticeable forms of stunted growth and chlorosis in plants and also marked anatomical change in plant tissues are responses to heavy metal toxicity.⁶ Oil spillage on land retards vegetative growth for a period of time and in extreme cases, leads to the destruction of vegetation. It also increases potential for hazards and renders the soil unfit for cultivation. Any hydrocarbon solvent is liable to penetrate into plants through lipophilic surface, roots and once inside, it dissolves the cell membranes and cause loss of cell sap and in some cases, accumulates in the tissue of fruits of crops.⁷ Particularly, dangerous soil contamination includes pollution with petroleum derivatives, which is very often observed in municipal soils around industrial plant and in areas where petroleum and natural gas are obtained.⁸

Bioaccumulation of hydrocarbons in plant appears to be related to the lipid content of the plant tissue, the greater the hydrocarbon accumulation.⁹ Plants may be killed by oil pollution or suffer reduced growth and reproductive rates due to combination of physical coating, altered soil chemistry and toxic effects of crude oil components.⁵ The contamination of soil environment can undoubtedly limit its protective function, upset metabolic activity, unfavorably affect its physicochemical characteristics, reduce fertility and negatively influence plant production.¹⁰ The above features are very much influenced by anthropogenic factors, which include the contamination of soil with petroleum derived products. Changes in some soil properties resulting from contamination with petroleum derived substances, and particularly those related to physic-chemical composition, brings about some changes in the biological composition of soil which in consequence, can lead to water and oxygen deficits, as well as to a shortage of available forms of nitrogen and phosphorus.¹⁰

Since contamination of soil with refinery products deteriorates its biochemical and physicochemical properties, it also limits the growth and development of plants, whose nutritive and technological value can be low and often questionable. In this connection,

Correspondence: Ronke Justina Komolafe, Department of Plant Science and Biotechnology, Federal University of Oye, Oye-Ekiti, Ekiti State, Nigeria. Tel.: +23.4813.8106512. E-mail: ronke.komolafe@fuoye.edu.ng

Key words: Biomass; mitotic index; seedlings; pollutant; micrograph; anatomy.

Contributions: RJK and OMA designed the experiment; RJK carried out the experiment and wrote the initial draft; OJA reviewed the paper and made necessary correction.

Conflict of interest: the authors declare no potential conflict of interest.

Received for publication: 21 February 2015.

Revision received: 2 April 2015.

Accepted for publication: 2 April 2015.

This work is licensed under a Creative Commons Attribution NonCommercial 3.0 License (CC BY-NC 3.0).

©Copyright R.J. Komolafe et al., 2015
Licensee PAGEPress srl, Italy
International Journal of Plant Biology 2015; 6:5883
doi:10.4081/pb.2015.5883

this present study has been undertaken to determine the effect of soil contamination with petrol and spent oil on the growth of guinea corn. The major objectives of this research were to study: i) the effect of petrol and spent oil pollutants on the growth traits (such as root length, stem length, leaf area and biomass) of guinea corn; ii) their effect on the changes in epidermal layer of Guinea Corn leaf; iii) their effect on the mitotic index of Guinea Corn leaf.

Materials and Methods

Seeds procurement and germination experiment

The seeds of Guinea Corn (*Sorghum bicolor* L.) were procured from the market in Lagos and its viability was tested. Three kg of soil sample was weighed and put inside plastic buckets. The soil in each bucket was treated with 5%, 10%, 15%, and 20% concentrations of petrol and spent lubricating oil. Another plastic bucket containing soil did not receive any treatment with petrol and spent lubricating oil; this serves as control. Each treatment was then replicated three times. Five seeds of guinea corn were sown into the soil in the plastic buckets. The soil in the plastic buckets was regularly watered to ensure that the soil was moist enough for plant germination.

Determination of biomass

Fresh and dry weights of each seedling were determined. This was carried out by measuring the weight of the fresh leaf in each treatment using a weighing balance. The dry weights of the air dried leaves were also determined. This was done by oven-drying the leaves at $80 \pm 5^\circ\text{C}$ for 48 hours.

Determination of leaf area

The leaf areas of the samples were calculated according to the method of Pearcy *et al.*¹¹ using the formula: $LA = L \times W$, where L represents the length of the leaf and W the width of the leaf. The leaf was placed on a plain sheet of paper, the length and the width of the leaf was then measured using a ruler.

Determination of the leaf lower and upper epidermal layers

Plant samples were cut into smaller pieces with the sharp razor blade and were placed inside the glass Petri dishes. Twenty cm^3 of concentrated nitric acid was carefully added into each glass Petri dishes to cover the small pieces of plant samples. The glass Petri dishes were covered with their lids and kept in a safe place for 48 hours to enable the concentrated nitric acid to start the bleaching and detachment of the mesophyll layer between the lower and the upper epidermal layers. The process was completed as soon as the greenish coloration of the leaves turned to light-yellow coloration. After the bleaching, the plant samples were carefully removed from the glass petri dishes and washed in tap water to remove the traces of the acid.

The concentration of nitric acid inside the specimen containers were replaced with tap water, the plant samples were then returned into it using a dissecting needle and were kept in a safe place for 24 hours. The separation of the lower and upper epidermal layers commenced as soon as bubbles of water was seen forming on top of the plant samples. Pieces of the separated layers were seen floating on top of tap water inside the specimen container.

Preparation of root tip for mitotic indices

Each root concentration was fixed in a specimen bottle using acetic acid alcohol. The root in each concentration was placed on a clean plain glass slide using a forceps and a razor blade was used in cutting its tip 5 mm long and the remaining parts discarded. A drop of normal HCl was used to dehydrate and soften its tissue for maceration for 2 minutes. The excess normal HCl was neatly removed with filter paper. A dissecting needle was then used to macerate the root tip after which a drop of acetic orcein stain was placed on the tissue to stain for 15-20 minutes.

After staining the tissue, the specimen on the slide was gently covered with a cover slip, the stain was allowed to spread evenly over the square parts of the cover slip without a bubble. The slide with the specimen was then placed in between two folds of the filter paper and using the blunt end of biro, gentle tapping and pressure was applied around the square area of the cover slip for evenly squashing of the specimen.

Finally, the square edges of the cover slip or squashed slide was sealed with the white transparent nail hardener. This was then viewed under the microscope to observe its mitotic stages and chromosomal aberrations for photomicrographs.

Determination of soil pH

The soil PH was determined following the method of Eckert *et al.*¹² The soil samples were first air dried and 5 g of the air-dried soil was mixed with 5 mL of distilled water and stirred. The mixture was allowed to stand for thirty minutes to allow it to settle. The slurry was decanted into a test tube. A portable pH meter with combine glass and calomel electrode was put into the slurry. The pH meter was standardized with buffer solutions of pH 4.0, 7.0 and 9.2 and the pH read off.

Results

Germination experiment

Table 1 shows the percentage germination of guinea corn under different treatment. Germination of seeds begins 4 days after planting in control and treated seeds. The percentage of seeds germinated varies according to the concentrations of the petroleum products. On the fifth and eighth day of planting, 45% and 85% germination were recorded. In 5% concentration of petrol, 45% germination was recorded five days after treatment, 25% germination

was recorded in 10%. Germination then increased till the eighth day to 50%, 25%, 20% and 15% in pot treated with 5%, 10%, 15% and 20% concentrations respectively while in the control experiment, 85% were recorded eighth day after planting. These values were maintained respectively till the fortieth day. From these values, it was observed that the rate of germination was lower in the treated experiment than in control. It was also observed that with increase in concentration, percentage germination reduced for the treated experiment. For sample treated with 5% spent oil, percentage germination on the fifth day was 15%, 30%, 15% and 5% in sample treated with 5%, 10%, 15% and 20% concentrations of spent oil. In the control experiment the percentage germination was 85% and this was maintained throughout the experiment.

Comparing the rate of germination of seed with the different concentrations of petrol and spent oil, it was discovered that germination was slower in sample treated with spent oil than in petrol (Table 1).

Fresh and dry weight

Table 2 shows the effect of the petrol and spent oil pollutants on fresh weight and dry weight of the seedlings sown in different concentrations of the pollutants and control. The control has the greater value of fresh and dry weight of 3.7 g and 0.43 g respectively with loss of 3.36 g. In 5% petrol treated plant, the fresh weights 0.97 g and the dry weight is 0.20 g with a loss of 0.77 g, there is 0.45 g and 0.26 g fresh weights; 0.06 g and 0.04 g dry weights of plant treated with 15% and 20% petrol respectively. The trend shows a decrease in fresh weight and dry weight with increasing concentration of petrol pollutant. In seeds treated with spent oil pollutants, there is a decrease from 0.97 g of fresh weight to 0.19 g of dry weight with loss of 0.78 g from seed treated with 5% concentration. The seed treated with 10% concentration has high value of fresh weight of 1.53 g, dry weight of 0.20 g with a loss of 1.33 g. The value

Table 1. Percentage germination of seeds of Guinea corn in different concentrations of petrol (in days).

Days after treatment	Control	5% petrol	10% petrol	15% petrol	20% petrol
4	45	25	20	15	10
5	55	35	25	20	15
6	65	35	25	20	15
7	75	40	25	20	15
8	85	50	25	20	15
9	85	55	25	20	15
10	85	60	30	20	15
11	85	60	30	25	20
12	85	60	-	25	20

decreased to 0.80 g fresh weight and 0.11 g of dry weight with loss of 0.69 g in 15% concentration. Twenty percent concentration had a fresh weight value of 0.40 g, 0.05 g dry weight with a loss of 0.35 g.

Growth parameters

Stem length characteristics

Table 3 shows the effect of different concentration of the pollutants on the stem length of the seedlings of guinea corn. The control seedlings were observed to have the highest stem length of 32.50 ± 0.50 cm compared with the 20% concentration of petrol with the lowest mean stem length of 20.33 ± 0.28 cm as observed 40 days after planting. The stem length increased with time (in days) in each treatment concentration while it decreased with increased concentration. Statistical analysis revealed that the treatment effect were highly significant ($P < 0.05$) on the stem length of guinea corn.

Leaf-area characteristics

Table 4 shows the effect of different concentrations of petrol and spent oil pollutants on the leaf area of experimental seedlings of guinea corn. Leaf area increased with time (in days) in each treatment whereas it decreased as the concentration of the pollutant increased except 10% concentration of spent oil whose leaf area is greater than its 5% concentration

as shown in Figure 1. The largest leaf area was observed on the 40th day in the control with a leaf area of 95.83 cm^2 compared with the least leaf area of 16.83 cm^2 in 20% concentration of spent oil. The spent oil had greater effect on the leaf area of plants having the smallest leaf areas were significant ($P < 0.05$) for all treated seeds. It was observed that in petrol pollutant, the mean leaf area decreases as the concentration of treatment increases from control ($95.833.51 \text{ cm}^2$) to (77.80) at 20% concentration as shown in Figure 1A, while in spent oil pollutant, the leaf area increases at 10% concentration even more than the control ($29.33 \pm 0.76 \text{ cm}^2$) and decrease to (16.83 ± 0.57

cm^2) at 20% concentration at 40th day of planting as shown in Figure 1B. It was shown that the mean difference of the spent oil is significant at the 0.05 level ($P < 0.05$).

Mitotic index

The results of the mitotic indices of guinea corn plant are shown in Table 5. This shows the number of dividing cells and the mitotic index of the one thousand cells counted. 35 of the counted cells were found to be dividing in the control with the mitotic index of 3.5. The 5% concentration of petrol has the highest dividing cell with the mitotic index of 2.5. It was observed that the greater the concentration of the petrol pollutant, the

Table 2. The effect of petrol and spent oil pollutants on the fresh and dry weight of guinea corn seedlings.

Concentration	Fresh weight	Dry weight	Difference in weight (weight loss)
Control	3.79	0.43	3.36
5% petrol	0.97	0.20	0.77
10% petrol	0.90	0.11	0.82
15% petrol	0.45	0.06	0.39
20% petrol	0.26	0.04	0.22
5% spent oil	0.97	0.19	0.78
10% spent oil	1.53	0.20	1.33
15% spent oil	0.80	0.11	0.69
20% spent oil	0.40	0.05	0.35

Table 3. Mean of the stem length of Guinea Corn seedlings in petrol and spent oil pollutants.

Days after treatment	Petrol					Spent oil				
	Control	5%	10%	15%	20%	Control	5%	10%	15%	20%
5	4.57±0.40	3.22±8.73	2.92±0.10	2.70±0.17	1.93±0.40	5.53±5.77	4.17±0.20	4.77±0.23	3.07±0.40	2.90±0.65
10	6.40±0.10	5.89±0.19	4.50±0.50	4.17±0.20	3.73±0.20	7.90±0.60	7.10±0.10	7.89±7.63	4.43±0.37	4.07±0.11y
15	10.23±0.25	8.27±0.25	8.07±0.11	7.83±0.35	7.10±0.17	10.80±0.26	9.33±0.28	10.80±0.17	7.47±0.61	7.30±0.43
20	14.50±0.50	10.77±0.25	10.00±0.50	9.50±0.50	8.18±0.27	14.50±0.50	12.67±0.28	16.00±0.50	11.33±0.76	10.33±0.76
25	16.67±5.77	14.17±0.28	13.33±0.76	12.40±0.17	12.50±0.50	18.50±0.50	14.80±0.26	20.17±0.28	14.17±0.28	14.00±0.50
30	21.73±0.25	17.15±0.18	16.27±0.25	15.83±0.28	15.17±0.28	20.50±0.50	17.17±0.28	22.13±0.32	16.17±0.28	15.83±0.28
35	26.33±0.28	20.73±0.40	19.83±0.28	17.83±2.02	18.27±0.25	22.00±0.50	18.47±0.45	25.50±0.50	18.00±0.50	17.57±0.40
40	32.50±0.50	22.60±0.65	21.27±0.75	20.83±0.28	20.33±0.28	24.50±0.50	21.50±0.50	29.33±0.76	20.83±0.28	20.00±0.50

Table 4. Effect of different concentrations of petrol and spent oil on the leaf area of Guinea corn.

Days after treatment	Petrol					Spent oil				
	Control	5%	10%	15%	20%	Control	5%	10%	15%	20%
5	5.70	1.87	1.28	1.10	1.08	4.90	2.47	3.37	1.96	1.85
10	9.18	6.11	5.15	4.73	3.82	5.92	5.93	6.07	5.36	4.68
15	21.50	14.55	9.97	9.73	9.52	9.37	8.89	13.77	8.63	7.37
20	40.50	30.00	25.00	17.83	16.67	11.50	10.65	20.00	10.00	9.50
25	50.50	45.40	37.60	35.50	33.85	13.85	12.00	21.33	11.00	10.67
30	60.50	56.50	51.33	46.17	45.83	15.17	12.83	24.50	12.02	11.18
35	84.83	73.67	70.67	70.33	64.17	18.50	15.50	26.00	15.00	14.33
40	95.83	90.47	89.67	89.47	77.80	20.00	17.33	29.33	17.33	16.83

lower the number of dividing cells and mitotic index. In spent oil pollutant, the number of dividing cells increased in 10% concentration with 2.0 mitotic index and lowest in 20% concentration with 1.1 mitotic index. This shows that the greater the concentration of the pollutants, the lower the mitotic indices and number of dividing cell of guinea corn.

Upper epidermal layer (adaxial)

The micrograph of the upper and lower epidermal layer of guinea corn leaf at different concentration of the pollutant is shown in Figure 2.

Discussion

Toxic effect of petrol and spent oil pollutants were evaluated on germination pattern, stem length, leaf area, root growth, dry and fresh weight. The effect on the internal morphology of the tissues of guinea corn plant and the mitotic indices of guinea corn were also investigated. Germination rate was low in 20% concentration of spent oil during the fifth day of planting of the seeds. It has moderate percentage of germination at 10% concentration of spent oil at day twelve of planting while there

was moderately low percentage germination at 5% concentration of petrol at day twelve of planting. The low rate of germination was probably due to toxicity resulting from pollutant contamination around the seeds.¹³ Low rate of germination agrees with the findings of Dulta and Boissyna,¹⁴ who worked on the effect of paper mill effluent on germination of rice seed and growth behavior of its seedlings discovered that pollutants particularly at higher concentration inhibit germination. Arora and Chauhan,¹⁵ reported in their investigation that the effect of tannery effluent on seed varieties of *Hordeum vulgare* L. showed that the effluent caused a significant reduction in germination percentage.

Stem length decreased with increase in concentration in all seeds treated with the petrol pollutant. This is in accordance with the findings of Ramasubramanian *et al.*¹⁶ who discovered that seedling length of *Phaseolus mungo* grown in sand culture decreased with an increase in concentration of effluents obtained from match dye industries. In spent oil pollutant, the stem length of seeds treated with 10% concentration of spent oil is greater than other and even the control experiment. This is in accordance with the findings of Agbogidi *et al.*¹⁷ who showed that the effect of crude oil pollution on plants is dependent on the level of pollution and that small amounts of minerals oils and oil products may actually be beneficial to plants.

Due to the toxic effect of the pollutant, there was reduction in fresh and dry weight with increase in concentration of both petrol and spent oil, except in seedlings treated with 10% spent oil which experiences an increase in dry weight and wet weight due to nutrient accumulation at that concentration. At high concentration of the pollutants, there was low fresh and dry weight of the seedlings. This is in agreement with that of Ramasubramanian *et al.*,¹⁶ who showed that there was a decrease in plant dry weight at high concentration of industrial effluent. Arora Rajini *et al.*¹⁵ also observed a significant reduction in the total biomass in almost all the varieties of *Hadeum vulgare* L.

The micrograph of the internal anatomy of the upper and lower epidermal layers shows the effect of the pollutant at various concentration on the arrangement of the epidermal cells. The higher concentration of the pollutants is responsible for the broken and scattered epidermal cells and smaller sizes of the stomata. The effect of petrol and spent oil on the mitotic indices of guinea corn shows that the mitotic index is high at low concentration of petrol and it is a little higher in 10% concentration spent oil. This shows that a high concentration of petrol pollutant affect the growth of the root and thereby affecting the mitotic index of the plant.

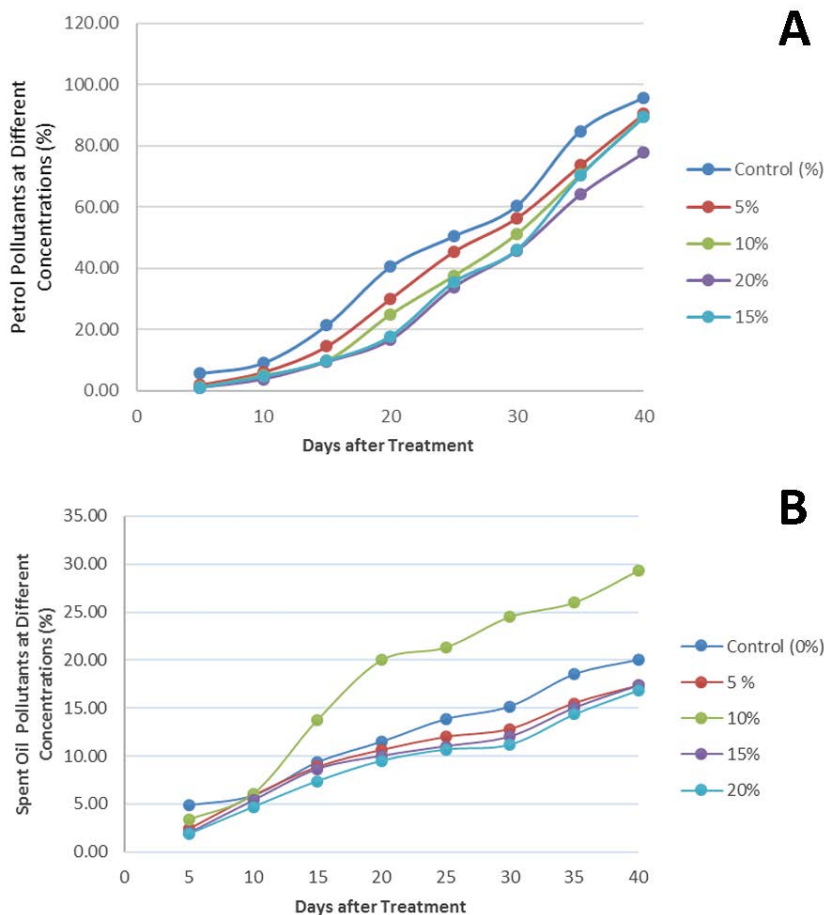


Figure 1. Graph of A) petrol pollutant and B) spent oil against days after treatment.

Table 5. Effect of petroleum products on the mitotic indices of Guinea corn.

	Control	5%	10%	15%	20%
Petrol					
No of cells counted	1000	1000	1000	1000	1000
No of dividing cells	35	25	24	19	12
Mitotic index	3.5	2.5	2.4	1.9	1.2
Spent oil					
No of cells counted	1000	1000	1000	1000	1000
No of dividing cells	35	19	20	14	11
Mitotic index	3.5	1.9	2.0	1.4	1.1

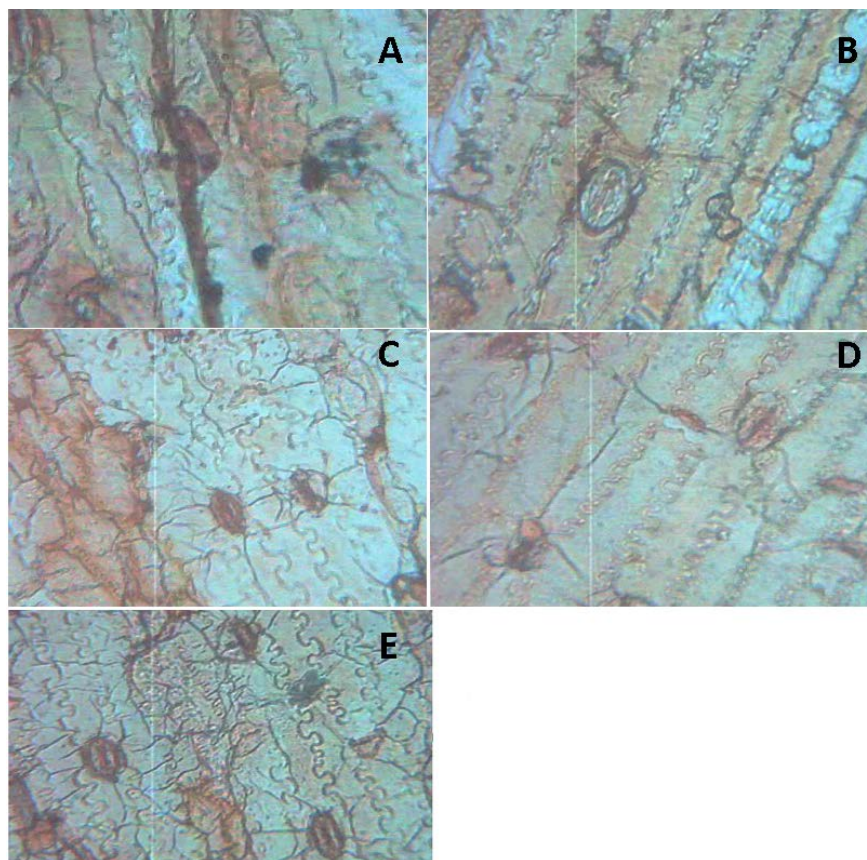


Figure 2. A) Upper epidermal layer guinea corn leaf exposed to 5% petrol; B) upper epidermal layer guinea corn leaf exposed to 10% petrol; C) Upper epidermal layer of guinea corn leaf unexposed (control); D) upper epidermal layer guinea corn leaf exposed to 20% petrol; E) upper epidermal (Adaxial) layer guinea corn leaf exposed to 20% spent oil.

Conclusions

This study revealed that petroleum pollutant adversely affected germination, growth and development of guinea corn. The damage done to the plant at higher concentration of the pollutant is more severe than at a lower concentration. However, petroleum products like spent oil can provide nutrition necessary for growth and yield of plant at low concentration. The petrol and spent oil pollutants affected the internal anatomy of the upper and lower epidermal layer of guinea corn leaf. The higher concentration of the pollutants is responsible for the broken and scattered epidermal cells and smaller sizes of the stomata. The high concentration of the pollutants also affected the growth of the root and thereby affecting the mitotic index of the plant.

This result clearly presents the effect of petrol and spent oil on the growth of Guinea

Corn; values recorded are representative of environmental responses of this plant to similar environmental stress and can be used as references in similar study.

References

1. Lastmer SD, Darall MS, Thomas CD, Ellgaard EG. Dendo chronology and heavy metal deposition in tree rings. *J Environ Qual* 1996;25:1411-9.
2. Bragg DC, ed. *Oil spill simulation 2nd International Oil Spill Research and Development forum*, London; 1995.
3. Davies MS. Effects of toxic concentration of metals on the root growth and development. In: Alkinson D, ed. *Plant root growth*. London: Blackwell; 1991. pp 211-227.
4. Bala R, Setia RC. *Some aspect of Lead toxicity in plants*. New Dehli: Narendia Publishing House; 1990.
5. Leighton FA. Petroleum oils and wildlife. 2000. Available from: http://fr.cwhc-rcsf.ca/wildlife_health_topics/oil.htm
6. Cox PE, Christensen JC, McGrath SP. Speciation of cadmium and zinc with application to soil solution. *J Environ Qual* 1995;24:183-90.
7. Gallagher D, ed. *Current status of the environmental health program. Second international oil spill research and developmental forum*. 23-26 May 1995, London.
8. Adam G, Gamoh K, Morris DG, Duncan H. Effect of alcohol addition on the movement of petroleum hydrocarbon fuels in soil. *Sci Total Environ* 2002;286:15-25.
9. Edwards NT. Polycyclic aromatic hydrocarbons (PAH) in the terrestrial environment. A review. *J Environ Qual* 1983;12:427-41.
10. Wyszowski M, Wyszowska J, Ziokowska A. Effect of soil contamination with diesel oil on yellow lupine yield and macro-element content. *Plant, Soil Environment* 2004;50:218-26.
11. Percy R, Ehleringer J, Mooney H, Rundel P. *Plant physiological ecology: methods and instrumentation*. London: Chapman and Hall; 1989.
12. Eckert D, Sins TJ. Recommended soil pH and lime requirement tests recommended soil testing procedures for the Northeastern United States. p. 11-16. In Sims JT, Wolf A (eds.). *Recommended soil testing procedures for the Northeastern United States*. Northeast Regional Bulletin #493. Agricultural Experiment Station, University of Delaware, Newark, USA.
13. Komolafe RJ. Effect of petrol and spent oil on the growth of Guinea corn (*Sorghum bicolor* L.) Lagos: University of Lagos; 2009.
14. Duita SK, Boissyna CL. Effect of paper mill effluents on germination of rice seed (*Oryza sativa* L. Var. masuri) and growth behaviour of its seedling. *J Industrial Pollut Control* 1997;13:41-7.
15. Arora R, Chauhan S. Effect of tannery effluent on seed germination and total biomass in some varieties of *Hordeum vulgare* L. *Acta Ecologica* 1996;18:112-55.
16. Ramasubramanian S. Analysis of industrial effluent and their impact on the growth and metabolism of *Phaseola mungo* L. *Commun Soil Sci Plant Analysis* 1993;24:2241-9.
17. Agbogidi OM, Eruotor PG, Akparobi SO. Effect of time of application of crude oil to soil on the Growth of maize (*Zea mays*). *Res J Environ Toxicol* 2007;1:116-23.

Phyllosphere and carposphere bacterial communities in olive plants subjected to different cultural practices

Silvia Pascazio,¹ Carmine Crechchio,¹
Patrizia Ricciuti,¹ Assunta Maria Palese,²
Cristos Xiloyannis,² Adriano Sofo³

¹Department of Soil, Plant and Food Sciences, University of Bari, Aldo Moro;

²Department of European and Mediterranean Cultures: Architecture, Environment and Cultural Heritage, Basilicata University, Matera; ³School of Agricultural, Forestry, Food and Environmental Sciences, Basilicata University, Potenza, Italy

Abstract

The aim of this study was to characterize phyllosphere and carposphere bacterial communities of olive trees subjected for 13 years to two different soil management systems (sustainable and conventional) in a mature olive grove located in Southern Italy. Amplified DNA fragments of the 16S ribosomal RNA eubacterial gene (16S *rRNA*) of bacteria living on leaf and fruit surface, and in fruit pulp were analyzed by denaturing gradient gel electrophoresis (DGGE). A clone library of 16S *rRNA* amplicons extracted from the bacteria living in pulp homogenates and a phylogenetic analysis was performed. Generally, the DGGE patterns of the bacteria from both the treatments clustered separately. The medium-term sustainable orchard management resulted in a higher number of bacterial species from olive fruit pulp. Phyllosphere and carposphere communities evaluated by DGGE were affected by the type of the agricultural practices adopted. A better understanding of phyllosphere and carposphere microbiota of cultivated olive plants could be useful for the promotion of plant growth, a better plant protection and a higher crop quality.

Introduction

Leaf, flower and fruit represent a substantial multiple of the soil and plant surface area and often have complex topographical features on which microbial colonization can occur.^{1,2} The potential population size of microorganisms associated to these three additional surfaces can be impressive, exceeding by 100 to 1000 times that of soil.^{3,4} The aerial habitat part of

plants for microorganisms, namely phyllosphere for leaves and carposphere for fruits, is normally colonized by a variety of bacteria, yeasts and fungi. Bacteria are by far the most numerous colonists, often being found at levels of 10^6 – 10^7 cells cm^{-2} of leaf surface.⁴ Phyllosphere and carposphere are unique and dynamic habitats, with microbial communities subjected to irregular, and sometimes relatively large changes in temperature, UV radiation, relative humidity, nutrient availability upon the plant surface, and leaf wetness.^{5,6} Despite these environmental constraints, microorganisms flourish on both leaf and fruit surfaces, where they can also protect their hosts from disease or promote growth.^{3,6}

Leaf surface topography and nutrients are generally recognized as important regulators of phyllosphere microbial communities. Much of the interest in phyllosphere and carposphere microbiology has been driven by the need of better understanding the behavior and control of plant pathogens and the factors affecting food quality and safety.^{2,3} Phyllosphere microorganisms often also have a direct positive influence on plants, altering plant surface properties, enhancing nitrogen fixation, and promoting the growth of plants, the control of plant pathogens, and the degradation of organic pollutants.^{1,4}

In semi-arid Mediterranean agricultural areas, soil degradation and water shortage phenomena are frequent and can have a strong negative impact on the agro-ecosystems and on food products.⁷ Thus, the adoption of sustainable soil and plant management practices, such as minimum tillage or no-till, recycling of locally derived organic matter and adequate irrigation, are urgently required to save water, restore soil organic matter, and reduce erosion and environmental pollution.⁸ In olive groves, the positive influence of sustainable management systems on soil microbiota has been described in the last decade.^{9–11} While the ecology of epiphyte microorganisms is both of scientific and economic importance, little research has been done on the changes phyllosphere and carposphere microbiota in response to the adoption of different cultural practices. On this basis, the aim of this study was to characterize phyllosphere and carposphere bacterial communities in olive trees subjected for a medium term (13 years) to two different orchard management systems, namely sustainable (S) and conventional (C), by using a combination of different culture-independent techniques including 16S *rRNA* fingerprinting and cloning. On the basis of previous researches on soil microbiota carried out in the same system,^{8,11} we hypothesize that a sustainable soil and plant management could significantly affect the bacterial community composition of olive phyllosphere and carposphere.

Correspondence: Adriano Sofo, School of Agricultural, Forestry, Food and Environmental Sciences, Basilicata University, Viale dell'Ateneo Lucano 10, 85100 Potenza, Italy.
Tel.: +39.0971.206228.
E-mail: adriano.sofa@unibas.it

Key words: Bacterial diversity; carposphere; endophytic bacteria; *Olea europaea* L.; phyllosphere; sustainable soil management.

Contributions: SP, 16S *rRNA* fingerprinting; CC, fruit and leaf sampling and DNA extraction; PR, 16S *rRNA* amplicons cloning and phylogenetic analysis; AMP, plant management; CX, soil management; AS, manuscript writing and statistical analysis.

Conflict of interest: the authors declare no potential conflict of interest.

Received for publication: 13 May 2015.

Revision received: 28 May 2015.

Accepted for publication: 28 May 2015.

This work is licensed under a Creative Commons Attribution NonCommercial 3.0 License (CC BY-NC 3.0).

©Copyright et al., 2015
Licensee PAGEPress srl, Italy
International Journal of Plant Biology 2015; 6:6011
doi:10.4081/pb.2015.6011

Materials and Methods

Experimental site and olive orchard management

The trial was carried out in 2013 in a 2-ha mature (>50 years) olive grove located in Southern Italy (Ferrandina, Basilicata Region, Italy; 40°29' N, 16°28' E). Trees belonged to *Maiatica* cultivar, an autochthonous olive variety for production of both table olives and olive oil, were vase-trained and planted at a distance of 8×8 m. The climate in the area is semi-arid, with an annual precipitation of 574.1 mm (mean 1976–2009) which falls mostly in the winter; the mean annual temperature ranges from 15 to 17°C. The soil of the experimental grove is a sandy loam, a Haplic Calcisol with a mean bulk density of 1.5 t m⁻³. The top 60 cm of the soil had an average pH (\pm standard deviation) of 7.4 \pm 0.4, an organic carbon content of 7.0 \pm 3.8 g kg⁻¹, a total nitrogen content of 0.8 \pm 0.2 g kg⁻¹ (Kjeldahl method), and extractable phosphorus (Olsen method) and potassium of 11.7 \pm 5.9 and 104 \pm 70 mg kg⁻¹, respectively.

In 2000, the olive orchard was divided into two 1-ha plots managed according to different orchard management systems: a sustainable (S) treatment and a conventional (C) treatment. The S treatment was irrigated with

municipal wastewater treated by a pilot unit, as described by other authors.^{7,12} The reclaimed wastewater was generally distributed from May to October by drip irrigation (6 self-compensating drippers per tree, each delivering 8 L h⁻¹). The annual irrigation volume was around 300 mm. In the S treatment, soil was totally and permanently covered by spontaneous self-seeding weeds (mainly graminaceous and leguminosae) which were mowed at least twice a year and residues were left on the ground as mulch. Olive trees were pruned lightly each year, in order to improve fruiting potential by controlling the amount of fruiting wood and enhancing flower bud differentiation. Similarly to herbaceous residues, pruning residues (4.4 t ha⁻¹ yr⁻¹ organic carbon) were shredded and then left on the ground as mulch. The average amounts of mineral elements yearly distributed by the wastewater used for irrigation were around 60 kg ha⁻¹ for N and K and 3 kg ha⁻¹ for P.⁷ An integrative amount of N (40 kg ha⁻¹ year⁻¹) was distributed by fertirrigation, in order to entirely satisfy the annual N plant needs, taking into account wastewater and soil chemical composition, and mineral element balance in the orchard system (cover crops and pruning material contributions, amount of fruit removed from the olive grove). Pest and disease control was performed according to the regional service recommendations for commercial olive groves.^{7,13} The olives from the C treatment were grown under rainfed conditions and managed according to the traditional and horticultural practices of the area usually adopted by the farmers,¹³ that is: tillage (milling at 10 cm depth) performed 2-3 times per year to control weeds; empirical soil fertilization carried out in early spring using ternary compounds (NPK 20-10-10 fertilizer at doses ranging from 300 to 500 kg ha⁻¹), without considering the plant needs and their partitioning along the various phenological phases of the annual vegetative cycle; and severe pruning carried out every two years, with pruned residues removed from the olive orchard. After 13 year of different management, the S practices resulted in an increase of soil organic carbon in the 0-10 cm soil layer up to 22.1 g kg⁻¹, compared to 11.8 g kg⁻¹ of the C treatment.

Leaf and fruit collection and sample preparation

In November 2013, leaves and olive fruits were collected in both the treatments (S and C). For each treatment, two composite leaf and fruit samples were randomly collected using sterile gloves and equipment from plants located at the central part of each plot, in order to avoid border interferences. Fully expanded leaves and well-developed fruits selected from each plant along the median segment of new-growth shoots, with similar light exposition

and position in the canopy, were chosen. Leaf samples, placed at approximately 1.0 m from the drippers (for the S treatment) and at 1.5 m from the ground, were collected. Leaf and fruit samples were stored immediately at 4°C in sterilized plastic pots before analysis. In order to desorb bacteria from leaf (leaf; L) and fruit surface (pericarp; P), the method of Redford and Fierer was used,¹⁴ starting from 40 leaves (L) or 20 olives (P), respectively. In order to extract bacteria from fruit pulp (mesocarp; M), the same 20 olives were homogenized with 40 ml of sterilized Ringer solution, and the homogenate was then filtered under sterile conditions. The wash solution and the filtrate were centrifuged at 4000 rpm for 10 min at 4°C. The supernatant was discarded, and the resulting pellet was used for DNA extraction.

DNA extraction

DNA was extracted from 0.50 g of pellet using the FastDNA® SPIN Kit for soil in combination with the Thermo Savant FastPrep® System homogenizer (MP Biomedicals LLC, Cleveland, OH, USA). The yield and fragmentation of the DNA were checked by agarose gel electrophoresis (0.7% w/v agarose-0.5 xTris-Borate-EDTA) and UV visualization of the stained gels Gel Red™ (Biotium, Inc., Hayward, CA, USA). The quality and concentration of DNA extracts were determined by spectrophotometric measurement at 260, 280 and 230 nm using a NanoDrop®ND-1000 UV-Vis spectrophotometer (Thermo Fisher Scientific, Inc., Waltham, MA, USA).

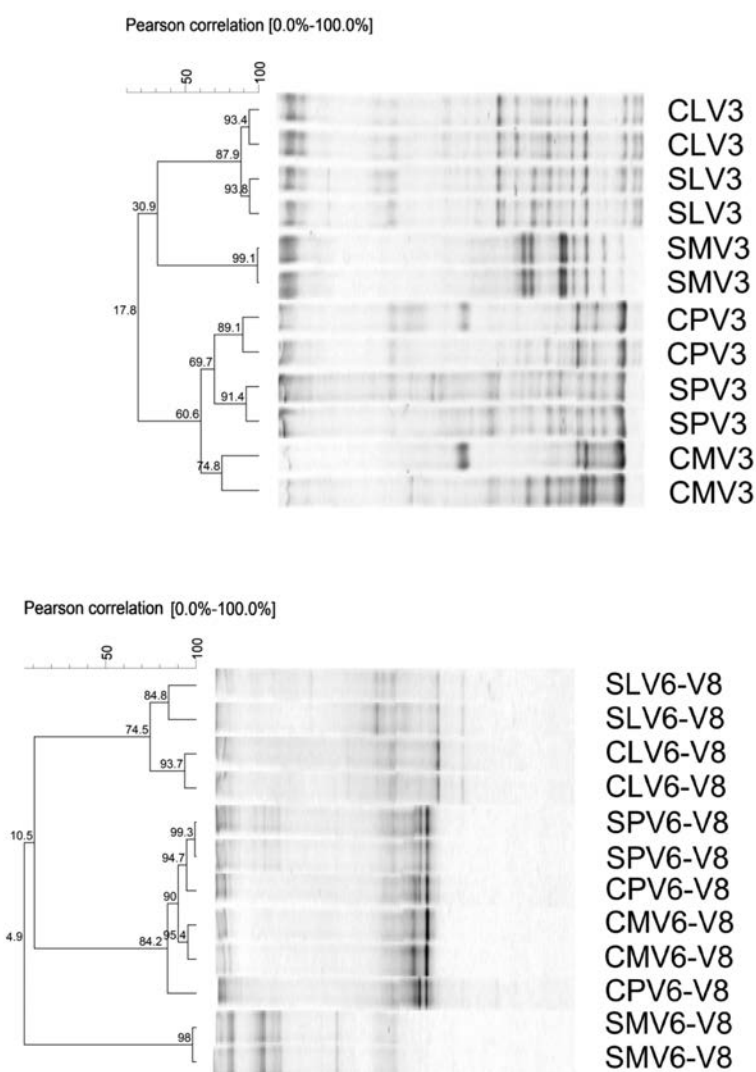


Figure 1. 16S denaturing gradient gel electrophoresis fingerprints ($n=2$) of phyllosphere and carposphere bacterial communities of olive plants based on the amplification of the V3 region (A) and V6-V8 region (B) of the small subunit *rRNA* eubacterial gene. Clustering was carried out using the UPGMA method based on the Pearson correlation coefficient. S: sustainable, C: conventional, L: leaf surface, P: pericarp surface, M: mesocarp.

16S rRNA fingerprinting by PCR-DGGE

DNA fragments in the V3 and V6-V8 regions of the 16S ribosomal RNA eubacterial gene (16S *rRNA*) were amplified by using the primer sets F357-R518 and 968F-1401R,^{15,16} respectively. For separating the 16S *rRNA* bacterial communities in a DGGE gel, a GC clamp was added at the end of the primer F357 and 968F. Each PCR mixture contained 50 pmol of

each primer, 10 nmol of each 2'-deoxynucleoside 5'-triphosphate, 3U of Taq DNA polymerase (EuroTaq; EuroClone, Milan, Italy), 2.5 mM MgCl₂, and 20-40 ng of template DNA. All PCR amplifications were performed using a MyCycler™ thermal cycler (Bio-Rad Laboratories, Inc., Hercules, CA, USA). Amplification products were checked by electrophoresis on 1.5 % (w/v) agarose gels.

PCR products were then loaded onto dena-

turing gradients. The region V3 and V6-V8 regions, were separated, respectively, in a 8% and 6% (w/v) polyacrylamide gels (acrylamide *N,N'*-methylenebisacrylamide, w/w, 37.5:1) in 1× TAE buffer with a linear chemical denaturing gradient ranging from 25-50% and 45-60% denaturant, respectively. Electrophoresis was carried out at 60°C for 10 min at 20V and then for 3 h at 200 V for the V3 region, and for 15h at 75V for the V6-V8 region, using the method

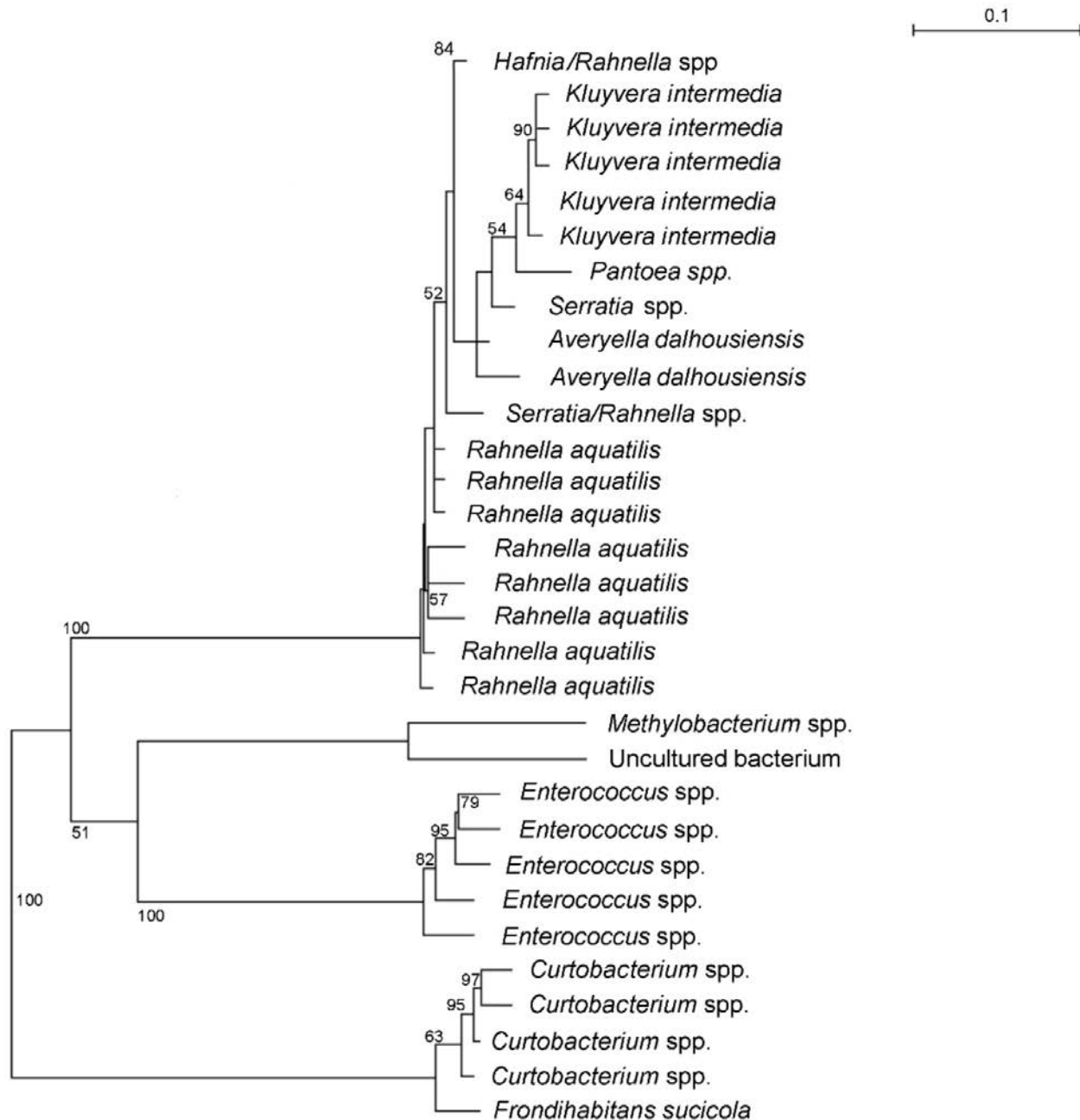


Figure 2. Phylogenetic tree of 16S *rRNA* sequences of bacteria isolated from olive mesocarp of the sustainable treatment. Clustering was carried out using the maximum likelihood method. The branches are scaled in terms of the expected number of substitutions per site (scale bar=0.1 substitutions per nucleotide position). Numbers adjacent to the branches are support values from 100 ML bootstrap replicates. Bootstrap values ≥ 50 are shown.

of Crecchio *et al.*¹⁷ DGGE profiles comparison and bacterial phylogenetic tree were constructed using the BioNumerics software (version 4.5; Applied Maths, Sint-Martens-Latem, Belgium) by the unweighted pair-group method with the arithmetic average clustering algorithm (UPGMA) based on the Pearson product-moment correlation coefficient (*r*).

16S rRNA amplicons cloning and phylogenetic analysis

A clone library was constructed using DNA extracted from fruit homogenates. The total region 16S *rRNA* was amplified with the universal primer for bacteria 8L-1513R.¹⁸ The clone library was generated by ligating PCR products into the pGEM-T (Promega; Madison, WI, USA), which were then transformed into competent *Escherichia coli* JM109 cells. A number of 100 clones from mesocarp of the sustainable treatment and from the mesocarp of the conventional treatment, containing the insert of the correct size were sequenced (Primm Biotech, Inc., Milano, Italy) for both strands with the primer 357F-1401R.¹⁹ The resultant sequences were aligned to the NCBI database using BLASTn (NCBI BLAST®; National Center for Biotechnology Information, Bethesda, MD, USA). These sequences were aligned separately or as a concatenated matrix using the multiple sequence alignment software ClustalW2 (EMBL-EBI, European Bioinformatics Institute, Cambridge, UK). Phylogenetic trees were carried out using a multiplatform graphical user interface for sequence alignment and phylogenetic tree building (SeaView, version 4) using the maximum likelihood (ML) method.²⁰

Results and Discussion

In our work, the bacterial communities of

the phyllosphere of the S treatment (SLV3) were discriminated from the patterns of the phyllosphere of the C treatment (CLV3), with a Pearson similarity coefficient of 87.9% (Figure 1A). The DGGE patterns of the bacteria of pericarp surface (SPV3 and CPV3) highlighted a clear separation between sustainable (S) and conventional (C) treatments and clustered separately at a lower value of similarity (69.7%), compared to phyllosphere (Figure 1A). The DGGE fingerprints showed a clear discrimination between S and C sites for mesocarp bacteria, with a Pearson similarity coefficient of only 17.8% (Figure 1A). The DGGE dendrogram of bacterial 16S DGGE fingerprint based on the amplification of the V6-V8 region paralleled that obtained by the amplification of the V3 region, evidencing that the S treatment clustered separately from the C treatment for phyllosphere, pericarp surface and mesocarp bacteria, with Pearson similarity coefficient values 74.5, 84.2 and 4.9%, respectively (Figure 1B). DGGE was successfully used to evaluate the influence of various plant genotypes, and the inoculation of the nitrogen-fixing bacterium *Azospirillum brasilense* upon the epiphyte community of tomato phyllosphere.²¹ Such DGGE-based methods for studying phyllosphere microbial communities also included quantitative PCR to estimate the abundance of specific bacterial taxa on a plant, *rRNA* gene amplicon pyrosequencing to assess fungal and bacterial abundance/diversity on tree foliage, and proteogenomics to uncover the most abundantly expressed genes in the phyllosphere environment.¹

The electrophoretic profiles relative to both V3 and V6-V8 regions of 16S *rRNA* showed that the bacterial communities of fruit mesocarp of both S and C treatments clustered at higher values of Pearson correlation coefficient, compared to those of fruit or leaf surfaces (Figure 1). On this basis, we decided to study in detail the bacteria present in olive mesocarp. The

classification of the bacterial groups isolated from olive fruit pulp (mesocarp) and the corresponding phylogenetic analysis are reported in Table 1 and Figure 2, respectively. Sequence homology search for the bacteria living in mesocarp of the sustainable treatment revealed 70 sequences of olive chloroplast genome and 30 belonging to bacterial genomes. For the mesocarp bacteria of C treatment, most of the sequences (98) derived from olive chloroplasts and only two belonged to bacterial genomes. The results showed that the DNA sequences (identity $\geq 97\%$) of the bacteria isolated from olive mesocarp belonged to the phyla the Proteobacteria, Actinobacteria, Firmicutes, with sequences of Proteobacteria being the most abundant (20 and 2 species in S and C, respectively) (Table 1). The data on the bacterial groups isolated from olive fruit pulp (mesocarp), identified on the basis of their genomic sequences (Table 1 and Figure 2), reflected the results found by other authors on phyllosphere bacteria of tree species of temperate and tropical regions,¹⁴ and of herbaceous species.⁵ In our experiment, the most abundant bacteria belonged to the family Enterobacteriaceae (19 and 2 species in S and C, respectively) (Table 1). This result is not surprising, considering their massive presence on the aerial surfaces of plants and within healthy plant tissues and seeds.⁶ Interestingly, insects can play an important role in the composition of plant-associated bacterial communities. For instance, many species of plant bacteria uses flies or other insects as vectors,²² even if it is not always clear if bacterial strains found in the insect digestive tract originate from plants (as for *Serratia* spp.) or it is the opposite (as for *Enterococcus* spp.).^{23,24} Leff and Fierer demonstrated,⁶ by 16S *rRNA* pyrosequencing that some fruits and vegetables harbored different bacterial communities. Some products showed a higher number of bacteria belonging to the family Enterobacteriaceae, while some other

Table 1. Classification of the bacterial species from olive fruit pulp (mesocarp) identified on the basis of their genomic sequences (NCBI BLAST® hits).

N. species	Phylum	Class	Order	Family	Genus	Species
Sustainable						
8	Proteobacteria	γ -Proteobacteria	Enterobacteriales	Enterobacteriaceae	<i>Rahnella</i>	aquatilis
5	Firmicutes	Bacilli	Lactobacillales	Enterococcaceae	<i>Enterococcus</i>	unknown
5	Proteobacteria	γ -Proteobacteria	Enterobacteriales	Enterobacteriaceae	<i>Kluyvera</i>	intermedia
4	Actinobacteria	Actinobacteridae	Actinomycetales	Microbacteriaceae	<i>Curtobacterium</i>	unknown
2	Proteobacteria	γ -Proteobacteria	Enterobacteriales	Enterobacteriaceae	<i>Averyella</i>	dalhousiens
1	Actinobacteria	Actinobacteridae	Actinomycetales	Microbacteriaceae	<i>Fronthabitans</i>	suicicola
1	Proteobacteria	γ -Proteobacteria	Enterobacteriales	Enterobacteriaceae	<i>Hafnia/Rahnella</i>	alvei
1	Proteobacteria	α -Proteobacteria	Rhizobiales	Methylobacteriaceae	<i>Methylobacterium</i>	unknown
1	Proteobacteria	γ -Proteobacteria	Enterobacteriales	Enterobacteriaceae	<i>Pantoea</i>	unknown
1	Proteobacteria	γ -Proteobacteria	Enterobacteriales	Enterobacteriaceae	<i>Serratia/Rahnella</i>	unknown
1	Proteobacteria	γ -Proteobacteria	Enterobacteriales	Enterobacteriaceae	<i>Serratia</i>	unknown
Conventional						
2	Proteobacteria	γ -Proteobacteria	Enterobacteriales	Enterobacteriaceae	<i>Pantoea</i>	agglomerans

products had higher abundance of Actinobacteria, Bacteroidetes, Firmicutes, and Proteobacteria phyla. They also stated that conventionally and organically farmed varieties could contribute to the variations in the bacterial communities. Unfortunately, these authors did not sample plant material directly from the field, following all the steps of production and deeply monitoring soil and plant management, but they studied the commercial product found on the market, that were likely affected by other variable, such as storage type and time.

Given that large volumes of water are needed for irrigation in tree crops, water demand cannot always be met with the available potable water. The type of irrigation system can influence the risk of crop contamination: overhead irrigation, for instance, usually causes more microbial contamination than furrow and drip irrigation.²⁵ In our case, this risk was avoided, as the bacterial species found in the S treatment (Table 1 and Figure 2) were completely different from those monitored and found at very low concentrations by Palese *et al.*⁷ (total coliforms, fecal coliforms, *Escherichia coli*, and *Salmonella* spp.) in the same system. Therefore, the risk of soil contamination in S treatment by such bacteria deriving from wastewater, that then eventually translates into fruit contamination, can be considered negligible.^{7,12}

Conclusions

Our results demonstrated that a medium-term sustainable orchard management determined a higher number of bacterial species from olive fruit pulp (mesocarp), identified on the basis of their genomic sequences. Moreover, phyllosphere and carposphere communities evaluated by DGGE were altered by the application of the two different agricultural practices. A better understanding of epiphytic and endophytic microbiota of cultivated olive plants grown under different agronomic systems could be useful for the promotion of plant growth, a better plant protection and a higher crop quality.

References

- Meyer KM, Leveau HHJ. Microbiology of the phyllosphere: a playground for testing ecological concepts. *Oecologia* 2012;168:621-9.
- Vorholt JA. Microbial life in the phyllosphere. *Nat Rev Microb* 2012;10:828-40.
- Lindow SE, Brandl MT. Microbiology of the phyllosphere. *Appl Environ Microb* 2003;69:1875-83.
- Xie WY, Su JQ, Zhu YG. Phyllosphere bacterial community of floating macrophytes in paddy soil environments as revealed by illumina high-throughput sequencing. *Appl Environ Microb* 2015;81:522-53.
- Delmotte N, Knief C, Chaffron S, et al. Community proteogenomics reveals insights into the physiology of phyllosphere bacteria. *Proc Natl Acad Sci USA* 2009;26:16428-33.
- Leff JW, Fierer N. Bacterial communities associated with the surfaces of fresh fruits and vegetables. *PLoS One* 2013;8:e59310.
- Palese AM, Pasquale V, Celano G, et al. Irrigation of olive groves in Southern Italy with treated municipal wastewater: effects on microbiological quality of soil and fruits. *Agric Ecosyst Environ* 2009;129:43-51.
- Sofo A, Ciarfaglia A, Scopa A, et al. Soil microbial diversity and activity in a Mediterranean olive orchard managed by a set of sustainable agricultural practices. *Soil Use Manage* 2014;30:160-7.
- Benitez E, Nogales R, Campos M, et al. Biochemical variability of olive-orchard soils under different management systems. *Appl Soil Ecol* 2006;32:221-31.
- Moreno B, Garcia-Rodriguez S, Cañizares R, et al. Rainfed olive farming in southeastern Spain: long-term effect of soil management on biological indicators of soil quality. *Agric Ecosyst Environ* 2009;131:333-9.
- Sofo A, Palese AM, Casacchia T, et al. Genetic, functional, and metabolic responses of soil microbiota in a sustainable olive orchard. *Soil Sci* 2010;175:81-8.
- Lopez A, Pollice A, Lonigro A, et al. Agricultural wastewater reuse in Southern Italy. *Desalination* 2006;187:323-34.
- Xiloyannis C, Martinez Raya A, Kosmas C, et al. Semi-intensive olive orchards on sloping land: requiring good land husbandry for future development. *J Environ Manage* 2008;89:110-9.
- Redford AJ, Fierer N. Bacterial succession on the leaf surface: a novel system for studying successional dynamics. *Microb Ecol* 2009;58:189-98.
- Temmerman R, Scheirlinck I, Huys G, et al. Culture-independent analysis of probiotic products by denaturing gradient gel electrophoresis. *Appl Environ Microb* 2003;69:220-6.
- Heuer H, Smalla K. Application of denaturing gradient gel electrophoresis and temperature gradient gel electrophoresis for studying soil microbial communities. In: van Elsas JD, Wellington EMH, eds. *Modern soil microbiology*. New York: Marcel Dekker, 1997. pp 353-273.
- Crecchio C, Curci M, Mininni R, et al. Short-term effects of municipal solid waste compost amendments on soil carbon and nitrogen content, some enzyme activities and genetic diversity. *Biol Fert Soils* 2001;34:311-8.
- Wang GCY, Wang Y. Frequency of formation of chimeric molecules as a consequence of PCR coamplification of 16S rRNA genes from mixed bacterial genomes. *Appl Environ Microb* 1997;63:4645-50.
- Yu Z, Morrison M. Comparisons of different hypervariable regions of rrs genes for use in fingerprinting of microbial communities by PCR-denaturing gradient gel electrophoresis. *Appl Environ Microb* 2004;70:4800-6.
- Gouy M, Guindon S, Gascuel O. SeaView Version 4: a multiplatform graphical user interface for sequence alignment and phylogenetic tree building. *Mol Biol Evol* 2010;27:221-4.
- Correa OS, Romero AM, Montecchia MS, et al. Tomato genotype and *Azospirillum* inoculation modulate the changes in bacterial communities associated with roots and leaves. *J Appl Microb* 2007;201:781-6.
- Kuzina LV, Peloquin JJ, Vacek DC, et al. Isolation and identification of bacteria associated with adult laboratory Mexican fruit flies, *Anastrephaludens* (Diptera: Tephritidae). *Curr Microb* 2001;42:290-4.
- Devriese L, Baele M, Butaye P. The Genus *Enterococcus*: taxonomy. *Prokaryotes* 2006;4:163-74.
- Kado CI. *Erwinia* and related genera. *Prokaryotes* 2006;6:443-50.
- Telias A, White JR, Pahl DM, et al. Bacterial community diversity and variation in spray water sources and the tomato fruit surface. *BMC Microbiol* 2011;11:81.

Constitutive expression of the barley dehydrin gene *aba2* enhances *Arabidopsis* germination in response to salt stress

Cristina Calestani,^{1,3} Meena S. Moses,^{1,4} Elena Maestri,² Nelson Marmioli,² Elizabeth A. Bray¹

¹Department of Botany and Plant Sciences, University of California, Riverside, CA, USA; ²Department of Biosciences, University of Parma, Italy; ³Department of Biology, Valdosta State University, GA, USA; ⁴EMD Millipore Corporation, Temecula, CA, USA

Abstract

Dehydrins (DHNs) are a sub-family of the late embryogenesis abundant proteins generally induced during development of desiccation tolerance in seeds and water deficit or salinity stress in plants. Nevertheless, a detailed understanding of the DHNs function is still lacking. In this work we investigated the possible protective role during salt stress of a *Dhn* from *Hordeum vulgare* (L.), *aba2*. The coding sequence of the *aba2* gene was constitutively expressed in transgenic lines of *Arabidopsis thaliana* (L.). During salt stress conditions germination rate, cotyledon expansion and greening were greatly improved in the transgenic lines as compared to the wild type. Between 98 and 100% of the transgenic seeds germinated after two weeks in media containing up to 250 mM NaCl, and 90% after 22 days at 300 mM NaCl. In conditions of 200 mM NaCl 93% of the transgenic cotyledons had greened after two weeks, outperforming the wild type by 45%. Our study provides further evidence that DHNs have an important role in salt stress tolerance. The production of plants constitutively expressing DHNs could be an effective strategy to improve plant breeding programs.

Introduction

Salinity stress can impact plant growth and development at all stages of the plant life cycle.

Plants respond to abiotic stress in many ways that are controlled by complex regulatory processes functioning at cellular and whole-plant levels, which are still not completely understood. A major response is the change in gene expression and synthesis of different types of proteins like those encoded by dehydrins (DHNs), a sub-family of group 2 Late

Embryogenesis Abundant (LEA D-11).¹⁻³ DHNs are a distinct group of proteins, which may accumulate up to 1% of total soluble proteins in mature embryos and in response to stresses involving cellular dehydration.¹⁻³

DHNs are conserved proteins, being identified from higher to lower plants. Presently, public databases contain over 4300 deduced amino acid sequences encoding DHNs (<http://www.ncbi.nlm.nih.gov/protein/?term=ddehytrin>). Recently, DHNs have also been identified in animal taxa such as rotifers, tardigrades, insects and nematodes.⁴ The molecular weights of DHNs vary within a broad range from 9 to 200 kDa.^{5,3} DHNs have been classified into different sub-groups based on their amino acid composition and domain architecture.^{1,5-8} Typically DHNs have one to 11 copies of a highly conserved domain of 15 amino acids, called the K segment.^{5,3} The K segment is predicted to form an amphipathic α -helix and it is required for binding to anionic phospholipid membranes, supporting the hypothesis that DHNs stabilize cell membranes during dehydration.^{5,9-11} Many DHNs have a tract of serine residues, called the S-segment,⁵ which has been proposed to be a site of protein activity regulation through phosphorylation.¹²⁻¹⁵ Another conserved domain, the Y-segment, is located near the N-terminus of several DHNs.^{5,3} Previous studies suggests that the Y-segment has a role in the protection from desiccation and salt stress.¹⁶

Although much is known about dehydrin gene structure and expression patterns, their function has not been completely elucidated.^{2,11} Data obtained through different methods of investigation support the hypothesis that DHNs protect the cell from osmotic and ionic stress. First, LEA protein accumulation correlates with the development of desiccation tolerance of seeds,¹⁷⁻²⁰ and also occurs during periods of environmental stress in vegetative parts of the plant.²¹ Second, a greater DHN level is positively associated with an increased degree of stress resistance.²²⁻³⁰ Enhancement of tolerance to salinity, drought and osmotic stress has also been observed in transgenic *Arabidopsis* plants overexpressing the maize *Rab17* or the wheat dehydrin *Dhn5*.^{22,23,26} *Dhn5* and *Rab17* are both YSK₂ DHNs homologous to the barley *aba2*.²¹ Third, several *Dhn* genes have been mapped within confidence intervals of QTLs associated with dehydration and low temperature tolerance in cereals and other plants.^{6,31,32} The *Dhn* gene used in this study, *aba2*, maps on the long arm of chromosome 5H of barley within a major QTL controlling freezing tolerance,^{32,33} on the 5AL chromosome of wheat within the confidence interval of a QTL associated with abscisic acid (ABA) accumulation during drought stress,³⁴ and with different traits determining salt tolerance.³⁵

Correspondence: Cristina Calestani, Department of Biology, Valdosta State University, 1500 N. Patterson St., Valdosta, GA 31698, USA.
Tel.: +1.229.333.7175 - Fax +1.229.245.6585.
E-mail: ccalestani@valdosta.edu

Key words: Dehydrin; late embryogenesis abundant; germination; salt stress; transgenic plant.

Acknowledgements: authors thank Dr. T.J. Close for providing the DHN antibody and for helpful discussions, Dr. E.M. Meyerowitz for providing the pCGN18 plasmid vector, Dr. R.W.M. Sablowski and Dr. K.J. Bradford for technical advice and helpful discussions. We also thank Professor Robert J. Beaver for his help with the statistical analysis of germination data.

Contributions: CC, NM, EAB project conception and research design; CC, MSM data acquisition; CC, NM, EM, NM, EAB data analysis and results interpretation; CC manuscript writing; EM, NM, EAB manuscript reviewing

Conflict of interest: the authors declare no potential conflict of interest.

Funding: this work was supported by the Ministero delle Risorse Agricole, Alimentari e Forestali Program "Piano Nazionale Biotecnologie Vegetali"; the National Research Council "Progetto Finalizzato Biotecnologie"; the Ministero dell'Università e della Ricerca Scientifica e Tecnologica (MURST) COFIN "Constitutive vs. induced adaptation to stress (abiotic) in plants", and the Department of Botany and Plant Sciences, UCR. C.C. was supported by a fellowship from MURST.

Received for publication: 23 January 2015.
Revision received: 22 May 2015.
Accepted for publication: 22 May 2015.

This work is licensed under a Creative Commons Attribution NonCommercial 3.0 License (CC BY-NC 3.0).

©Copyright C. Calestani et al., 2015
Licensee PAGEPress srl, Italy
International Journal of Plant Biology 2015; 6:5826
doi:10.4081/pb.2015.5826

In this work we investigated the biological function of a *Dhn* from *Hordeum vulgare* (L.), *aba2* (National Center for Biotechnology Information accession number CAA66970), and specifically its possible protective role during salt stress. ABA2 was originally identified in barley coleoptiles, and its expression was induced by treatment with ABA.³⁶ By using a transgenic approach, we constitutively expressed *aba2* in *Arabidopsis thaliana* with the goal to unveil, if present, a role of *aba2* in protecting from the damages of salt stress. The *aba2* is the cv. Georgie allele of the barley gene

Dhn1 and it codes for a protein with a molecular mass of 22 kDa.^{1,7} We tested germination, cotyledon expansion and greening, and seedling growth on medium containing NaCl concentrations that were restrictive to the *Arabidopsis* control plants.

When evaluating the effects of the heterologous expression of the barley *aba2* in *Arabidopsis* plants, it must be considered whether the observed effects result from engineering a novel gene into the *Arabidopsis* genome or from a change in the expression pattern of a *Dhn* with a function similar to *Arabidopsis*' native *Dhn* genes. For this purpose we obtained a phylogenetic tree including ABA2 and the native DHNs encoded in the *Arabidopsis* genome.

Materials and Methods

Construction of the plasmid vector for plant transformation

The *EcoRI-NheI* 530 bp fragment containing the *aba2* cDNA was isolated from the plasmid pGEM-3Zf+-ABA2, filled-in with DNA polymerase I Klenow fragment, and ligated into the *SpeI* site of pBlueScript II KS+ (Stratagene, now Agilent Technologies, Santa Clara, CA, USA), resulting in the plasmid pBSA2. To construct pCGN18A2, the *BamHI-XbaI* fragment from pBSA2 was cloned between the *BamHI* and *XbaI* sites of the binary vector pCGN18,³⁷ downstream of the constitutive promoter CaMV 35S.

Production of transgenic plants

The plasmid construct pCGN18A2 was transformed into *Agrobacterium tumefaciens*, strain ASE.³⁸ Transformed *A. tumefaciens* was selected on chloramphenicol (30 µg/mL⁻¹), gentamicin (25 µg/mL⁻¹), and kanamycin (50 µg/mL⁻¹). Seeds of *Arabidopsis thaliana* (L.) ecotype Landsberg *erecta* (*Ler*) were sown on a soil mixture of fine vermiculite, peat moss and coarse vermiculite (1:2:1 v v⁻¹), saturated with modified Hoagland's solution (3.0 mM KNO₃, 2.5 mM Ca(NO₃)₂, 1.5 mM MgSO₄, 0.5 mM KH₂PO₄, 68.0 mM Fe-EDTA, 23.0 mM H₃BO₃, 4.55 mM MnCl₂, 0.385 mM ZnSO₄, 0.16 mM CuCO₄, and 0.04 mM Na₂MoO₄.³⁹ Seeds were stratified for 3 days in the dark at 4°C. Plants were grown in 0.1 L pots with 2-3 plants per pot at 23°C, with fluorescent light at 150 mEm⁻²s⁻¹ and a photoperiod of 16 h. Four-week-old plants were transformed by vacuum infiltration of *A. tumefaciens* carrying the pCGN18A2 plasmid.⁴⁰ Seeds produced by the infiltrated plants (T₁ generation) were surface sterilized and sown in Petri dishes on solid Murashige and Skoog (MS) medium,⁴¹ containing 50 µg/mL⁻¹ of kanamycin. Kanamycin-resistant

plants were transferred to soil and grown as described above.

Analyses of ABA2 protein synthesis in transgenic plants

ABA2 protein accumulation was analyzed in kanamycin-resistant three weeks old *Arabidopsis*

plants of the T₂ and T₄ generation (Figure 1). Plants were grown in 0.1 L pots with 2-3 plants per pot. Total proteins were extracted from fresh leaf material (50-100 mg) by homogenizing in ice-cold 50 mM sodium borate and 50 mM citric acid buffer, pH 9, with 1 mM phenylmethanesulfonyl-fluoride (PMSF), followed by centrifugation at

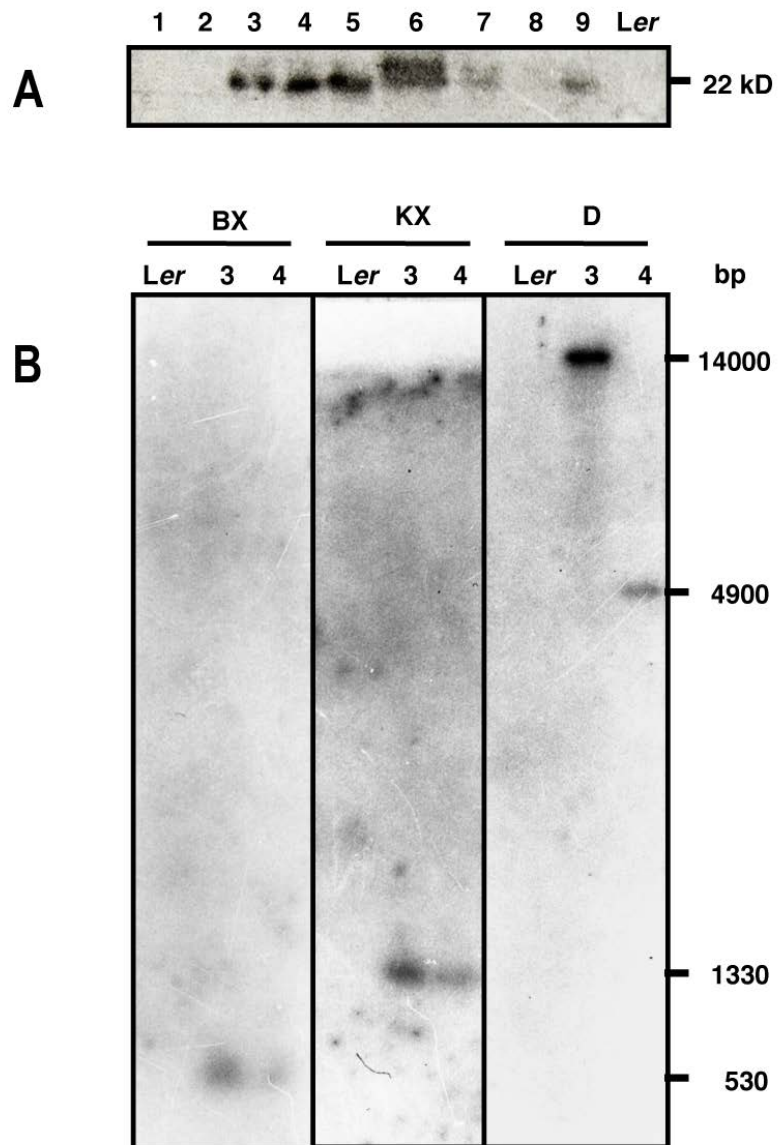


Figure 1. Characterization of ABA2 expression in *Arabidopsis* transgenic lines. A) Immunoblot analysis of ABA2 protein accumulation in leaves of transgenic *Arabidopsis* plants. Transgenic lines A2-1 through 9 (lanes 1-9) and *Ler* (non-transformed plants) are shown. B) Southern blot analysis of genomic DNA isolated from transgenic plants (T₃ generation) hybridized with a ³²P-labeled *aba2* cDNA. Genomic DNA was digested with *Bam*HI and *Xba*I (BX) to release a 530 bp *aba2* sequence; *Kpn*I and *Xba*I (KX) to release a 1330 bp fragment corresponding to the 35S CaMV promoter and the *aba2* sequence; and *Dra*I (D) which cuts once within the T-DNA sequence. The sizes of individual bands expressed in bp are indicated on the right. *Ler*, non-transformed plants; 3, transgenic line A2-3; 4, transgenic line A2-4.

12000 × g for 10 min at 4°C. Proteins were also extracted from 10 mg of seedlings using the same procedure. Seedlings were extracted when the cotyledons began to expand: after 2 days on MS and after 4 days on MS supplemented with 150 mM NaCl (Figure 2). Protein concentration was determined using the Bradford Assay (Bio-Rad Laboratories). For immunoblot analyses, 10 µg of total protein extract was separated by 13% acrylamide SDS-PAGE using Mini-Protean II electrophoresis cells (Bio-Rad Laboratories) and electrophoretically transferred onto nitrocellulose membrane (Micron Separations, Westborough, MA, USA) with Mini Trans-Blot Cells (Bio-Rad Laboratories). After transfer, the nitrocellulose membrane was blocked with 3% (w v⁻¹) gelatin in Tris-Buffered Saline (TBS; 50 mM Tris-Cl, 150 mM NaCl, pH 7.5). Polyclonal antibodies raised against the carboxy terminal consensus peptide of DHN were used to recognize ABA2.⁴² The secondary antibody, which binds to the primary antibody, was a goat anti-rabbit IgG conjugated to alkaline phosphatase (Southern Biotechnology Associates, Inc., Birmingham, AL). A colorimetric detection was performed by incubating the membrane in 0.05% (w v⁻¹) 4-nitroblue tetrazolium chloride and 0.05% (w v⁻¹) 5-bromo-4-chloro-3-indoyl-phosphate (Sigma-Aldrich, St. Louis, MO, USA). In a control experiment for antibody specificity, the antiserum was incubated with the DHN carboxy terminal peptide for 30 min at 37°C prior to incubation with the nitrocellulose membrane and no bands were observed (data not shown). Proteins molecular weight were derived by using the Prestained SDS-PAGE Standards Low Range (BioRad Laboratories).

Southern blot analyses

Genomic DNA was extracted from 200-500 mg of one-week-old seedlings using a method modified from Doyle and Doyle.⁴³ Fresh tissue was homogenized in 300 µL extraction buffer [2.5% (w v⁻¹) sorbitol, 1% (w v⁻¹) N-lauroyl sarcosine, 0.8% (w v⁻¹) CTAB, 0.8 M NaCl, 20 mM EDTA, 1% (w v⁻¹), pH 8] and incubated for 30 min at 65°C. Samples were extracted once with phenol:chloroform (1:1 v v⁻¹) and ethanol precipitated following standard procedures.⁴³ For DNA blot analyses, 0.6 µg of genomic DNA of transgenic and control plants were restricted with *Bam*HI and *Xba*I, with *Kpn*I and *Xba*I, and with *Dra*I. Restricted DNA was size-fractionated on a 0.8% agarose gel and transferred to nylon membrane (Hybond-N⁺ Amersham, GE Healthcare, Piscataway, NJ, USA) using an alkaline DNA blot transfer method.⁴⁴ The *aba2* cDNA was ³²P-labeled using the Oligolabeling Kit (Pharmacia Biotech, Piscataway, NJ, USA) and utilized for DNA hybridization.⁴⁵

Germination and seedling growth analyses in response to salt stress

Germination was analyzed on T₄ seeds of

transgenic lines and non-transformed *Ler* plants grown at the same time in the same growth chamber in approx. 0.1 L pots with 2-3 plants per pot. Seeds of each genotype were surface-sterilized with 95% ethanol for 5 min followed by 20 min in 30% bleach and sown on solid MS salt basic medium,⁴¹ with 0.3% sucrose, supplemented with increasing concentrations of NaCl from 150 to 300 mM, at 50 mM intervals. Approximately 50 seeds of a transgenic line and 50 seeds of *Ler* were sown in the same Petri dish. The Petri dishes with the seeds were incubated for 3 days at 4°C in the dark and then transferred to an incubator at 23°C, with light at 150 mEm⁻²s⁻¹ and a photoperiod of 16 h. Petri dishes were kept in a vertical position. Germination percentage, measured as seeds at radicle emergence stage, and cotyledon greening was monitored at daily intervals in four replicate Petri dishes. In Figure 2 we choose to test 150 mM salt concentration because at 200mM the non transgenic seedlings would become quickly chlorotic and die. The proportions of germinating seeds determined in two independent experiments were analyzed using the Minitab Probit Analysis (Minitab Inc., State College, PA, USA; Release 13.32) in which the factor considered was cumulative germination percentage on each day (time to germination). Two independent experiments were performed. Experiment 1 had four replicates for each NaCl concentration with either transgenic A2-3 or A2-4 and the wild type plated on each plate. Experiment 2 had three replicates for each NaCl concentration. The estimated mean times to germination were analyzed as growth models. The estimated mean time to germination differences between the wild type (C) and

either of the mutants (A2-3 or A2-4) were tested using a two-sample t-test assuming unequal variance.

Phylogenetic analysis

Proteins containing the conserved lysine-rich domain K were identified in the Arabidopsis genome from Pfam (<http://pfam.xfam.org/family/PF00257#tab-view=tab7>) and verified in TAIR (<https://www.arabidopsis.org/>). The nine Arabidopsis DHNs amino acid sequences, the barley ABA2/DHN1, the wheat DHN5 and the maize RAB17 were aligned using ClustalW version 2.1 (<http://clustalw.ddbj.nig.ac.jp/>)⁴⁶ A neighbor-joining tree was constructed using FigTree version 1.4.2 (<http://tree.bio.ed.ac.uk/>).

Results

Production of transgenic Arabidopsis plants constitutively expressing *aba2*

The level of accumulation of the 22 kDa ABA2 protein in unstressed leaves was analyzed for nine transgenic lines (Figure 1A). Line 3, 4 and 5 showed the highest level of ABA2 accumulation; line 6, 7 and 9 accumulated ABA2 to a lesser extent, with line 6 showing an additional protein of 23 kDa; line 1, 2 and 8 did not show any detectable accumulation of ABA2 (Figure 1A). Lines 3 and 4 (A2-3 and A2-4) were used for further studies. Both lines A2-3 and -4 have the *aba2* gene inserted at a single locus and they were produced from inde-

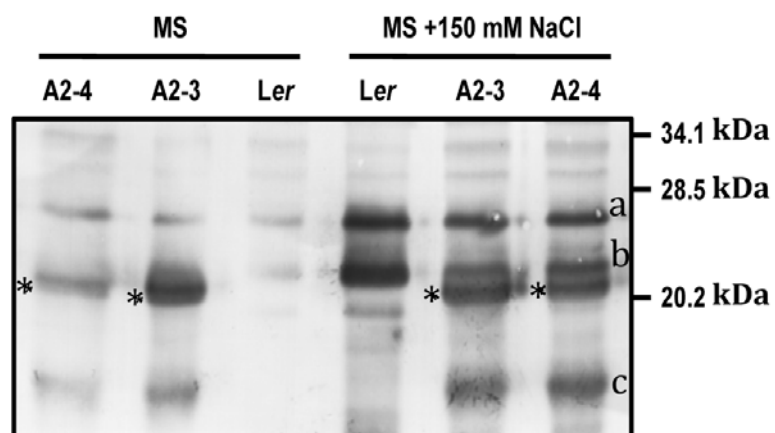


Figure 2. Immunoblot analyses of the accumulation of ABA2 and other DHNs in seedlings of transgenic lines and *Ler*. Seeds of control (*Ler*) and transgenic plants (A2-3 and A2-4) were germinated on MS or MS with 150 mM NaCl. DHNs having the same molecular mass as ABA2 are indicated (*).

pendent transformation events as verified by genomic DNA blot analyses (Figure 1B).

Constitutive expression of *aba2* enhances salt-stress resistance during seed germination

Seed germination on media containing NaCl, measured as percentage of radicle emergence, was compared between seeds from the T₄ generation of two independent transgenic lines (A2-3 and A2-4) and the wild type plants (Figure 3, Table 1). At 200, 250 and 300 mM NaCl, the final germination percentage was greater for the transgenic lines than the wild type (Figure 3B-D, Table 1). On control MS medium, the final germination percentage for the wild type *Ler* was 92% after 2 days and 100% for both transgenic lines (Figure 3A). Up to 250 mM NaCl, both transgenic lines achieved between 98% to 100% germination, while the wild type a maximum of 85.2% and 70.6% on 200 and 250 mM NaCl respectively, after 12-14 days (Figure 3B,C). When seeds were imbibed and germinated on 300 mM NaCl, the transgenic line reached 90% germination after 20 days whereas after the same period of time the germination percentage for *Ler* was 45% (Figure 3D).

The transgenic lines overexpressing ABA2 showed a decreased time to germination in response to salt stress. The mean time to germination, as estimated by probit analysis, was shorter for the two transgenic lines than for the wild type when seeds were exposed to 200, 250 and 300 mM NaCl (Table 1, Experiment 1). An additional replicate experiment showed similar results (germination time courses are not shown; Table 1, Experiment 2). There are no significant differences between the final germination percentages of the A2-3 and A2-4 transgenic lines.

Cotyledon emergence and greening was measured as a cumulative percentage at daily intervals (Figure 4). On MS medium, cotyledons had emerged by Day 2 in both the wild type and transgenic lines, however, 15% of the wild type cotyledons did not green (Figure 4A). Exposure to 200 mM NaCl reduced greening to 48% in the wild type seedlings whereas 91-93% of the transgenic cotyledons were greened after 2 weeks (Figure 4B,C).

To verify the accumulation of ABA2 in stressed and non-stressed seedlings, immunoblot analyses were done on proteins extracted from the transgenic and control seedlings sown on MS media or MS media with 150 mM NaCl (Figure 2). The ABA2 protein was present in the transgenic lines in stressed and non-stressed conditions while it was absent in *Ler*. The immunoblot analysis also detected the native DHNs, which as expected accumulated at higher levels under salt stress conditions (Figure 2, bands a, b and c). It

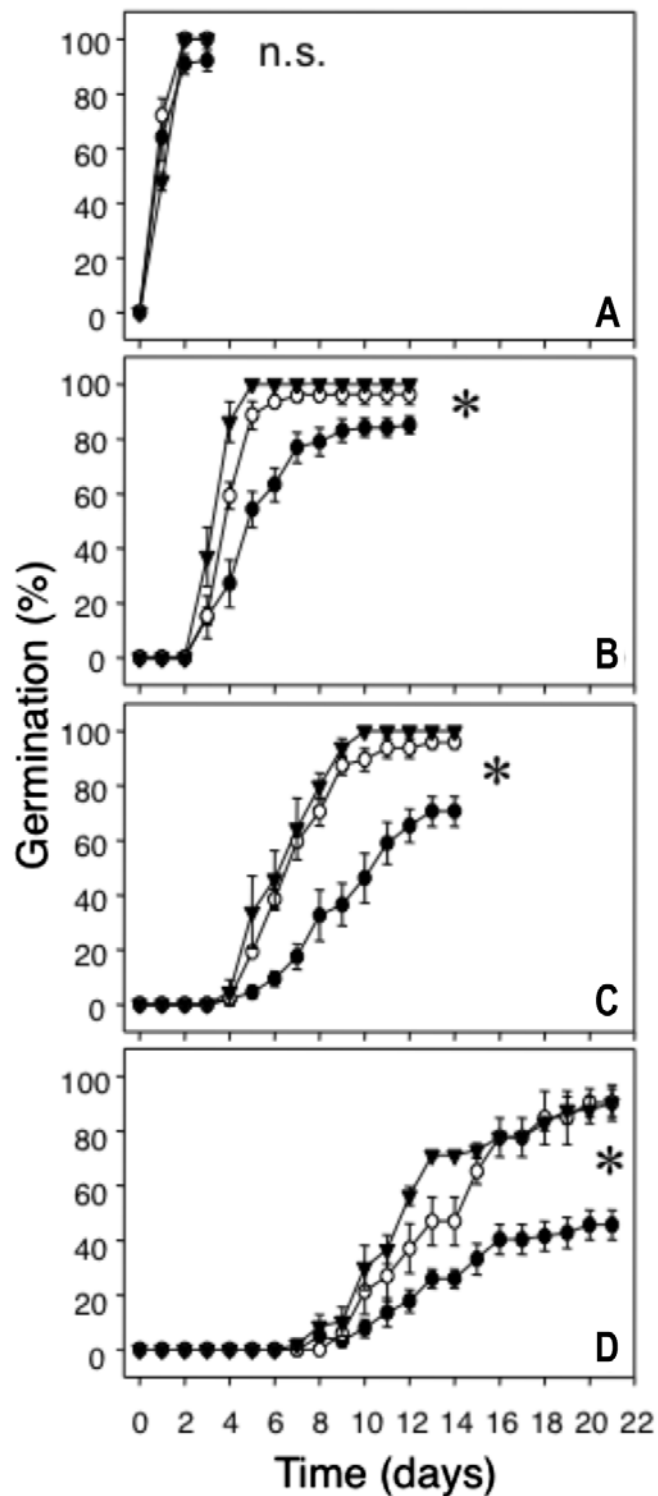


Figure 3. Germination time course of transgenic seeds constitutively expressing ABA2 and control *Ler* seeds during salt stress. Seeds of the transgenic plants (T₄ generation) A2-3 (○), A2-4 (▼) and non-transformed *Ler* plants (●) were plated on MS media (A; after the second day there was no change in percent germination in the control conditions, data not shown) and on MS supplemented with different concentrations of NaCl (B, 200 mM; C, 250 mM; D, 300 mM). Approximately 50 seeds of a transgenic line and *Ler* were plated in the same Petri dish; three replicate plates were analyzed for each transgenic line at each NaCl concentration. Germination was measured as a cumulative percentage of radicle emergence at daily intervals for 3 weeks. Data are the average germination percentage ± s.e. Significant differences of the final germination percentages are indicated (*). A representative experiment out of five independent experiments is shown.

should be noted though that under stress some of the native DHNs appear to accumulate at lower levels in the transgenic lines as compared to *Ler* (Figure 2, bands a and b). Interestingly, an additional protein, smaller than 20 kDa, was present in the transgenic lines only, and it was expressed at higher levels during salt stress conditions (Figure 2, band c).

The barley ABA2 is closely related to Arabidopsis dehydrins

The barley ABA2 protein sequence was phylogenetically compared to the native DHNs encoded in the Arabidopsis genome, to the wheat DHN5 and to the maize RAB17. The Arabidopsis genome contains nine genes that code for DHN proteins, as defined by the presence of the conserved K segment.⁵ To determine the phylogenetic relation between the barley gene ABA2 and the Arabidopsis genes, a neighbor-joining tree of the nine Arabidopsis was built (Figure 5). Two main clades were identified: one containing the Y_nSK_2 proteins and the other with the $SK_{2,3}$ proteins. As predicted, ABA2 was in the clade with Y_nSK_2 proteins from Arabidopsis, DHN5 and RAB17. Arabidopsis *Dhn* genes can be grouped into three types based on the presence of previously identified amino acid domains: four YSK_2 , four $SK_{2,3}$ and one K_6 . A new domain was identified in the Arabidopsis SK type genes with the consensus RGL/MFDLXKKXEEVXE.

Discussion

In this study, we produced transgenic *A. thaliana* plants constitutively expressing the barley *aba2* gene. The transgenic lines had greater resistance to salt stress during seed germination than did the wild type. The presence of a constitutively expressed DHN in Arabidopsis correlated with an increase of the final germination percentage in salt stress conditions at 200 mM NaCl and above (Figure 3), and a decrease of the mean time to germination as compared to the wild type at all the NaCl concentrations tested (Table 1). The transgenic plants reached 90-100% final germination in salt stress conditions, while the wild type plants underperformed by 15%, 30% and 45% as the NaCl concentration in the growth media was increased (Figure 3).

According to our results, it seems unlikely that the observed effects are caused by novel functional aspects of the barley ABA2 transferred into the Arabidopsis genome. In fact, Arabidopsis has nine DHNs, four of which have the same Y_nSK_2 domain structure as ABA2 and two of which cluster into the same clade with ABA2 (Figure 5). Although this does not

ensure identical function, it does indicate that they are closely related and are likely to have the same role.

We also observed that seed lots produced at

different time varied in NaCl tolerance during germination, but this did not alter the difference between the genotypes *Ler*, A2-3 and A2-4. The transgenic seeds expressing the barley

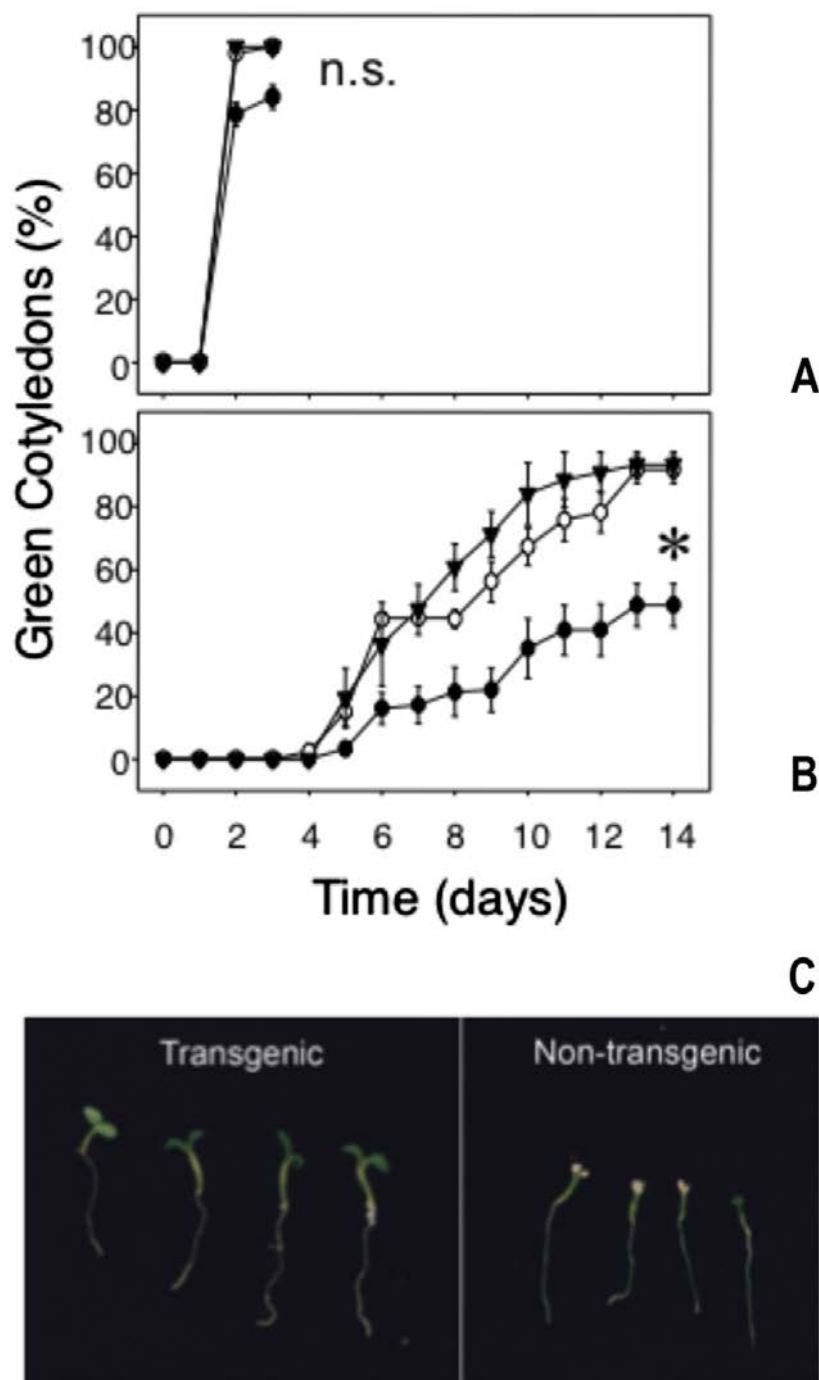


Figure 4. Cotyledon greening time course of transgenic lines constitutively expressing ABA2 and control *Ler* seeds during salt stress. Cotyledon greening of germinated seeds of the transgenic plants A2-3 (○) and A2-4 (▼), and of non-transformed *Ler* plants (●) was recorded as a cumulative percentage at daily intervals. Seeds were plated on MS media (A; after day three there was no change in percent germination, data not shown) or MS supplemented with 200 mM NaCl (B). The average percentage \pm s.e of seedlings with green cotyledons is shown. Significant differences of the final cotyledon greening percentages are indicated (*). C) A representative sample of one-week old *Ler* and transgenic seedlings grown on 150 mM NaCl.

aba2 had a greater ability to germinate than wild type seeds produced at the same time in the same growth conditions in all of the seed lots tested. It has previously been reported that NaCl tolerance of Arabidopsis seeds at germination is variable. Salt tolerance of seeds appears to vary with plant nutrition as well as the length of time seeds are permitted to develop before drying.⁴⁷ Natural variation for salt tolerance at germination has also been recently described in Arabidopsis.⁴⁸

Therefore, our data suggest that the constitutive expression of *aba2* directly or indirectly improves germination in response to salinity. Transgenic Arabidopsis plants overexpressing the maize *Rab17* or the wheat dehydrin *Dhn5* also shown an enhancement of tolerance to salinity, drought and osmotic stress.^{22,23,26} In the Rab17 study salt stress was applied to 1-week-old seedlings, therefore the effects of the DHNs overexpression on germinating seeds were not tested. Whereas the wheat *Dhn5*, expressed in a Columbia ecotype background, did show a similar level of germination rate improvement as compared to our study with the barley ABA2 expressed in a *Ler* ecotype.²² Transgenic approaches employing the overexpression of a DHN have also been tested in plants other than Arabidopsis. A recent study shows that the constitutive expression of the tomato dehydrin *tas14* in tomato improves salt and drought tolerance.³⁰ In this case, the effects on germination were not tested. Transgenic plants over-expressing *tas14* accumulate ABA earlier and at higher levels, and counteract the osmotic stress by intracellular accumulation of K⁺, Na⁺ and sugars.³⁰ This suggests that the constitutive expression of Y_nSK₂ DHNs in transgenic plants may be an effective approach for the enhancement of salt tolerance in different plant species.

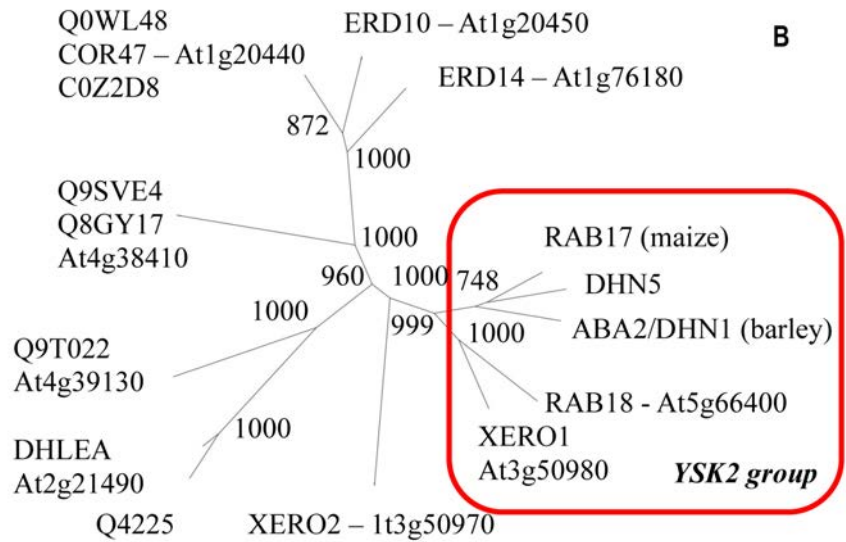
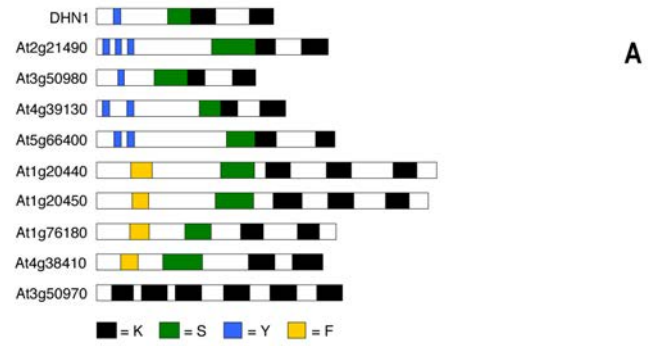


Figure 5. Phylogenetic relationships among the barley ABA2 and Arabidopsis DHNs. A) Protein conserved domains comparison of ABA2 and nine DHNs identified in the Arabidopsis genome. The Arabidopsis loci names are indicated and the DHNs conserved domains K, S, Y, and F are color-coded. B) Unrooted neighbor-joining tree of the barley ABA2 and the Arabidopsis DHNs. Bootstrap values are shown.

Table 1. Statistical analysis of the time to germination during salt stress conditions.

NaCl (mM)	Mean C (SE _C)	Mean A2-3 (SE _{A2-3})	Mean A2-4 (SE _{A2-4})	z-value A2-3 ^A	P-value A2-3	z-value A2-4 ^A	P-value A2-4
Experiment 1							
0	B	B	B	-	-	-	-
200	3.50 (0.61)	1.83 (0.01)	1.21 (0.16)	2.71, df=5	0.042*	3.61, df=5	0.015*
250	7.70 (0.65)	3.95 (0.14)	3.21 (0.48)	5.62, df=5	0.002*	5.54, df=6	0.001*
300	14.06 (1.4)	8.05 (0.95)	6.84 (0.18)	3.61, df=6	0.011*	5.26, df=5	0.003*
Experiment 2							
0	0.71 (0.11)	0.87 (0.24)	B	-0.61, df=1	0.653	-	-
150	3.08 (0.03)	2.43 (0.28)	2.48 (0.10)	2.26, df=2	0.152	5.57, df=3	0.011*
200	5.47 (0.23)	4.14 (0.06)	5.39 (0.51)	5.66, df=7	0.001*	0.14, df=4	0.896
250	10.60 (0.49)	8.63 (0.12)	8.68 (0.55)	3.91, df=7	0.006*	2.62, df=7	0.035*
300	27.61 (2.00)	17.39 (1.10)	17.89 (0.38)	4.49, df=9	0.002*	4.80, df=7	0.002*

The estimated mean times to germination were analyzed as growth models using the Minitab Probit Analysis. Indicated in parenthesis are the standard errors for the controls (SE_C), and the transgenic lines A2-3 or A2-4 (SE_{A2-3}, SE_{A2-4}). Significant differences of the estimated mean time to germination between the wild type (C) and either of the mutants (A2-3 or A2-4) are indicated (*P<0.05).

^AThe z-value is given by:

$$\frac{\hat{\mu}_C - \hat{\mu}_A}{\sqrt{SE_C^2 + SE_A^2}}$$

^B The values of the estimates of mean time to germination did not converge: no tests possible for this level of salt treatment. μ_C equals the mean of the combined controls and μ_A is the mean of the transgenic line A2-3 or A2-4.

Interestingly, in addition to the constitutive expression of the barley *aba2*, the transgenic plants we produced showed the salt-stress induction of an additional protein recognized by the DHN antibody, which is not present in the wild type plants in control or salt stress conditions (Figure 2, band c). We cannot exclude that the enhancement of the salt tolerance observed in our transgenic plants is actually the results of the combined effects of the barley ABA2 and the additional stress-induced native DHN. In this regard, similar results were also observed in transgenic Arabidopsis plants overexpressing the wheat *Dhn5* or the maize *Rab17*.^{23,26} The transcriptome analysis of the *Dhn-5* transgenic plants showed the induction of abiotic and biotic stress related proteins, including other LEA proteins, specifically a LEA7, the low temperature induced LTI30/XERO2, and RAB18/XERO1. Interestingly the latter is a Y₂SK2 DHN of 13 kDa, similar in size to the additional DHN induced in the transgenic plants produced in our study (Figure 2, band c). Likewise, transgenic Arabidopsis overexpressing the maize *Rab17* also showed the induction of a LEA7.^{23,26} The molecular function of *Dhn5* and *Rab17* is not known but under stress conditions they are both translocated to the nucleus,^{13,22} consequently they might have a role in the transcriptional regulation of other stress responsive genes. In the case of RAB17 it has been shown that nuclear targeting is mediated by a stress-induced phosphorylation of the S-segment.^{49,50}

DHN and other LEA proteins may have a role in protecting the embryo during seed desiccation and rehydration.^{2,17,51} It is known that DHN content increases during the late stages of seed development, is high in dormant embryos, and usually decreases upon seed imbibition and germination, together with a decline in seed desiccation tolerance.¹⁷⁻¹⁹ It has been shown that re-drying (imbibition followed by dehydration) soybean seeds during the period of radicle emergence results in a decrease in germination frequency. Instead, if re-drying is accompanied by imbibition with ABA or with PEG, which results in accumulation of LEA proteins in the seeds, the seed desiccation tolerance is maintained.¹⁷ Thus a change in the timing or location of expression of a DHN may permit increased viability during seed germination under stress conditions.

Another possible role of DHNs may be the facilitation of water uptake during seed imbibition on low osmotic potential media. It has been proposed that LEA proteins may act as a hydration buffer in the cell in the presence of sugars.^{11,52} In fact, heat-soluble protein preparations in the presence of sugars absorb 2-3 times more water than a lysozyme/sugar preparation^{11,52} Thus, overexpression of DHNs may alter the seeds capacity to absorb water during imbibition promoting germination on

media containing a concentration of NaCl that is restrictive to wild type germination. Alternatively, DHNs may promote cellular detoxification. Experiments studying the molecular function of DHNs have pinpointed lipid binding,^{10,53} Ca²⁺,¹² or metal binding.⁵⁴ The binding capacities of DHNs may in turn participate in the ability to inhibit lipid peroxidation.²⁴

Conclusions

In conclusion, transgenic plants expressing the barley ABA2 showed a significant improvement of the germination process in conditions of increased salinity and low osmotic potential. Therefore the modification of *aba2* expression via transgenic approaches could greatly benefit plant improvement programs aimed at the environmental adaptation of different types of crops.

References

1. Close TJ. Dehydrins: a commonality in the response of plants to dehydration and low temperature. *Physiol Plant* 1997;100:291-6.
2. Tunnacliffe A, Wise MJ. The continuing conundrum of the LEA proteins. *Naturwissenschaften* 2007;94:791-812.
3. Hanin M, Brini F, Ebel C, et al. Plant dehydrins and stress tolerance. *Plant Signal Behav* 2011;6:1503-9.
4. Hand SC, Menze MA, Toner M, et al. LEA proteins during water stress: not just for plants anymore. *Ann Rev in Physiol* 2011;73:115-34.
5. Close TJ. Dehydrins: Emergence of a biochemical role of a family of plant dehydration proteins. *Physiol Plant* 1996;97:795-803.
6. Campbell SA, Close TJ. Dehydrins: genes, proteins and associations with phenotypic traits. *New Phytol* 1997;137:61-74.
7. Choi D-W, Zhu B, Close TJ. The barley (*Hordeum vulgare* L.) dehydrin multigene family: sequences, allele types, chromosome assignments, and expression characteristics of 11 Dhn genes of cv. Dicktoo. *Theor Appl Genet* 1999;98:1234-47.
8. Houde M, Daniel C, Lachapelle M, et al. Immunolocalization of freezing tolerance-associated proteins in the cytoplasm and nucleoplasm of wheat crown tissues. *Plant J* 1995;8:583-93.
9. Dure L III. Structural motifs in Lea proteins. In: Close TJ, Bray EA, eds. *Plant responses to cellular dehydration during environmental stress*. Rockville: American Society of Plant Physiologists; 1993. pp 91-

- 103.
10. Koag MC, Wilkens S, Fenton RD, et al. The K-segment of maize ABA2 mediates binding to anionic phospholipid vesicles and concomitant structural changes. *Plant Physiol* 2009;150:1503-14.
11. Hara M. The multifunctionality of dehydrins. *Plant Signal Behav* 2010;5:503-8.
12. Alsheikh MK, Heyen BJ, Randall SK. Ion binding properties of the dehydrin ERD14 are dependent upon phosphorylation. *J Biol Chem* 2003;278:40882-9.
13. Goday A, Jensen AB, Culiñez-Macià FA, et al. The maize abscisic acid-responsive protein Rab17 is located in the nucleus and interacts with nuclear localization signals. *Plant Cell* 1994;6:351-60.
14. Plana M, Itarte E, Eritja R, et al. Phosphorylation of maize RAB-17 protein by casein kinase 2. *J Biol Chem* 1991;266:22510-4.
15. Vilardell J, Goday A, Freire MA, et al. Gene sequence, developmental expression and protein phosphorylation of RAB17 in maize. *Plant Mol Biol* 1990;14:423-32.
16. Graether SP, Boddington KF. Disorder and function: a review of the dehydrin protein family. *Front Plant Sci* 2014;5:576.
17. Blackman SA, Wettlaufer SH, Obendorf RL, et al. Maturation proteins associated with desiccation tolerance in soybean. *Plant Physiol* 1991;96 868-74.
18. Blackman SA, Obendorf RL, Leopold AC. Desiccation tolerance in developing soybean seeds: the role of stress proteins. *Physiol Plant* 1995;93:630-8.
19. Han B, Hughes DW, Galau GA, et al. Changes in late-embryogenesis-abundant (LEA) messenger RNAs and dehydrins during maturation and premature drying of *Ricinus communis* L. seeds. *Planta* 1997;201:27-35.
20. Farrant JM, Moore JP. Programming desiccation-tolerance: from plants to seeds to resurrection plants. *Curr Opin in Plant Biol* 2011;14:340-5.
21. Bray EA. Plant responses to water deficit. *Trends Plant Sci* 1997;2:48-54.
22. Brini F, Hanin M, Lumberras V, et al. Overexpression of wheat dehydrin DHN-5 enhances tolerance to salt and osmotic stress in Arabidopsis thaliana. *Plant Cell Rep* 2007;26:2017-26.
23. Brini F, Yamamoto A, Jlaiel L, et al. Pleiotropic effects of the wheat dehydrin DHN-5 on stress responses in Arabidopsis. *Plant Cell Physiol* 2011;52:676-88.
24. Cheng Z, Targolli J, Huang X, et al. Wheat LEA genes, PMA80 and PMA1959 enhance dehydration tolerance of transgenic rice (*Oryza sativa* L.). *Mol Breeding* 2002;10:71-82.
25. Hara M, Terashima S, Fukaya T, et al. Enhancement of cold tolerance and inhibi-

- tion of lipid peroxidation by citrus dehydrin in transgenic tobacco. *Planta* 2003;217:290-8.
26. Figueras M, Pujal J, Saleh A, et al. Maize Rab17 overexpression in Arabidopsis plants promotes osmotic stress tolerance. *Ann Appl Biol* 2004;144:251-7.
 27. Houde M, Dallaire S, N'Dong D, et al. Overexpression of the acidic dehydrin WCOR410 improves freezing tolerance in transgenic strawberry leaves. *Plant Biotechnol J* 2004;2:381-7.
 28. Puhakainen T, Hess MW, Mäkelä P, et al. Overexpression of multiple dehydrin genes enhances tolerance to freezing stress in Arabidopsis. *Plant Mol Biol* 2004;54:743-53.
 29. Shekhawat UKS, Srinivas L, Ganapathi TR. MusaDHN-1, a novel multiple stress-inducible SK₃-type dehydrin gene, contributes affirmatively to drought- and salt-stress tolerance in banana. *Planta* 2011;234:915-32.
 30. Munoz-Mayor A, Pineda B, Garcia-Abellán JO, et al. Overexpression of dehydrin tas14 gene improves the osmotic stress imposed by drought and salinity in tomato. *J Plant Physiol* 2012;169:459-68.
 31. Alm V, Busso CS, Ergon A, et al. QTL analyses and comparative genetic mapping of frost tolerance, winter survival and drought tolerance in meadow fescue (*Festuca pratensis* Huds.). *Theor Appl Genet* 2011;123:369-82.
 32. Choi DW, Koag MC, Close TJ. Map locations of barley Dhn genes determined by gene-specific PCR. *Theor Appl Genet* 2000;101:350-4.
 33. Hayes PM, Blake T, Chen THH, et al. Quantitative trait loci on barley (*Hordeum vulgare* L.) chromosome 7 associated with components of winter-hardiness. *Genome* 1993;36:66-71.
 34. Quarrie SA, Steed A, Semikhodski A, et al. Identification of quantitative trait loci regulating water- and nitrogen-use efficiency in wheat. In: Leigh RA, Blake-Kalff MMAM, eds. Proceedings of the second STRESS-NET conference. Luxembourg: European Commission, Directorate General VI; 1995. pp 175-180.
 35. Semikhodskii AG, Quarrie SA, Snape JW. Mapping quantitative trait loci for salinity responses in wheat. In: Jevtic S, Pekic S, eds. Proceedings of international symposium on drought and plant production. Belgrade: Agricultural Research Institute; 1997. pp 83-92.
 36. Gulli M, Maestri E, Hartings H, et al. Isolation and characterization of abscisic acid inducible genes in barley seedlings and their responsiveness to environmental stress. *Plant Physiol (Life Sci Adv)* 1995;14:89-96.
 37. Krizek BA, Meyerowitz EM. The Arabidopsis homeotic genes APETALA3 and PISTILLATA are sufficient to provide the B class organ identity function. *Development* 1996;122:11-22.
 38. Fraley RT, Rogers SG, Horsch RB, et al. The SEV system: a new disarmed Ti plasmid vector system for plant transformation. *Biotechnology* 1985;3:629-35.
 39. Bernstein L, Francois LE, Clark RA. Interactive effects of salinity and fertility on yields of grains and vegetables. *Agron J* 1974;66:412-21.
 40. Bechtold N, Ellis J, Pelletier G. In planta Agrobacterium-mediated gene transfer by infiltration of adult Arabidopsis thaliana plants. *C R Acad Sci Paris Life Sci* 1993;316:1194-9.
 41. Murashige T, Skoog F. A revised medium for rapid growth and bio assays with tobacco tissue cultures. *Physiol Plant* 1962;15:473-97.
 42. Close TJ, Fenton RD, Moonan F. A view of plant dehydrins using antibodies specific to the carboxy terminal peptide. *Plant Mol Biol* 1993;23:279-86.
 43. Doyle JJ, Doyle JL. Isolation of plant DNA from fresh tissue. *Focus* 1990;12:13.
 44. Sambrook J, Fritsch EF, Maniatis T. Molecular cloning: a laboratory manual. Cold Spring Harbor: Cold Spring Harbor Laboratory Press; 1989.
 45. Sharp PJ, Kreis M, Shewry PR, et al. Location of b-amylase sequences in wheat and its relatives. *Theor Appl Genet* 1988;75:286-90.
 46. Larkin MA, Blackshields G, Brown NP, et al. ClustalW and ClustalX version 2. *Bioinformatics* 2007;23:2947-8.
 47. Bradford K. Water relations in seed germination. In: Kigel J, Galili G, eds Seed development and germination. New York: Marcel Dekker Inc; 1995. pp 351-396.
 48. DeRose-Wilson L, Gaut BS. Mapping salinity tolerance during Arabidopsis thaliana germination and seedling growth. *PLoS ONE* 2011;6:e22832.
 49. Jensen AB, Goday A, Figueras M, et al. Phosphorylation mediates the nuclear targeting of the maize Rab17 protein. *Plant J* 1998;13:691-7.
 50. Riera M, Figueras M, Lopez C, et al. Protein kinase CK2 modulates developmental functions of the abscisic acid responsive protein Rab17 from maize. *Proc Natl Acad Sci USA* 2004;101:9879-84.
 51. Skriver K, Mundy J. Gene expression in response to abscisic acid and osmotic stress. *Plant Cell* 1990;2:503-12.
 52. Walters C, Ried JL, Walker-Simmons MK. Heat-soluble proteins extracted from wheat embryos have tightly bound sugars and unusual hydration properties. *Seed Sci Res* 1997;7:125-34.
 53. Koag MC, Fenton RD, Wilkens S, et al. The binding of maize ABA2 to lipid vesicles. Gain of structure and lipid specificity. *Plant Physiol* 2003;131:309-16.
 54. Kruger C, Berkowitz O, Stephan UW, et al. A metal-binding member of the late embryogenesis abundant protein family transports iron in the phloem of *Ricinus communis* L. *J Biol Chem* 2002;277:25062-9.

Growth, photosynthesis and pollen performance in saline water treated olive plants under high temperature

Georgios C. Koubouris,
Nikolaos Tzortzakos,
Nektarios N. Kourgialas, Marina Darioti,
Ioannis Metzidakis

Hellenic Agricultural Organization
"Demeter", Institute for Olive Tree and
Subtropical Plants, Chania, Greece

Abstract

Olive cultivation in hot arid areas is hindered by the scarcity of irrigation water. The exploitation of saline water has been proposed as a solution to partially cover plant water demands. This paper presents the effects of salinity [0, 60 and 120 mM sodium chloride (NaCl)] on physiological and reproductive functions of cultivars *Koroneiki* and *Amphissis* in a closed hydroponic system. Shoot growth was markedly reduced in high salinity dose in *Amphissis* (–81%) and *Koroneiki* (–75%). The photosynthetic rate was significantly reduced at 120 mM NaCl for both cultivars, as well as chlorophyll and carotenoids content (43% and 44%, respectively). The Na⁺ content in all plant parts increased in both salinity doses especially in *Amphissis* while K concentration decreased for both cultivars. Inflorescences in *Amphissis* were severely damaged due to salinity. Consequently, pollen sampling and *in vitro* germination study was only feasible for *Koroneiki*. Indeed, *Koroneiki* pollen germination was reduced at 60 mM NaCl (–42%) and at 120 mM NaCl (–88%). Pollen tube length was also reduced by 15% and 28% for the middle and high salinity dose, respectively. The results of the present study indicate that *Amphissis* is more sensitive in high salinity doses compared to *Koroneiki* and that reproductive functions are severely affected by salinity.

Introduction

Agriculture in hot arid areas is hindered by the scarcity of irrigation water. The exploitation of saline water has been proposed as a solution to partially cover plant water demands. Most of the world's olive production is situated in the Mediterranean region and the olive is considered to be the major tree crop in this area.¹ Compared to other tree crops, the olive tree is moderately tolerant to

salinity. Olive cultivation often occurs in locations that are unsuitable for other crops, due to summer drought and lack of good quality water for irrigation, which leads to salinity building up in the soil. The conflicting demands for water between agriculture, civil use and tourism, all reaching higher levels, in late spring, summer, and early autumn, when water is less abundant; lead to an over-pumping of groundwater which in turn generates saltwater intrusion in several agricultural areas. Taking into consideration that olive cultivation is more and more supplemented with irrigation, salinity due to saltwater intrusion is becoming a major problem on the yield of olive crop.²

In general, salinity is an environmental stress that limits growth and development in plants. Various effects of salinity on olive tree have been demonstrated.³ Shoot growth is affected more than root growth under a saline environment, resulting in an increased root:shoot ratio.⁴ There are also several genotypic variations for salt tolerance among the cultivars.⁵

In recent years, many studies employ hydroponic culture to study the effects of salinity on crops,⁶ in which the experimental process can be controlled in a more appropriate way than in field applications, excluding the plant-soil interaction interference. However, according to our best knowledge, there are limited studies dealing with olive trees in hydroponics and indeed no studies employed NFT system, which is considered suitable method for nutrition studies.⁷ Nevertheless, a number of unresolved issues regarding the impact of salinity on olive trees still exist.

Under Mediterranean conditions, salinity stress commonly occurs simultaneously with other environmental constraints such as high temperature and high solar irradiance.⁸ High temperature reduces photosynthetic and pollen performance of olive,^{9,10} while the impact of solar irradiance is considered as more complex due to qualitative components *i.e.* spectrum composition and light intensity. Aim of the present study was to investigate the effects of two NaCl salinity levels under enhanced temperature on physiological and reproductive functions of two olive cultivars of major importance for Greece – olive oil cv. *Koroneiki* and table olive cv. *Amphissis*.

Materials and Methods

Plants of *Koroneiki* and *Amphissis* were developed in a hydroponic system (Nutrient Film Technique-NFT) in an unheated glasshouse with a north-south orientation of the Institute of Olive Tree and Subtropical Plants of Chania. The average minimum and

Correspondence: Georgios Koubouris, Hellenic Agricultural Organization "Demeter" (formerly, NAGREF - National Agricultural Research Foundation), Institute for Olive Tree and Subtropical Plants, Agrokipion, 73100 Chania, Greece.
E-mail: koubouris@nagref-cha.gr

Key words: *Olea europaea* L.; photosynthesis; pollen germination; salinity.

Acknowledgements: this work was supported by General Secretariat for Research and Technology in the framework of Greek-Egyptian Bilateral Cooperation 2006-2008 (contract no. GSRT-271-e).

Contributions: GCK, experimental plan, experimental work, writing the paper; NT, experimental work, writing the paper; NNK, manuscript writing, statistical analysis; MD, experimental work; IM, experimental work supervision.

Conflict of interest: the authors declare no potential conflict of interest.

Received for publication: 26 May 2015.

Revision received: 22 June 2015.

Accepted for publication: 22 June 2015.

This work is licensed under a Creative Commons Attribution NonCommercial 3.0 License (CC BY-NC 3.0).

©Copyright G.C. Koubouris et al., 2015
Licensee PAGEPress srl, Italy
International Journal of Plant Biology 2015; 6:6038
doi:10.4081/pb.2015.6038

average maximum temperature in the greenhouse were 18 and 38.8°C, respectively. Each plot (three replicate plots per salinity treatment per cultivar) consisted of a separated (twin trough with a 3% slope) NFT system containing at least 10 plants. Two-year-old olive trees were fed with a complete nutrient solution.¹¹

Plants were grown for 6 months with a basic nutrient solution. Plants were subjected to 60 mM and 120 mM of NaCl which were added to the basic solution starting on the 2nd week after transplanting. To avoid osmotic shock NaCl was applied in stepped up 4-days increments of approximately 20 mM until the final level was reached. The nutrient solution was renewed regularly to avoid phenomena of toxicity or deficiency. The setpoints for pH and EC were 6 and 6 dS·m⁻¹, respectively.

During the cultivation period (6 months), the consumption of nutrient solution from the cultivars was recorded on a monthly basis. For the determination of Na and K, pooled samples of roots, young shoots, old shoots, young leaves and old leaves from 3 plants were taken, dried at 65°C for 48h, and then grounded. After extraction with diluted nitric acid for 24 h, Na

and K were determined using flame photometry (PFP-7, Barloworld Scientific T/As Jenway, Gransmore Green, UK). Regarding the plant physiology parameters that were studied, new vegetation (cm/plant) and consumption of nutrient solution (Li) were measured for comparing the tolerance of the two cultivars in the various salinity treatments.

Additionally, gas exchange measurements were made at the end of the experimental period. Ten leaves for each treatment were used to measure photosynthetic rate, stomatal conductance and intercellular CO₂ concentration (Ci) using a portable gas exchange system (LI-6400, Li-Cor Biosciences, Lincoln, NE, USA).

In order to assess pollen performance of plants grown in saline culture medium, pollen was collected from freshly opened flowers and subsequently incubated at room temperature (~22°C) in the dark for 24 h, in a growth chamber (Kottermann 2770, D3162; Hanigsen, Germany) before counting pollen germination and pollen tube length. Throughout the experiment, pollen was cultured on solid medium consisting of 0.8% (w/v) agar, 15% (w/v) sucrose, 100 ppm boric acid and 60 ppm tetracycline hydrochloride, according to Koubouris *et al.*¹⁰ Pollen germination was evaluated on five petri dish fields containing over 50 pollen grains for each treatment. Pollen tube length was measured for approximately 60 pollen tubes for each treatment.

Data were analyzed using SPSS (SPSS Inc., Chicago, USA) and were subjected to one-way analysis of variance (ANOVA). Significantly different means were calculated at P≤0.05 using least significant difference (LSD) test.

Results and Discussion

Vegetative growth of both olive cultivars was significantly affected by high salinity dose (120 mM NaCl). Indeed, overall new shoot growth was reduced both for *Koroneiki* (–75%) and *Amphissis* (–81%) (Figure 1A). However, the results of the present study indicated that *Koroneiki* may grow sufficiently at mild salinity as there were no differences among 60 mM NaCl and control treatments. In contrast, a major reduction of shoot growth (–65%) even at mild salinity (60 mM NaCl) indicates higher sensitivity of *Amphissis* under salinity conditions. Shoot elongation was reduced by salinity (up to 80 meq l⁻¹ NaCl) in *Koroneiki* but was unaffected in *Amphissis* in a previous study.¹² In fact, different salinity doses were then tested and shoot elongation was measured in four selected shoots per plant, in contrast with the present study where total plant shoot growth was monitored. Shoot elongation was also affected by salinity in other olive varieties.²

Absorption of nutrient solution from the

plants was studied as an indicator of plant nutrition functionality, since it is generally well established that saline conditions limit the vegetative development of olives, mainly as a result of interference with the osmotic balance in the root system zone.¹³ Significant reduction in the absorption of nutrient solution from the plants was recorded at high salinity dose (120 mM NaCl) both for *Koroneiki* (–86%) and *Amphissis* (–85%) (Figure 1B). Mild salinity dose (60 mM NaCl) had no effect for *Koroneiki* but suppressed nutrient absorption for *Amphissis* (–64%), which is directly related with the reduced shoot elongation and/or increased sensitivity to salinity. Reduced water absorption by olive plants grown in sand-perlite (1/1) culture in a saline medium was also reported by Therios & Misopolinos.¹²

The antagonistic role of Na⁺ and K⁺ and the negative effect of salinity on plant nutrition

were confirmed by plant tissue analysis. The Na⁺ content increased in both salinity doses compared to the control plants (Table 1). Indeed, Na accumulation was higher in *Amphissis* compared to *Koroneiki* in all plant parts. It was previously shown that salinity induces detrimental effects by specific toxic accumulation of chloride and sodium ions in the leaves.¹⁴ In the present study, the Na accumulation was increased in salinity treatments in all plant tissues – roots, stems, shoots, leaves – in both cultivars, in agreement with Melgar *et al.*¹⁵ For both *Koroneiki* and *Amphissis*, it was observed that the higher the salinity dose the higher the reduction of K concentration in plant tissues (Table 1). Similar effect was reported by several studies (*e.g.* Chartzoulakis *et al.*¹⁶) while, in contrast, higher K accumulation in salt-stressed olive leaves was reported by Melgar *et al.*¹⁵

The leaf photosynthetic rate was signifi-

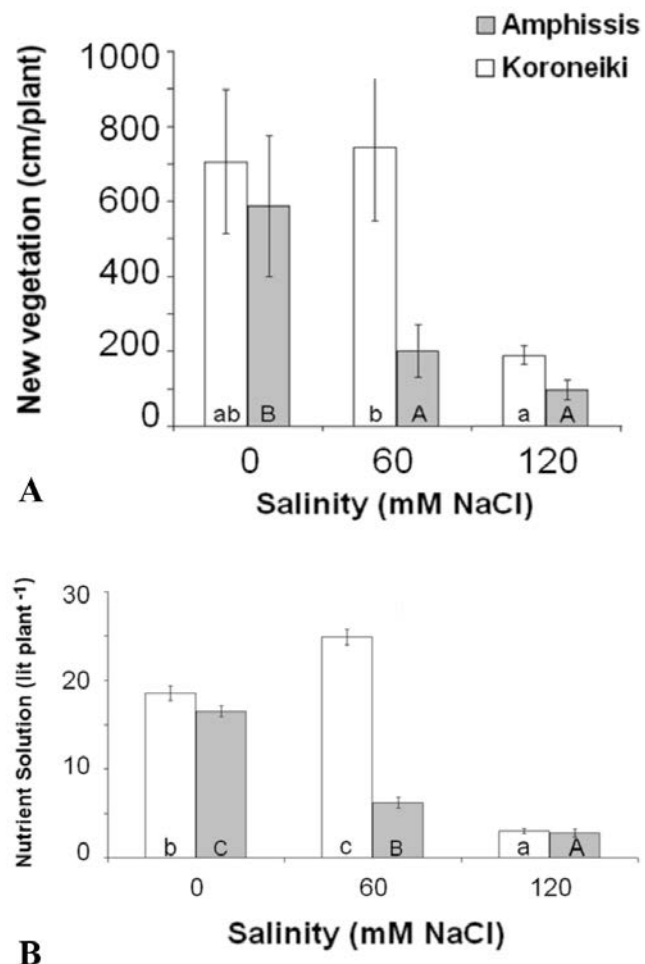


Figure 1. Influence of NaCl salinity (60 mM and 120 mM) on shoot growth of hydroponically grown olive tree *Koroneiki* and *Amphissis* in NFT (A) and on total consumption of nutrient solution of hydroponically grown olive tree *Koroneiki* and *Amphissis* in NFT (B). Each bar is mean ± standard error for each treatment. Bars with the same letter were not significantly different at P<0.05 [LSD test; n=10 (A) and n=3 (B)].

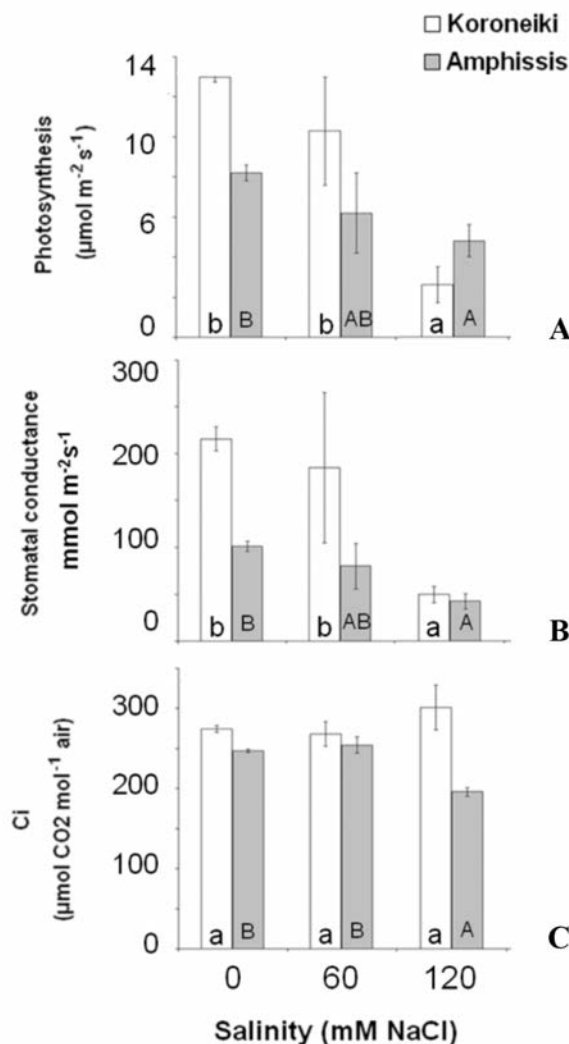


Figure 2. Influence of NaCl salinity (60 mM and 120 mM) on (A) photosynthesis rate, (B) stomatal conductance, and (C) substomatal CO_2 concentration (C_i) of hydroponically grown olive tree *Koroneiki* and *Amphissis* in NFT. Each bar is the mean \pm standard error for each treatment. Bars with the same letter were not significantly different at $P < 0.05$ (LSD test, $n=10$).

Table 1. Influence of NaCl salinity (60 mM and 120 mM) on K and Na content in different plant tissues of hydroponically grown olive tree *Koroneiki* and *Amphissis* in NFT. A composite sample from 4 plants was analyzed for each case.

Salinity (mM NaCl)	Variety	Element	% dw				
			Root	Young leaves	Old leaves	Young shoots	Old shoots
0	Koroneiki	K	1.58	2.05	2.00	1.68	0.96
60	Koroneiki	K	0.67	1.73	1.38	1.25	0.99
120	Koroneiki	K	0.70	1.20	1.03	0.92	0.81
0	Amphissis	K	0.31	2.53	2.17	2.72	1.78
60	Amphissis	K	0.49	2.29	1.73	2.47	1.43
120	Amphissis	K	0.35	1.78	1.20	1.20	0.57
0	Koroneiki	Na	0.27	0.24	0.25	0.31	0.20
60	Koroneiki	Na	0.27	0.44	0.57	0.39	0.36
120	Koroneiki	Na	1.70	1.33	1.87	1.56	1.05
0	Amphissis	Na	0.08	0.19	0.16	0.25	0.21
60	Amphissis	Na	0.71	1.19	1.16	1.76	1.09
120	Amphissis	Na	1.01	1.96	2.34	2.28	0.78

cantly reduced at 120 mM NaCl for both cultivars with greater effects observed in *Koroneiki* (Figure 2A). This result is in agreement with Loreto *et al.*¹⁷ who reported that when olive trees exposed to salt stress, cultivars with inherently high photosynthesis showed the highest photosynthetic reductions. However, sufficient carbon assimilation was retained at intermediate salinity level (60 mM) for both cultivars compared to reference values reported for olive at normal conditions.^{18,19}

Besides photosynthetic rate, in both cultivars, stomatal conductance was influenced by salinity in a very similar way (Figure 2B). Specifically, the reduction on stomatal conductance declined to high salinity for *Koroneiki* (–78%) and for *Amphissis* (–60%) which is in accordance with previous studies.¹⁶ In the present study, salinity (120 mM) significantly reduced intercellular CO_2 concentration (C_i) of *Amphissis*, however, no such effect of either salinity doses was observed for *Koroneiki* (Figure 2C). These results show that the reduction of photosynthesis in salt-stressed *Koroneiki* leaves is attributable to stomatal resistance, while for *Amphissis* both stomatal and mesophyll resistances are involved as it has been also reported previously for other olive cultivars.²⁰ The simultaneous existence of biochemical limitations to photosynthesis such as carboxylation rate and efficiency is also common in salt-stressed olive leaves.²⁰ Impairment of the photosynthetic apparatus by salinity was also indicated by a reduction in chlorophyll and carotenoids content (43% and 44%, of the controls respectively at 120 mM NaCl; data not shown).

Inflorescences in *Amphissis* were severely damaged due to salinity. Consequently, pollen sampling and *in vitro* germination study was only feasible for *Koroneiki*. This also highlights the increased sensitivity to salinity damage of *Amphissis* compared with *Koroneiki* as

the reproductive phase of the tree, being more sensitive and susceptible to stresses, was more damaged compared to the vegetative part of the tree (*i.e.* stems and leaves). Indeed, *Koroneiki* pollen germination was reduced at 60 mM NaCl (–42%) and at 120 mM NaCl (–88%) as presented in Figure 3A. Pollen tube length was also reduced by 15% and 28% for the mild and high salinity dose, respectively (Figure 3B).

Data on olive pollen germination in response to salinity are scarce. In olive, pollen performance is reduced at high temperature,¹⁰ similarly with photosynthetic activity.⁹ A number of previous studies are in agreement with the present results highlighting the increased importance and scientific interests on salinity effects on crops. In a previous study on 5 *Pistacia* species, pollen was found to be more sensitive to salinity compared to seeds.²¹ Exposure of 3 *Cicer arietinum* L. varieties to salinity induced reduction of pollen production, germination and tube length, especially at higher doses.²² Similarly, reduced pollen viability and germination was observed for *Brassica napus* L. plants previously irrigated with sea water solutions.²³ In a relevant study on *B. napus* L., pollen germination was shown

to better reflect overall plant sensitivity to salt stress compared to pollen tube length,²⁴ which also reflects and supports the present findings as the pollen germination provided clearer evidence on salinity effects compared to data pertaining to pollen tube length.

In order to overcome the water deficit due to increased water needs in agriculture, many countries may have to use water of lower quality such as saline water or treated waste water. In order to achieve that, however a detailed study of the effects of salinity on plants must be performed. This study elucidates the response to salinity stress of two major olive cultivars in Greece, *Koroneiki* and *Amphissis*, through several physiological and reproductive indicators. Specifically, the findings of this work indicate that *Amphissis* physiological processes are more sensitive in high salinity doses compared to *Koroneiki*. However, olive tree response to salinity may vary as influenced by agronomic practices *e.g.* proper leaching methodology,²⁵ soil type and precipitation intensity and distribution in the area of cultivation. The results of the present study also indicate that reproductive functions are severely affected by salinity. Therefore, future salinity studies would benefit from addition of

reproductive indicators to investigate whether a plant can not only grow but also produce sufficiently under saline conditions.

References

1. Paranychianakis NV, Chartzoulakis KS. Irrigation of Mediterranean crops with saline water: From physiology to management practices. *Agricult Ecosyst Environ* 2005;106:171-87.
2. Perica S, Goreta S, Selak GV. Growth, biomass allocation, and leaf ion concentration of seven olive (*Olea europaea* L.) cultivar under increased salinity. *Sci Hort* 2008;117:123-9.
3. Tattini M, Traversi ML. On the mechanism of salt tolerance in olive (*Olea europaea* L.) under low or high-Ca²⁺ supply. *Environ Exper Bot* 2008;65:72-81.
4. Chartzoulakis K, Loupassaki M, Bertaki M, Androulakis I. Effects of NaCl salinity on growth, ion content and CO₂ assimilation rate of six olive cultivars. *Sci Hort* 2002;96:235-47.
5. Benlloch M, Ojeda MA, Ramos J, Rodriguez-Navarro A. Salt sensitivity and low discrimination between potassium and sodium in bean plants. *Plant Soil* 1994;166:117-23.
6. Chondraki S, Tzerakis C, Tzortzakis N. Influence of NaCl and calcium foliar spray on hydroponically grown parsley in NFT system. *J Plant Nutr* 2012;35:1457-67.
7. Tzortzakis NG. Influence of NaCl and calcium nitrate on lettuce and endive growth using nutrient film technique. *Int J Veget Sci* 2009;15:1-13.
8. Chaves MM, Maroco JP, Pereira JS. Understanding plant responses to drought-from genes to the whole plant. *Funct Plant Biol* 2003;30:239-64.
9. Koubouris GC, Kavroulakis N, Metzidakis IT, et al. Ultraviolet-B radiation or heat cause changes in photosynthesis, antioxidant enzyme activities and pollen performance in olive tree. *Photosynthetica* 2015;53:279-87.
10. Koubouris GC, Metzidakis IT, Vasilakakis MD. Impact of temperature on olive (*Olea europaea* L.) pollen performance in relation to relative humidity and genotype. *Environ Exper Bot* 2009;67:209-14.
11. Economakis CD, Daskalaki AA, Metzidakis IT. Seasonal variation in water and nutrient uptake by olive plants grown in solution culture. *Proceedings of the International Symposium on the Olive Tree and the Environment* 2003;85.
12. Therios I.N, Misopolinos ND. Genotypic response to sodium chloride salinity of four major olive cultivars (*Olea europaea*

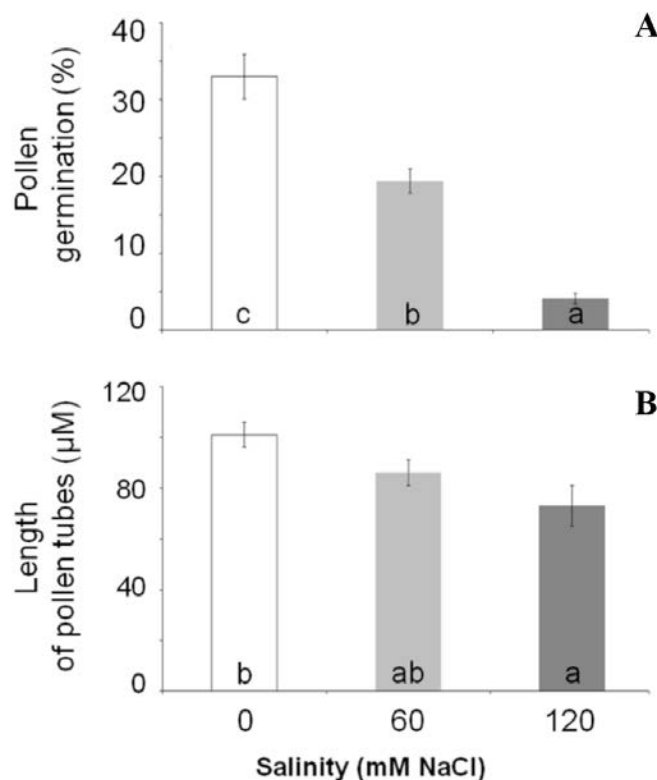


Figure 3. Effect of NaCl salinity (60 mM and 120 mM) on (A) pollen germination (n=250) and (B) length of pollen tubes (n=60) for hydroponically grown olive tree *Koroneiki* in NFT. *Amphissis* pollen was unavailable due to salinity-induced damaged inflorescences. Each bar is the mean \pm standard error for each treatment. Bars with the same letter were not significantly different at $P < 0.05$ (LSD test).

- L.). *Plant Soil* 1988;106:105-11.
13. Tattini M. Ionic relations of aeroponically-grown olive genotypes during salt stress. *Plant Soil* 1994;161:251-6.
 14. Hassan MM, Seif SA, Morsi ME. Salt tolerance of olive trees. *Egypt J Horticult* 2000;27:105-16.
 15. Melgar JC, Syvertsen JP, Martinez V, Garcia-Sanchez F. Leaf gas exchange, water relations, nutrient content and growth in citrus and olive seedlings under salinity. *Biol Plant* 2008;52:385-90.
 16. Chartzoulakis K, Psarras G, Vemmos S, et al. Response of two olive cultivars to salt stress and potassium supplement. *J Plant Nutr* 2006;29:2063-78.
 17. Loreto F, Centrito M, Chartzoulakis K. Photosynthetic limitations in olive cultivars with different sensitivity to salt stress. *Plant Cell Environ* 2003;26:595-601.
 18. Sofo A, Dichio B, Xiloyannis C, Masia A. Lipoxygenase activity and proline accumulation in leaves and roots of olive trees in response to drought stress. *Physiol Plant* 2004;121:58-65.
 19. Sofo A, Dichio B, Xiloyannis C, Masia A. Antioxidant defences in olive trees during drought stress: changes in activity of some antioxidant enzymes. *Funct Plant Biol* 2005;32:45-53.
 20. Centrito M, Loreto F, Chartzoulakis K. The use of low [CO₂] to estimate diffusional and non-diffusional limitations of photosynthetic capacity of salt-stressed olive saplings. *Plant Cell Environ* 2003;26:585-94.
 21. Martinez-Palle E, Herrero M, Aragues R, et al. Salt response of seeds and pollen of five *Pistacia* species. *Acta Hort* 1995;419:49-54.
 22. Dhingra HR, Varghese TM. Flowering and male reproductive functions of chickpea (*Cicer arietinum* L.) genotypes as affected by salinity. *Biol Plant* 1993;35:447-52.
 23. Gul H, Ahmad R. Effect of salinity on pollen viability of different canola (*Brassica napus* L.) cultivars as reflected by the formation of fruits and seeds. *Pak J Bot* 2006;38:237-47.
 24. Tyagi RK, Rangaswamy NS. Screening of pollen grains vis-à-vis whole plants of oilseeds brassicas for tolerance to salt. *Theor Appl Genet* 1993;87:343-6.
 25. Wiesman Z, Itzhak D, Ben Dom N. Optimization of saline water level for sustainable Barnea olive and oil production in desert conditions. *Sci Hort* 2004;100:257-66.

In vitro culture as an aid to conservation of indigenous ferns: *Diplazium proliferum*

Zubeir M. Golamaully,¹
Vishwakalyan Bhoyroo,¹
Nadeem Nazurally,¹
Vineshwar Gopal²

¹Faculty of Agriculture, University of Mauritius, Reduit; ²National Parks and Conservation Services, Reduit, Mauritius

Abstract

With the ever growing population and economic needs of Mauritius, the flora of Mauritius has never been in more danger and one group of vascular plants is even more in peril; ferns. *Diplazium proliferum* is indigenous to the Mascarene region and is considered as a rare species in Mauritius. The need to develop a tested *in vitro* propagation protocol is a must to protect the biodiversity of Mauritius. This experiment was geared towards the establishment of a proper sterilization technique and the effect of 6-benzylaminopurine (BAP) and light on *in vitro* culture of this fern. Sterilization with 0.05% Mercuric chloride was effective to eliminate fungal contamination and allow germination of spores. Culture media supplemented with BAP did not significantly increase growth rate of both gametophytes and sporophytes of *D. proliferum*. Present results suggest efficient sterilization methods to be a crucial stage for successful *in vitro* regeneration of ferns. The established protocol will be used as an optimized baseline protocol for the propagation of other indigenous ferns.

Introduction

Ferns are referred to as the *disaster taxa* since during intervals of environmental stress; they are the early pioneers to a newly stripped landscape.^{1,2} The ground work established on the status of ferns in Mauritius began with the project *Flore des Mascareignes*. The initiative was to describe all the higher plants species and ferns in the Mascarenes. While being near its completion, it has revealed more than 100 new species. Before its colonization, the island of Mauritius was entirely covered with forest. Today, not only about 5% of the native forest is remaining which sums up to about 100 km², but it is also threatened by alien invasive species. 40% of the native flora has been categorized as threatened and about 39 plant

species has been confirmed as extinct.

There are four main stages of the growth of a fern from its spore i) the sporophyte or fern plant, ii) nonsexual spores produced as a result of reduction division, iii) gametophyte or thallus plant, iv) oospores produced as the result of the conjugation of egg and sperm. When a spore germinates, it produces a small filament (protonema). Development of the gametophyte occurs through two stages. In the first stage, the plant shape is a linear aggregate and in the second stage, it is a solid aggregate. The thallus is hermaphrodite and hence can develop several spermaries and ovaries on the lower region. Fertilization occurs when a spermatozoid passes down the neck to the egg to conjugate with it. The developing embryo is completely parasitic to the parent plant which provides it with nutrients. Finally the embryo breaks free from the enlarged venter of the archegonium to grow roots in the ground below while a first leaf develops towards the light shifting from a parasitic stage to an independent one.³ Gametophytes that germinate from the single celled spore are the source from which a homosporous fern's bisexual gametophyte are mitotically derived. The self-fertilization of a sperm and egg of a single gametophyte that are genetically similar will yield a sporophyte that is instantly homozygous at all *loci* on its homologous chromosomes.⁴ *In situ* conservation of ferns and their allies in their natural habitats should always be the main aim. However, this is not always possible; hence, additional methods are required to support and complete the *in situ* methods which will increase the probability of survival of the individual species.⁵ Several reports of *in vitro* propagation of spores have shown success in their cultivation but have indicated a considerable loss of spores during the sterilization process, aseptic sowing or due to contamination which have led to the development of different spore sterilization and sowing methods.⁶ *In vitro* germination of spores and following prothallus development and subsequent sporophyte growth can bypass some of the difficulties linked with conventional methods. These difficulties include: low germination rates, contamination with prothalli from invasive species and the growth of too few sporophytes. Successful *in vitro* germination of rare species are *Cibotium schiedei* from Central America and *Angiopteris boivinii* from the Seychelles.⁷

Spores viability can vary drastically among pteridophytes; from a few days to a few years. It has been understood that the genetic make-up and a few physiological characteristics of spores need to be reviewed to understand the spores' viability variations.⁸ Factors such as spore type, chlorophyllous and non-chlorophyllous or taxonomic region can affect the viabil-

Correspondence: Vishwakalyan Bhoyroo, Department of Agricultural and Food Sciences, Faculty of Agriculture, University of Mauritius, Reduit, Mauritius.
Tel.: +230.797.8038; Fax: +230.403.7830.
E-mail: v.bhoyroo@uom.ac.mu

Key words: Ferns; *in vitro* culture; *Diplazium proliferum*; conservation.

Acknowledgements: this project was supported by the National parks and Conservation Services (Mauritius). Laboratory facilities were provided by the Faculty of Agriculture and the whole project was funded by the University of Mauritius. We also extend our gratitude to Mr Pynee of the MSIRI for providing accession numbers.

Contributions: the authors contributed equally.

Conflict of interests: the authors declare no potential conflict of interest.

Funding: this project was funded by the University of Mauritius and supported by the National Parks and Conservation Services.

Received for publication: 16 May 2015.

Accepted for publication: 24 July 2015.

This work is licensed under a Creative Commons Attribution NonCommercial 3.0 License (CC BY-NC 3.0).

©Copyright Z. M. Golamaully et al., 2015
Licensee PAGEPress srl, Italy
International Journal of Plant Biology 2015; 6:6020
doi:10.4081/pb.2015.6020

ity of spores The high rate of respiration or inability to recover photosynthetic properties after desiccation in green spores has been proposed as the cause of quick decrease of viability. Lloyd and Klekowski (1970) have compared the viability of green spores (chlorophyllous) and non-green spores (non-chlorophyllous) and noticed that green spores germinate faster than non-green spores; however, this property to germinate is lost quickly over time.⁹ Furthermore, their data has shown that under laboratory conditions, green spores have short life span (48 days) while the non-green spores live on to about 2.8 years. It has also been suggested that the short viability of green spores of *Equisetum hyemale* L. may be due to the loss of its photosynthetic ability when the spores are rehydrated following desiccation. While the factors influencing viability of spores are known, little is known about those affecting the spores under herbarium conditions.⁵

D. proliferum is a rare fern restricted to few forest areas in Mauritius and is listed among the top priorities for immediate propagation and conservation by The Nation Parks and Conservation Services. This study aims to

develop a tissue culture protocol for the propagation of this wild fern, including defining key stages for successful micropropagation such as sterilization steps and culture condition.

Materials and Methods

After acquisition of proper permits to collect samples, mature leaflets of *Diplazium proliferum* (accession number: MAU 26445) were kindly provided by the National Parks and Conservation. Mature leaflets (Figure 1A) were allowed to air dry prior to collection of spores. Dried leaves were scrapped with a scalpel on a sheet of paper and the spores that fell on the paper were transferred in a corning tube. Spore surface sterilization were carried in the 3 following methods i) treatment 1: 2% Sodium Hypochlorite;¹⁰ ii) treatment 2: 2% Sodium Hypochlorite and 1 g/L Nystatin (fungicide) and iii) treatment 3: 1%, 0.1% and 0.05% Mercuric chloride (HgCl₂). Basal Murashige and Skoog's (1962) media was used as control (n≥50) and 1 mg/L 6-Benzylaminopurine (n≥50) was tried as a growth promoter for spore germination.¹¹ Cultured pots were partly kept in total darkness in an incubator and partly in light condition for daily 16 hours photoperiod. All experiments were done in aseptic conditions. Following the growth of some sporophytes, the media became insufficient and sub-culturing had to be done. Sporophytes were removed from the media and cut in pieces and inoculated in fresh media (with and without BAP).

Growth rates were measured as surface areas of growing sporophytes using digital photography. Photographs of growing explants were taken with a scale stuck to the wall of culture pots. Surface areas were calculated using Scion Image software. The values obtained were calculated as mean and significant growth differences between treatments were calculated following Mann-Whitney U test in SPSS 16.0. Mann-Whitney U test was used since the samples obtained in the experiments were not normally distributed and had unequal sample size due to different contamination levels.¹²

Results

First response occurred after 35 days in light (Figure 1B). Different growth phases from the inoculation of spores to the development of green gametophyte stage and consequently to the sporophyte stage with appearance of first leaflets were observed (Figure 2A-C). Slurry like gametophyte usually dries up and then small callus started to form (Figure 2D-F).

Sterilization with 2% sodium hypochlorite gave too much contamination following the inoculation and the spores did not germinate at all. Supplementing with a fungicide, Nystatin, also gave high contamination levels. Treatments with 1% and 0.1% mercuric chloride resulted in minimal contamination levels but no germination were observed at all. Mercuric chloride at 0.05% was efficient for sterilization and the germination rate was 51% with this treatment (Figure 3A).

Germination occurred irrespective of presence or the absence of BAP. Furthermore, the rate of development of the gametophytes and sporophytes was not significantly faster (Mann-Whitney U, P>0.05) though higher rates were observed with BAP (Figure 3B,C). The growth rate over the 4 month appeared to

be favored by the presence of BAP in the culture media with greater rate of development beginning from the 2nd month. From month 3, the drop in surface area was due to the sub-culturing carried out. However quickly after in month 4, the growth rate spurred back.

Discussion and Conclusions

Although sodium hypochlorite was reported as an effective and non damaging surface sterilizer, it was not effective in this experiment and extensive contamination was obtained. Interestingly it was reported that surface sterilization of *Cyathea gigantea* spores at 30% sodium hypochlorite proved to be effective.¹³



Figure 1. *Diplazium proliferum*: A) mature leaves with Sporangia clusters on back of leaves; B) cells at gametophytic stage viewed under compound microscope.

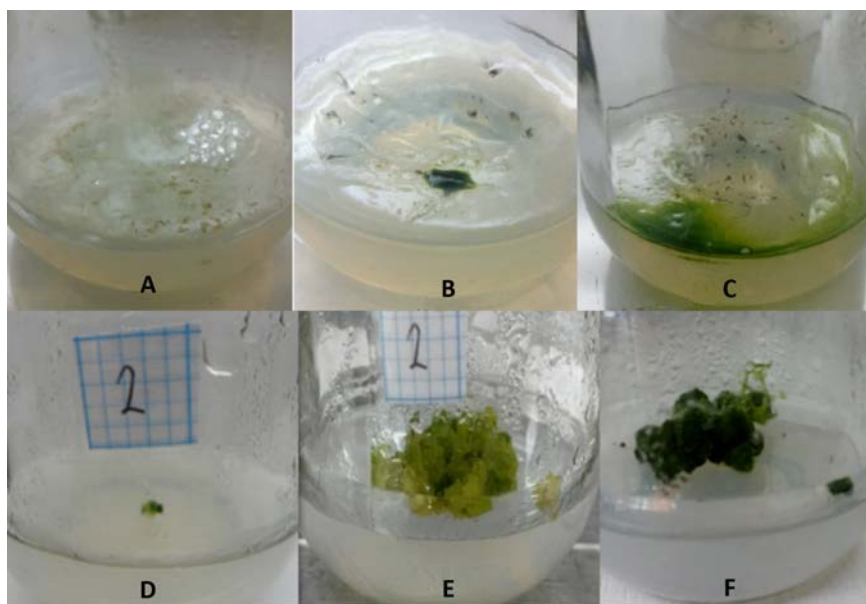


Figure 2. A-C) The development of spores to gametophytic stage: A) inoculated spores, B) initial growth of gametophytes, C) slurry of gametophytes. D-F) Development of sporophyte to small plantlets (shoots): D) initial subcultured tissue, E) increase in size of sporophyte, F) appearance of first leaves.

With lower concentration, the sterilization was not successful and when used above 30% the mortality rate was too high. However, for the sterilisation of spores of *Diplazium proliferum*, 2% sodium hypochlorite proved to be inefficient against fungal contaminants. Since most of the contamination present appeared to be fungal, a fungicide (Nystatin) was used in

addition to 2% sodium hypochlorite.¹⁴ However, this also proved to be inadequate since, fungal contamination persisted. A stronger sterilizing agent had to be used, since, no success had been made in neutralizing the unwanted microorganisms that were proving to be a major cause preventing germination. Since, mercuric chloride has shown

itself as a very strong decontamination agent, its use made sense. Several reports showed promising results from the use of mercuric chloride.¹⁵⁻¹⁷ The use of 1% and 0.1% was too strong and rendered the spores infertile however, the use of 0.05% produced viable sterile spores which led to the formation of gametophytes for *Diplazium proliferum*.

The germination of spores varies depending on their taxonomy.⁹ For spores to germinate, it must first have achieved maturation. This is difficult to determine specially in the understudied *Diplazium* family. Several factors may affect spore maturation such as the cause-effect relationship whereby dry weather, high temperature and low humidity favored release of mature spores.¹⁸ Once spores had germinated it would give rise to a gametophyte which produces a sporophyte if successful fertilization occurs. This series of events is dependent on many factors. While germination of a spore will most probably give rise to a prothallus, it will not necessarily guarantee a sporophyte. This can be explained by the fact that all the gametophytes that emerged were hermaphroditic that is without the presence of an egg and a sperm simultaneously, no sporophyte could emerge regardless of other factors. Presence of lethal or semi lethal genes following fusing of an egg and sperm will ensure that the sporophyte dies. The genotype of this gametophyte is deadly in the homozygous state. This phenomenon and found that in seven population of *Osmunda regalis* from which he obtained 109 sporophytes, all possessed at least 1 form of lethal gene in heterozygous condition.¹⁹ Though BAP was reported to positively affect the growth of ferns *in vitro*,²⁰ it did not significantly increase the growth rates for *Diplazium proliferum*. However, it should be noted that the non-uniformity in the data obtained was mainly due to the problem of contamination. This study proved that sterilization of spores for *in vitro* culture is a very crucial stage for successful *in vitro* propagation of ferns from spores.

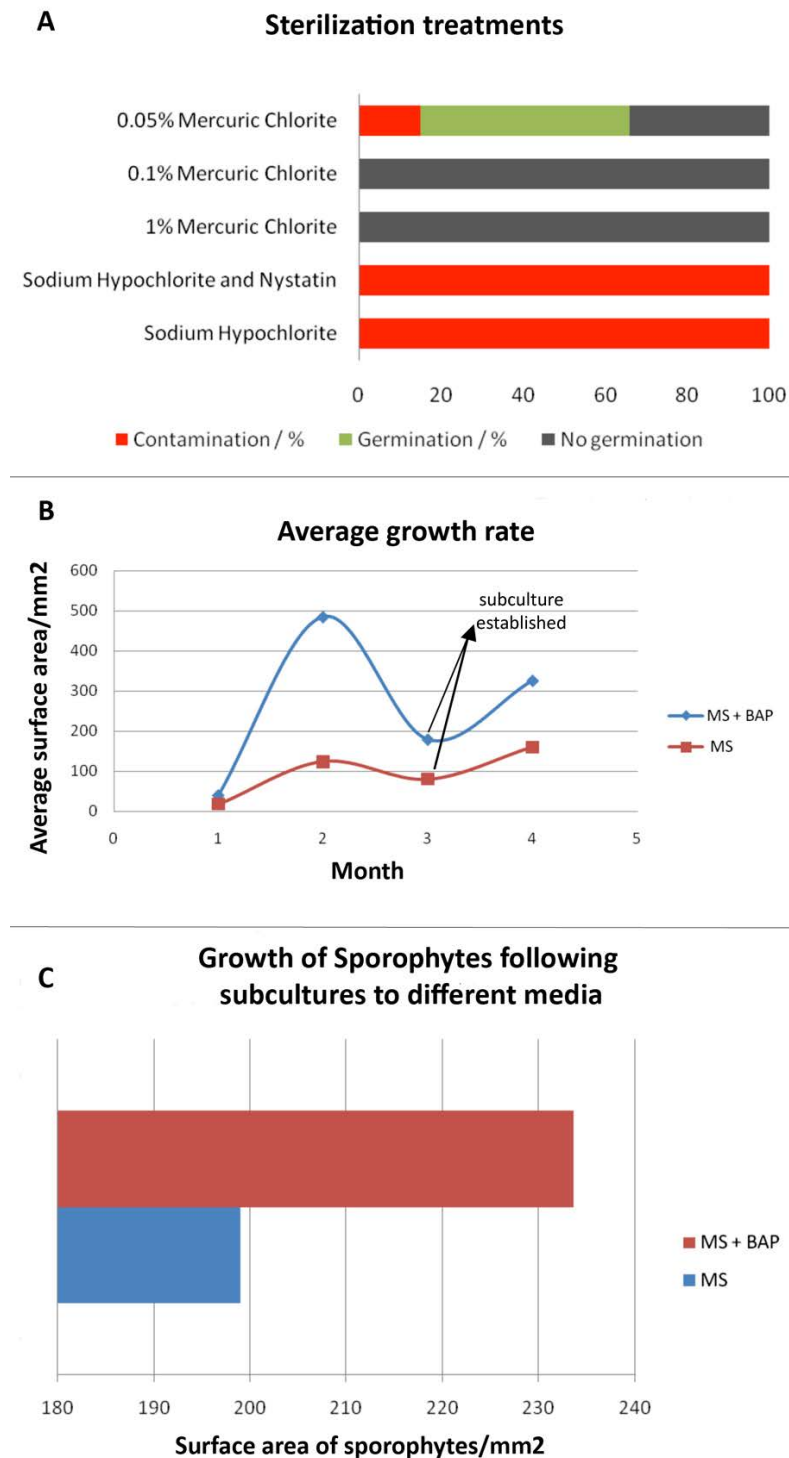


Figure 3. Efficiency of sterilization treatments (A), average growth rate from spores inoculated (B) and difference in growth of sporophytes after subculturing (C).

References

1. Tschudy RH, Pillmore CL, Orth CJ, et al. Disruption of the terrestrial plant ecosystem at the Cretaceous-Tertiary boundary, Western Interior. *Science* 1984;225:1030-2.
2. McElwain JC, Punyasena S. Mass extinction events and the plant fossil record. *Trends Ecol Evol* 2007;22:548-57.
3. Schaffner JH. A life cycle of a Homosporous pteridophyte. *Ohio J Sci* 1906;6:485-8.
4. Nakazato T, Jung MK, Housworth EA, et al. Genetic map-based analysis of genome structure in the homosporous fern

- Ceratopteris richardii. Genetics 2006;173:1585-97.
5. Magrini S, Olmati C, Onofri S, Scoppola A. Recovery of viable germplasm from herbarium specimens of *Osmundaregalis* L. *Am Fern J* 2010;100:159-60.
 6. Hua W, Chen PT, Yuan LP, Chen LQ. An efficient method for surface sterilization and sowing Fern spores in vitro. *Am Fern J* 2009;99:226-30.
 7. Fay MF. Conservation of rare and endangered plants using in vitro methods. *In Vitro Cell Dev Biol* 1992;28:1-4.
 8. Camloh M. Spore age and sterilization affects germination and early gametophyte development of *Platyserium bifurcatum*. *Am Fern J* 1999;89:124-32.
 9. Lloyd RM, Klekowski EJ Jr. Spore germination and viability in Pteridophyta: evolutionary significance of chlorophyllous spores. *Biotropica* 1970;2:129-37.
 10. Knauss JF. A partial tissue culture method of pathogen-free propagation of selected ferns from spores. *Proc Florida State Horticult Soc* 1976;8:848-52.
 11. Murashige T, Skoog F. A revised medium for rapid growth and bio-assays with tobacco tissue cultures. *Physiol Plant* 1962;15:473-97.
 12. Nachar N. The Mann Whitney U: a test for assessing whether two independent samples come from the same distribution. *Tutorials Quant Methods Psychol* 2008;4:13 20.
 13. Das B, Tania P, Kishori GA, et al. Evaluation of antioxidant potential & quantification of polyphenols of *Diplazium esculentum* Retz. with emphasis on its HPTLC chromatography. *J Pharm Res* 2013;6:93-100.
 14. Brumback WE. Raising the climbing fern from spores. *Arnoldia* 1985;45:27-9.
 15. Danso KE, Azu E, Elegba W, et al. Effective decontamination and subsequent plantlet regeneration of sugarcane (*Saccharum officinarum* L.) in vitro. *Int J Integr Biol* 2011;11:90-6.
 16. Puchooa D. In vitro regeneration of lychee (*Litchi chinensis* Sonn.). *Afr J Biotechnol* 2004;3:576-84.
 17. Badoni A, Chauhan JS. In vitro sterilization protocol for micropropagation of *solanum tuberosum* cv. Kufri Himalini. *Academia Arena* 2010;2:24-7.
 18. Arosa ML, Quintanilla LG, Ramos JA. Spore maturation and release of two evergreen macaronesian ferns, *Culcita macrocarpa* and *Woodwardia radicans*, along an altitudinal gradient. *Am Fern J* 2009;99:260-72.
 19. Klekowski EJ Jr. Populational and genetic studies of a homosporous fern-*osmunda regalis*. *Am J Botany* 1970;57:1122-38.
 20. Bonomo MC, Martínez OG, Tanco ME, et al. Spores germination and gametophytes of *Alsophila odonelliana* (Cyatheaceae) in different sterile media. *YTON* 2013;82:119-26.

Spatial constraints also regulates final achene mass in the sunflower (*Helianthus annuus* L.) capitulum

Luis F. Hernández

Laboratorio de Morfología Vegetal,
Departamento de Agronomía,
Universidad Nacional del Sur, Bahía
Blanca, Comisión de Investigaciones
Científicas de la Pcia de Buenos Aires, La
Plata, Argentina

Abstract

In capitula of the cultivated sunflower (*Helianthus annuus* L.) achene size and mass commonly decrease from proximal to distal positions. Temporal limitation of resources of the distal achenes over the proximal ones has been the common explanation for this response. Nevertheless, because the capitulum architecture and expansion dynamics also interacts with achene growth and development, also space exert a coupled effect with resources on achene size along the inflorescence radius. In this work we removed young achenes from different capitulum positions [inner sector (IS) and outer sector (OS)] and applied an artificial restriction to the capitulum/achenes radial expansion. Removal of outer achenes significantly increased the final dry mass of the remnant ones between 17.1 to 27.6%. Removal of inner achenes also produced the same effect but in less magnitude, between 9.3 to 17.9% of the outer ones. The removal of outer achenes with the application of an artificial peripheral constraint did not significantly increase the dry mass of the remnant ones (2.7% of the inner and 7.1% of the control). Percentage of empty achenes significantly diminished in the middle sector (MS) in capitula with the outer achenes removed and in capitula with the outer achenes removed plus a peripheral constraint but in the range of 7.1% (MS achenes) and 2.7 % (IS achenes). Percentage of empty achenes of the MS did not change when the outer achenes were removed but was significantly lower when the OS was removed and the peripheral constraint was applied. This results suggest that a part of the reduced growth and development of IS and MS achenes is not only controlled by the competition for resources but also is restricted by space and pressure exerted by the neighboring ones.

Introduction

Sunflower grain yield is mainly determined by the number of achenes produced in the inflorescence (capitulum) and their average mass.^{1,2} Also, in the production of hybrid sunflower seed, achene size and homogeneity are important determinants of seed quality.³ Achene size and/or achene set diminution into an inflorescence have been to occur in several species.⁴ These were attributed either to competition for resources,^{5,7} or to architectural constraints such as reduced vascular ways to supply photoassimilates to the sinks.⁸⁻¹⁰

The physiological mechanisms that regulate these processes are complex. Nevertheless experiments made in the sunflower, where the source/sink relationship was changed, show that achene size differences along the radial length of the capitulum, *i.e.* from the periphery towards its center (peripheral to distal positions), are due from insufficient assimilate supply from the sources.^{2,11-15} Besides these well documented evidences, few works on achene development in Asteraceae inflorescences have been focused on to the relationship of maximum achene mass or size and the positional incidence following achene or inflorescence growth. For example it has been observed in *Tragopogon porrifolius* L. (Asteraceae) that the removal of external achenes during capitulum development resulted in heavier internal achenes, while it was not the case when internal achenes were removed.¹⁶ On the other hand it is known that into a developing capitulum, space for floret or achene development changes on time and can play a relevant role in controlling the final floret number or achene size and eventually achene mass. For example, in young sunflower plants, the external application of cytokinins,¹⁷⁻¹⁹ or surgical removal of the involucre bracts at early stages of capitulum development,¹⁸ both ways to increase the size or the meristematic surface of the still undifferentiated receptacle into floret primordia, significantly increased the number of florets and, at maturity, the number of achenes per plant.

The selective removal of flowers in different sectors of the sunflower capitulum, external, middle and internal, generated a significant increase in the mass of achenes of the inner region of the capitulum as well as reduced the number of empty achenes, while it was not so and the effect was much smaller with the reverse treatment.²⁰ In this case, the experiment was able to show the positional effect in terms of the demand for photoassimilate in

Correspondence: Luis F. Hernández. Laboratorio de Morfología Vegetal, Departamento de Agronomía, Universidad Nacional del Sur, Bahía Blanca, 8000, Argentina.
Tel.: +54.0291.4566.130 - Fax: +54.0291.4595127.
E-mail: lhernan@criba.edu.ar

Key words: Architectural constraints; *Helianthus annuus* L.; flower removal; achene; sunflower.

Acknowledgements: Sunflower seed was kindly provided by Dr. C.A. Sala, Nidera Argentina. The valuable assistance in sample processing by Mrs. G.M. Abrego and Mr. M.E. Sanders is greatly appreciated.

Conflict of interest: the author declares no potential conflict of interest.

Funding: this work was supported by grants to L.F.H. of the Secretaría Gral. de Ciencia Tecnología (SeGCyT-UNS) and the Comisión de Investigaciones Científicas (CIC, La Plata) Argentina.

Received for publication: 13 May 2015.
Accepted for publication: 25 July 2015.

This work is licensed under a Creative Commons Attribution NonCommercial 3.0 License (CC BY-NC 3.0).

©Copyright L.F. Hernández, 2015
Licensee PAGEPress srl, Italy
International Journal of Plant Biology 2015; 6:6014
doi:10.4081/pb.2015.6014

different capitulum positions.

So not only available resources but also physical limitations (space) could be acting to control the final achene number and size into the capitulum.

Intra-flower competition in inflorescences have not been deeply studied. An unique and elegant example was given by Jeune and Barabé,²¹ who explored with a mathematical approach the geometrical and biophysical rules that affect the spatial arrangement of inflorescence components in the Araceae. They compared the structure of the compact inflorescences of this family with a theoretical structure, where the average number of sides of floral primordia neighboring an *n*-sided primordium was determined by physical laws. They observed that a discrepancy between the measured shape and organization of those inflorescences and those predicted by theory was accounted for by the effect of physical constraint due to the proximal environment of developing primordia.

In the present study we examined the relative

influences of capitulum architecture and whole plant resources as mechanisms for setting achene production in sunflower. So an accurate determination of the rate of development of the remaining achenes after performing the process of selective removal of flowers in various parts of the sunflower capitulum was performed.

Materials and Methods

Plant material

Seeds of the inbred line HA89-B were sown under field conditions in Pedro Luro, Argentina (39°26'S; 62°40'W). The soil of the experimental site is a Udic haplustol with sandy texture and low organic matter content (2.2%).²² Plants were grown at a crop population density at flowering of 6 plants/m². Plot size was 5 rows × 15 m with an inter-row spacing of 0.70 m.

The crop was managed according to the recommended conventional agronomical practices.²³ Environmental conditions during crop growth kept soil water content above 50% of maximum soil available water. When necessary, soil water was supplemented by furrow irrigation. Nutrient deficiencies were prevented with pre-planting and pre-flowering fertilization with nitrogen (60 Kg N.ha⁻¹) applied as NO₃K. Weeds were controlled manually. Insect pests were not an important factor during the whole growing season.

During the study, mean air temperature (°C) and solar radiation (μmol.m⁻²s⁻¹) were daily recorded with two-hour interval using a WS-GP1 Compact Automatic Weather Station (Delta-T Devices Ltd., Cambridge, UK). Maximum and minimum temperatures during the reproductive period as well as average

daily incident radiation were between the range of optimum magnitudes for sunflower.¹ Table 1 summarizes the seasonal pattern shown by the environmental variables registered during the experimental period.

Flower removal experiments

Crop phenology was followed every two-three days from emergence to harvest maturity. Vegetative and reproductive development observations followed the Schneider and Miller scale.²⁴ When plants reached first anthesis (FA; phenological stage R5.1)²⁴ 180 plants were labeled for experimentation.

Treatments started in these selected plants between late R7 and early R8.²⁴ At that time achene filling in the peripheral flowers had begun.²⁵ At R8 all flowers had reached full development within the inflorescence.

Four localized source/sink modifications treatments were performed: *outer flowers removed* (OR; Figure 1A), in which flowers in the outer third of the capitulum radius were removed, *inner flowers removed* (IR; Figure 1B), in which the inner third of flowers was removed. Control, in which inflorescences were not manipulated (Figure 1C) and *outer flowers removed + perimetral constraint*

(OR+PC; Figure 1D). In this treatment, after the flowers of the outer third of the capitulum radius were removed, a semi-elastic ring of high density expanded polystyrene 2.5 cm thick was applied to partly restrain its radial expansion during achene growth and capitulum maturation. To retain the ring onto the receptacle, 4 stainless steel clips equally distributed on the receptacle surface were used (Figure 1D). During the period of capitulum maturation, rings were observed to be always kept in position. At the beginning of this last procedure capitulum diameter of selected plants averaged 9.3±1.3 cm.

The number of flowers removed in the treatment where outer flowers were removed was between 5 to 10% higher than that in the treatment where inner flowers were removed.

Achene dry mass determination

Starting from the treatment day, achenes from three capitulum sectors, external (ES), middle (MS) and internal (IS), each equal to 1/3 of the capitulum radius were harvested every 3 to 7 days up to harvest maturity (HM). At each harvest time, 10 achenes per plant were taken from 3 selected plants per plot that had not been sampled previously. Ovaries were

Table 1. Mean environmental data for three developmental crop phases. Crop phase A represents the 15-d interval centered on the mean date of full anthesis. Crop interval S-A is the time elapsed between sowing and 7 days before the mean date of full anthesis. A-PM is the interval between 7 days after full anthesis the date of PM.

Environmental factor	Plant developmental phase		
	S-A	A	A-PM
Max. temperature, °C	22.6	25.2	31.5
Min. temperature, °C	13.2	17.1	14.8
Daily incident radiation, MJ m ⁻²	22.3	23.2	21.7

A, anthesis; S, seeding time; PM, physiological maturity.

Table 2. Effect of floret removal on average dry mass per filled achene at harvest maturity and percentage of empty achenes.

Treatment, capitulum sector	Max. achene mass (mg) and empty achenes (%) at harvest maturity in each capitulum sector					
	External		Middle		Internal	
	Max. achene mass, mg	Empty achenes per sector, %	Max. achene mass, mg	Empty achenes per sector, %	Max. achene mass, mg	Empty achenes per sector, %
Control						
External	61.5 (3.3) ^a	12.1 ^a	-	-	-	-
Middle	-	-	44.9 (2.6) ^a	15.3 ^a	-	-
Internal	-	-	-	-	33.1 (2.7) ^a	23.0 ^a
Outer ring removed						
Middle	-	-	56.2 (3.1) ^b [+27.6]	7.2 ^b	-	-
Internal	-	-	-	-	37.6 (2.9) ^b [+13.6]	19.7 ^a
Outer ring removed + PC						
Middle	-	-	49.8 (3.7) ^a [+7.1]	11.9 ^b	-	-
Internal	-	-	-	-	34.0 (3.2) ^a [+2.7]	18.4 ^b
Inner ring removed						
External	67.7 (2.9) ^b [+9.3]	13.2 ^a	-	-	-	-
Middle	-	-	53.6 (3.5) ^c [+17.9]	12.7 ^a	-	-

Values in column with different letters are significantly different (P<0.05). PC, perimetral constraint. Values in parentheses ±1SE. Values in the same column followed by different letters are significantly different (P<0.05). Values in brackets = percentage of achene dry mass (mg) change against control values for the same capitulum sector.

kept in a cooler with ice and taken to the laboratory within 90 minutes of sampling. The achenes were dried at 70°C for at least 48 h before weighing. Achene dry mass (ADM) was then calculated.

After ripening the collected capitula were taken to the laboratory and the achenes were separated from treated and control inflorescences. All achenes were taken from each capitulum separately in three concentric zones, equal in width (external, middle and internal). Total number of empty achenes per sector was counted and ADM was then measured.

Statistical analysis

Time course of achene mass increase was estimated fitting a bilinear regression to the data using a nonlinear routine of the Kaleidagraph version 4.1 software (Synergy Software, Reading, Pennsylvania, USA). The initial straight line is defined by $p=a_1+bX$ (for $X<c$) and the second straight line is defined by $p=a_2$ (for $X>c$), where p is the ADM (mg), X represents time (days from R7) a_1 is the intercept, b is the slope of the non-plateau section, (defines achene growth rate), a_2 is the value of the plateau of the function (indicates the maximum ADM (mg) and c , the unknown breakpoint (*i.e.*, the timing of maximum ADM).^{25,26}

All data were statistically analyzed by a two-way analysis of variance (ANOVA) using the Infostat statistical software package v. 2012.²⁷ The least significant difference (LSD) test was used to separate differences between capitulum sectors achene mass and their interactions.

Results

Flower removal affected achene mass after treatments of inner or outer achenes (Table 2; Figure 2). Achenes were heavier in those treatments in which internal or external flowers were removed in comparison with control ones (Table 2; Figure 2). Peripheral achenes of inflorescences where inner flowers were removed (Figure 1B) were significantly heavier (67.7 ± 2.9 g; $P<0.05$) than the outermost achenes of inflorescences of control plants (61.3 ± 3.3 g; $P<0.05$; Table 2).

Floret removal of the outer third capitulum ring significantly improved achene mass in the middle and center (Table 2; Figure 2B). In treated plants, the percentage of empty achenes in the middle sector was lower (7.2% and 11.9%, Table 2), than in control plants (15.3%, Table 2) as well as in the middle sector (19.7% and 18.4% *vs.* 23.0%). For IR treatment, maximum ADM in the external third and middle sector was observed 16 and 17 days respective-

ly after R7 (Figure 2B).

In the treatment when the inner third was removed (Figure 1B) final achene dry mass of the middle sector was attained 3.7 days later than in control plants (Figure 2A). On the other hand, in the treatment when the outer third was removed (Figure 1A) achenes of the middle sector attained its final dry mass 1.5 days earlier (Figure 2B). For OR treatment, maximum ADM in the internal third and middle sector was attained two days earlier than in control (Figure 2B).

Generally in all cases, except for the MS achenes in the IR treatments, the slope of the achene dry mass gain, was higher than in control (Figure 2; Table 2) indicating that the achenes were not only gaining higher mass compared with controls but also that this process was occurring faster. In the first case it may happen that the period of achene filling lengthens in the MS because there is no space limitations as a result of absent central achenes. In the second case, it can happen something similar but with an effect half controlled by the achenes of the MS. Also, as the ovaries of the IS may be in some cases smaller,¹⁴ these achenes gain mass before and quickly reach their maximum mass.

In capitula with outer ring floret removal (OR+PC) a peripheral constraint, which in turn is mechanically equivalent to being under compression, significantly reduced the final ADM of achenes of the MS compared with those plants with the peripheral removed ring

and no constraint (OR; Table 2). Nevertheless the final achene mass was significantly higher for the same capitulum sector in control plants (Figure 2B; Table 2).

Discussion

Following abundant evidence related with resource competition among achenes, independently of floral initiation order, appear to be that later developed achenes, affect the size of achenes produced earlier, so achenes from the IR treatment should be heavier than OS achenes in control inflorescences.

But, on the other hand, spatial effects where position also affects achene mass, suggest that the OS achenes from the IR treatment should be heavier than the OS achenes from the OR treatment, as the latter are in a relative inner position compared to the IR ones.

In this work ovary removal overall produced an increase in the size of the remaining achenes, suggesting competition for resources as one of the causes of the observed position effect. But on the other hand, the experimental manipulations of the source/sink ratio not only demonstrate that resource limitation is a major determinant of achene mass, in the capitulum,^{16,20} but that can mask a spatial effect on the development capacity of the remaining achenes. In this sense spatial issues should also be considered.

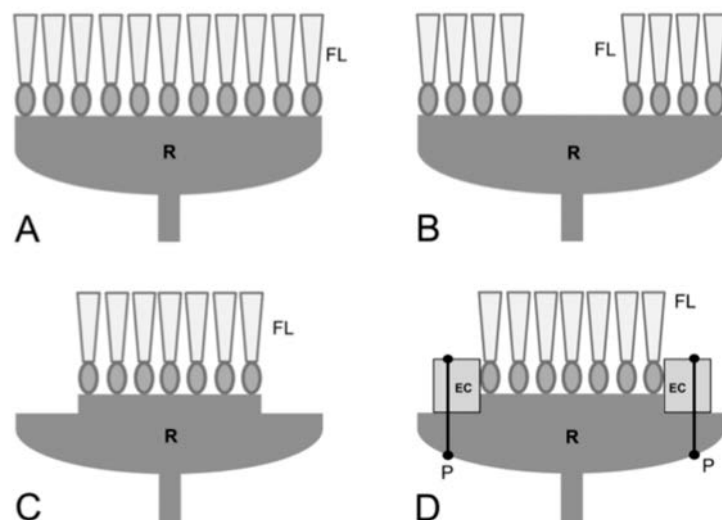


Figure 1. Schematic representation of the four treatments control (A), *inner flowers removed* (IR; B), *outer flowers removed*, (OR; C) and *outer flowers removed plus external constraint* (OR+PC; D), applied to capitula of sunflower in the experimental manipulation of flower competition. EC: Styrofoam ring to apply an artificial external constraint to the middle ovaries; R: receptacle; FL: florets; P: fixing pins of the EC onto the receptacle tissue.

In fact, in the experiment where a physical restriction of capitulum radial expansion was placed after removal of the OS ovaries (Figure 1D), resulted in lesser growth of the IS achenes than in the case of the removal of the OS ovaries without the external constraint (Table 2; Figure 2). Therefore, we should not ignore physical effect imposed by internal forces of expansion/compression of developing achenes in a whole capitulum.

In Figure 3 a conceptual expansion model in a post fertilized capitulum is presented. In this model an interpretation of how the forces of achene expansion and radial receptacle expansion would interact on a particular growing achene (Figure 3A).

We can infer that the dynamics of achene growth will result from the interrelation of the physiological component (assimilate input) plus two main geometrical components: the physical expansion of the receptacle surface (Figure 3B) and the rate at which achene growth is occupying this surface (Figure 3C).

The rate of achene growth will quickly increase as the receptacle surface cease its expansion growth probably produced by decrease competition for nutrients or growth substances by the proximal achenes, now engaged in active growth.

Exploratory work on determination of receptacle expansion after R8 using landmarks showed that radius growth, expansion rate diminishes from the center towards the periphery (Hernández, unpublished) an inverse finding previously reported,²⁸ in the interval in FS5 to 6 when the receptacle meristem is differentiating into floret primordia. In there, he found that capitulum expansion rate was higher at the periphery and slower or absent at the receptacle center. So if the disc center tends to grow rapidly (have excess surface)^{29,30} compared to the margins then the margins will respond, passively, with buckling,^{31,32} and it would necessarily result in the formation of a the rounded downwards rim observed in mature capitula after R8.³³

Conclusions

It is concluded that achene size is highly controlled by restrictions in space. Achenes that develop in the (external) proximal position of the capitulum have an advantage over those that develop in the (internal) distal portion thereof. Being the first to start developing and the most external, the radial expansion of the capitulum during grain filling and maturation diminishes the pressures between neighboring achenes but are higher as one moves towards the capitulum center. So, when more we move towards the center, significant coun-

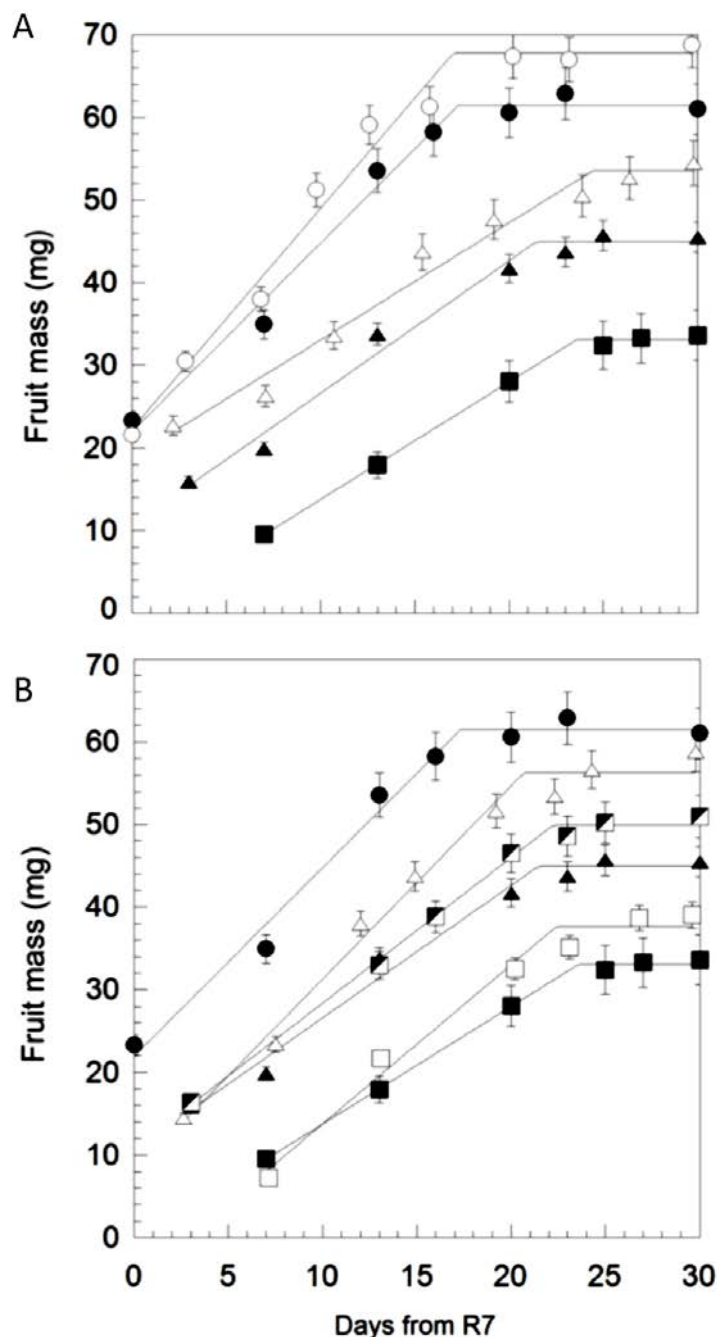


Figure 2. Evolution of achene dry mass (ADM) from R7 up to harvest maturity for the controls plants (closed symbols) and treated plants (open symbols) respectively. A) Control plants vs. external ring of florets removed (OR) and external ring removed plus a peripheral constraint (OR+PC). B) Control plants vs. internal ring of florets removed (IR). (●, ○) external achenes; (▲, △) middle achenes; (■, □) internal achenes, (◼) middle achenes when an artificial peripheral constraint was applied. For this last treatment data for the internal achene mass is not shown. Vertical bars: ± 1 SE. Fitted values are shown in the following equations:

$$\begin{aligned} \bullet & y=21.96+2.28x & R^2=0.996 \\ \circ & y=22.29+2.67x & R^2=0.993 \\ \blacktriangle & y=10.57+1.60x & R^2=0.992 \\ \triangle & y=18.84+1.42x & R^2=0.974 \\ \blacksquare & y=-0.46+1.42x & R^2=0.989 \\ \square & y=-5.45+1.94x & R^2=0.987 \\ \blacksquare & y=10.79+1.76x & R^2=0.979 \end{aligned}$$

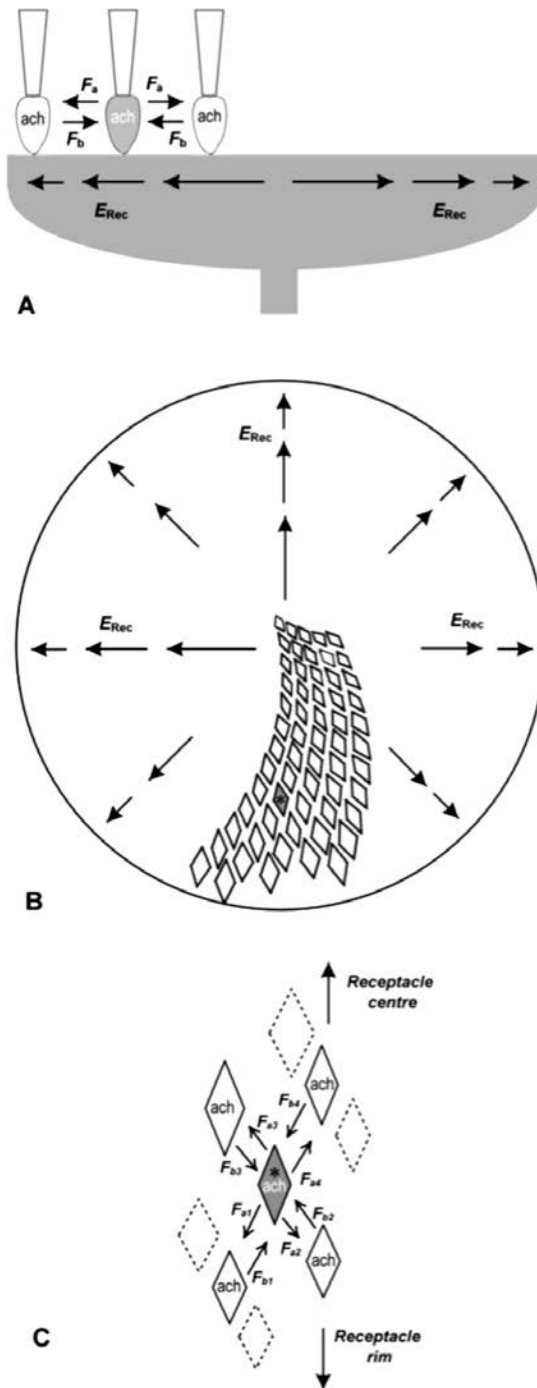


Figure 3. Schematic representation of the conceptual model of receptacle radial expansion, achene growth spatial competition. Simplified model of achene growth from the point of view of forces interacting during the development of a given achene on the receptacle surface. While the whole receptacle is radially expanding (A, B) each growing achene confronts with the competition for space with its neighbors (C). ach: achene; F_{a1-4} : expansion forces exerted by a particular achene. F_{b1-4} : expansion forces exerted by neighboring achenes. Regarding the neighboring achenes developmental age, because its relative position in the receptacle (C), then $F_{b1} > F_{b2} > F_{b3} > F_{b4}$. For simplification of the model, F_{a1-4} is equal in all directions. E_{Rec} : receptacle radial expansion. Different arrow length represents the expansion rate magnitude gradient into the receptacle after R8, as observed by Hernández (unpublished).

tervailing forces would begin to appear that would multiply from the outside in.

The results shown here constitute important experimental evidence supporting both resource competition and physical/spatial effects on achene size reduction within the sunflower inflorescence. The results also suggest that, similarly, the physical constraints during the capitulum development may limit the size/mass of internal achenes compared with the external ones, but the proximate mechanism of architectural effects remains uncertain.

References

1. Connor DJ, Hall AJ. Sunflower physiology. In: Schneiter AA, ed. Sunflower technology and production, agronomy monogr 35, ASA, CSSA, SSSA, Madison, USA. 1997. pp 113-182.
2. Lindström LI, Pellegrini CN, Aguirrezábal LAN, et al. Growth and development of sunflower fruits under shade during early pre and post-anthesis period. *Field Crops Res* 2006;96:151-9.
3. Robinson RG 1978. Production and culture. In: Carter JF, ed. Sunflower science and technology. Agronomy Monogr. 35, ASA, CSSA, SSSA, Madison, 1978. pp 89-143.
4. Diggle PK. Architectural effects on floral form and function: a review. In: Stuessy T, Hsrandl E, Mayer V, eds. Deep morphology: towards a renaissance of morphology in plant systematics. Koenigstein: Ganter Verlag; 2003. pp 63-80.
5. Medrano M, Guitián P, Guitián J. Patterns of achene and seed set within inflorescences of *Pacratium maritimum* (Amaryllidaceae): nonuniform pollination, resource limitation, or architectural effects? *Am J Bot* 2000;87:493-501.
6. Vallius E. Position-dependent reproductive success of flowers in *Dactylorhiza maculata* (Orchidaceae). *Func Ecol* 2000;14:573-9.
7. Kliber A, Eckert CG. Sequential decline in allocation among flowers within inflorescences: proximate mechanism and adaptive significance. *Ecology* 2004;85:1675-87.
8. Byrne M, Mazer SJ. The effect of position on fruit characteristics, and relationships among components of yield in *Phytolacca rivinoides* (Phytolaccaceae). *Biotropica* 1990;22:353-65.
9. Wolfe LM, Denton W. 2001. Morphological constraints on fruit size in *Linaria canadensis*. *Int J Plant Sci* 2001;162:1313-6.
10. Guitián J, Guitián P, Medrano M. Causes of fruit set variation in *Polygonatum odora-*

- tum (Liliaceae). *Plant Biol* 2001;3:637-41.
11. Hernández LF, Orioli GA. Participación de la diferentes hojas de la planta de girasol durante el llenado de los frutos. *Turrialba* 1991;41:330-4.
 12. Hernández LF, Palmer JH. Incorporation of ¹⁴C labelled metabolites into the developing sunflower capitulum. In: XIII International Sunflower Conf Proceedings, Pisa, Italy, 1992. pp 564-70.
 13. Alkio M, Diepenbrock W, Grimm E. Evidence for sectorial photoassimilate supply in the capitulum of sunflower (*Helianthus annuus*). *New Phytol* 2001;156:445-56.
 14. Lindström LI, Pellegrini CN, Hernández LF. Histological development of the sunflower fruit pericarp as affected by pre- and early post-anthesis canopy shading. *Field Crops Res* 2007;103:229-38.
 15. Dosio GAA, Tardieu F, Turc O. Floret initiation, tissue expansion and carbon availability at the meristem of the sunflower capitulum as affected by water or light deficits. *New Phytol* 2011;189:94-105.
 16. Torices R, Méndez M. Fruit size decline from the margin to the center of capitula is the result of resource competition and architectural constraints. *Oecologia* 2010;164:949-58.
 17. Palmer JH, Hernández LF. Techniques to change the Fibonacci control of the number of floret and seed rows in the sunflower capitulum. In: XII Intl. Sunflower Conf Proceedings, Novi Sad, Yugoslavia. 1988. pp.156-7.
 18. Hernández LF. Grain yield of the sunflower capitulum promoted by surgical removal of the involucral bract primordia. *Trends Agric Science* 1993;1:127-35.
 19. Beltrano J, Caldiz DO, Barreyro R, et al. Effects of foliar applied gibberellic acid and benzyladenine upon yield components in sunflower (*Helianthus annuus* L.). *Plant Growth Reg* 1994;15:101-6
 20. Alkio M, Schubert A, Diepenbrock W, et al. Effect of source-sink ratio on seed set and filling in sunflower (*Helianthus annuus* L.). *Plant Cell Env* 2003;26:1609-19.
 21. Jeune B, Barabé D. Interactions between physical and biological constraints in the structure of the inflorescences of the Araceae. *Ann Bot* 1998;82:577-86.
 22. Soil Survey Staff. Soil taxonomy: a basic system of soil classification for making and interpreting soil surveys. 2nd ed. Natural Resources Conservation Service. U.S. Department of Agriculture Handbook 436. 1999.
 23. Díaz Zorita M, Duarte GA, Plante E. El Cultivo de Girasol. Buenos Aires: ASAGIR; 2003. pp 5-9.
 24. Schneiter AA, Miller JF. Description of sunflower growth stages. *Crop Sci* 1981;21:901-3.
 25. Lindström LI, Hernández LF. Developmental morphology and anatomy of the reproductive structures in sunflower (*Helianthus annuus*): a unified temporal scale. *Botany* 2015;93:307-16.
 26. Hernández LF, Larsen AO. Maturation in sunflower. Visual definition of physiological maturity can be associated to the capitulum's quantitative color parameters. *Spanish J Agric Res* 2013;11:447-54.
 27. Di Rienzo JA, Casanoves F, Balzarini MG, et al. InfoStat, vers 2008, Grupo InfoStat, FCA, Universidad Nacional de Córdoba, Argentina. 2008.
 28. Hernández LF. Pattern formation in the sunflower (*Helianthus annuus* L.) capitulum. *Biophys Consid Biocell* 1995;19:201-12.
 29. Selker JM, Steucek GL, Green PB. Biophysical mechanisms for morphogenetic progressions at the shoot apex. *Developmental Biol* 1992;153:29-43.
 30. Holland MA, Kosmata T, Goriely A, et al. On the mechanics of thin films and growing surfaces. *Math Mechan Solids* 2013;18:561-75.
 31. Green PB. Pattern formation in shoots: a likely role for minimal energy configurations of the tunica. *Int J Plant Sci* 1992;153 S59-S75.
 32. Green PB. Connecting gene and hormone action to form, pattern, and organogenesis: biophysical transductions. *J Exp Botany* 1994;45:1775-88.
 33. Knowles PF. Morphology and anatomy. In: Carter JF, ed. *Sunflower Science and Technology*. Agron Monogr 19. ASA, CSSA,SSSA, Madison, USA. 1978. pp 55-88.

Proline content and yield components of local corn cultivars from Kisar Island, Maluku, Indonesia

Hermalina Sinay,^{1,2} Estri Laras Arumingtyas,¹ Nunung Harijati,¹ Serafinah Indriyani¹

¹Department of Biology, Faculty of Mathematics and Natural Sciences, Brawijaya University, Malang; ²Biology Education Programe, Faculty of Teaching and Education, Pattimura University, Ambon, Indonesia

Abstract

Proline is one of amino acid that usually accumulates inside the plant cell when facing drought stress. The accumulation of proline can protect the plant cell from damage during drought. The aim of this research was to determine proline content and yield components of local corn cultivars from Kisar Island, Maluku, Indonesia. The field trial was organized using randomized block design with three replicates. Six local corn cultivars found in Kisar Island (Deep Yellow, Early Maturing Yellow, Red Blood, Rubby Brown Cob, Waxy, and White) were used as plant materials and a recommended tolerance variety (*Srikandi*) was taken as reference group. Proline content was determined using ninhydrin method. Yield components variables included cob weight (at harvest, after air dry, after oven dried, at 12% of water content), cob water content at harvest, cob length, cob diameter, number of seed row per cob, number of seed per cob, and cob yield at 12% of water content. Data collected was analysed with analysis of variance followed by Duncan multiple range test at the significant level 0.05 using Statistical Analysis System/SAS software version 9.0. The result shows that highest proline content and yield components (except for cob water content) was showed by the Deep Yellow cultivar. The lowest proline content was showed by Rubby Brown Cob cultivar. The lowest corn yield components was showed by Red Blood local cultivar. Deep Yellow cultivar can be proposed as superior drought tolerance variety, and can be recommended for further wide cultivation in Maluku province.

Introduction

About 41% of Earth's land surface is covered

by dryland.¹ In Indonesia, as much as 40% of agricultural land is dryland.² Kisar Island is part of Southwest Maluku district in Maluku province that known as dry area with dry climates and very low rainfall (991-1102 mm/year, or 19.05-21.19 mm/week).³ In Maluku, this area also known as a major contributing area of corn. However, one of the problem associated with dryland and very low rainfall in this area is the low productivity of corn (1.0 t/ha with harvest area 16,460 ha).⁴⁻⁶

When experiencing to dryland or drought environment conditions, plant have a special mechanism to overcome the drought stress like synthesis of osmolyte.⁷ The synthesis and accumulation of osmolyte can protect plant cells from damage caused by drought stress.⁸ One of the osmolyte that accumulate in the plant cell during drought is proline.^{9,10} The increasing of proline accumulation during drought stress in various plant species have been reported by many researcher such as on peanut,¹¹ soybean,¹² and patchouli.¹³ In corn, proline accumulation due to drought have been reported at the germination stage,¹⁴ vegetative stage,¹⁵ and reproductive stage.^{7,16-18} Drought stress can also significantly affect plant production including corn.¹⁸⁻²⁰

Information regarding the potential yield and adaptability of the plants through the synthesis and accumulation of osmolyte is the most important factors that should be understandable by researcher or a breeder in order to obtain the best and stable genotype which can be used in a wider cultivation. This is caused by the phenotypic expression of a genotype can be changed in accordance with the ability to adapt to environmental conditions. In Kisar Island Southwest Maluku district, there are six local corn cultivars that have been cultivated by local people for a long time since many years. However, the potential yield and adaptability through proline synthesize and accumulation of six local cultivars has not been studied. The aim of this research was to determine the proline content and yield components, and wich one of these local corn cultivars that can be recommended for wider cultivation based on the proline content and yield components.

Materials and Methods

The plant materials consist of six local corn cultivars obtained from farmers in Kisar Island (Deep Yellow, Early Maturing Yellow, Red Blood, Rubby Brown, Waxy, and White) and one reference variety (*Srikandi*) from Research Institute for Cereals. The experiment was conducted in Yawuru District Kisar Island, South West Maluku Regency from December 2013 to March 2014, using random-

Correspondence: Hermalina Sinay, Department of Biology, Faculty of Mathematics and Natural Science, Brawijaya University, Jalan Veteran Malang 65145, East Java, Indonesia. Tel.:+62.0341.575841-Fax: +62.0341.575841 E-mail: herlinbio@yahoo.co.id

Key words: Proline; yield components; corn.

Acknowledgments: this research was a part of first author doctoral research project wich was funded by the Directorate of Higher Education Ministry of Research Technology and Higher Education The Republic of Indonesia. The authors greatly acknowledge for the availability of these funding.

Contributions: HS, performed most of experimental work, data collecting and analyzing, manuscript writing; ELA, NH, SI, supervised experimental work, helped correct the paper, perpermed the english language of the paper.

Conflict of interest: the authors declare no conflict of interest.

Conference presentation: part of this paper was presented at the International Biological Science Conference, 2014 Sept 29-30, Faculty of Science, Prince of Songkhla University, Phuket, Thailand

Received for publication: 9 June 2015.

Revision received: 12 August 2015.

Accepted for publication: 12 August 2015.

This work is licensed under a Creative Commons Attribution-NonCommercial 3.0 International License (CC BY-NC 3.0).

©Copyright H. Sinay et al., 2015
Licensee PAGEPress srl, Italy
International Journal of Plant Biology 2015; 6:6071
doi:10.4081/pb.2015.6071

ized block design with three replicates. The environmental condition were measured including temperature wich is ranging from 27.1°C (Dec 2013) and 28.5-28.9°C (January-March 2014). The rainfall was about 47.84 mm/week (Dec 2013), and 17-3-0.2 mm/week (January-March 2014).

Plots size was 1.5×1.5 m. One plot with nine planting holes planted with four seeds per hole and thinned at thirty days after planting. There was 50×50 cm space between each planting hole in each plot. There was no fertilizer and watering applied during planting season. Observation were carried out on 1 purposed selected plants leaves at 65 days after planting using the second leaf from tip for proline analysis, while yield components analysis were conducted after harvesting from 3 selected plants.

Proline analysis was conducted following the nynhidrin method.²¹ Fresh leaves with the weight of 0.25 g,¹⁷ was milled in mortar and

pestle, and homogenized with 10 mL of 3% sulphosalysilic acid (w/v). The homogenate then centrifugated at 6000 rpm for 15 minutes. The supernatant obtained was poured in-to new test tube and filtered using Whatman filter paper number 40. Two milliliters of supernatant was taken and added with 2 mL of glacial acetic acid and 2 mL of acid nynhidrin. The acid nynhidrin wich is consist of 60 mL of 2.5 grams nynhidrin in 100 mL of glacial acetic acid, 30 mL of aquadest and 10 mL of 85% phosphoric acid was prepared following the methods of Clausen.²²

The solution then heated at 100°C of boiling water for one hour, and incubated on ice for 5 minutes. The solution then extracted with 4 mL of toluene, and vortex vigorously for 10 second. The upper phase of solution was taken, and the absorbance was measured at 520 nm of wavelength by using UV-VIS Spectrophotometer. For the standart curve, series of proline concentration (2.5-20 µg/mL) was made using pure DL-prolin (Merck; Kenilworth, NJ, USA). Proline concentration then calculated and expressed as µmole/g fresh weight. The observation of corn yield was conducted when the husk turned to yellow or brownish.²³ The yield components observed were cob weight at harvest, cob weight after air dry, cob weight after oven dried, cob water content after air dry, cob weight at 12% of water content, cob length, cob diameter, number of seed row per cob, number of seed per cob, and cob yield at 12% of water content. Data then analysed using analysis of variance followed with Duncan multiple range test at the significant level of 0.05. Anova and Duncan was conducted with the assistance of statistical analytical system (SAS) version of 9.0.

The highest value of proline content was showed by Deep Yellow local cultivar and the lowest proline content was showed by Rubby Brown Cob local cultivar (Table 1). Proline is an organic compound that most accumulated in plant when experience to drought stress.²⁴ The function of proline in the plant cell was to keep the stability or turgidity of the cell, and protect the cell from damage due to drought.²⁴ With the accumulation of proline inside the plant cell, it is expected to give a positive effect to the physiological process wich lead to the increase of plant yield.

The highest value of cob weight at harvest was showed by Deep Yellow cultivar, and the lowest one in the Red Blood cultivar (Table 1). Cob weight showing the accumulation of water and organic materials contained in the seed. Accumulation of organic material associated with photosynthesis and distribution of photosynthate from the source to the plant organs wich serve as a place for the dumping of photosynthesis products (sink), in this case is corn seed. Similar to cob weight at harvest data, after the cob was air dried, the highest weight value also showed by the Deep Yellow local cultivar and the lowest one was obtained by the Red Blood local cultivar. After air dried for 30 days, cob weight become decreased about 2-6 grams compared with the cob weight at harvest. This was allegedly associated with the reduced of water content in the cobs. The water content in the cob can be decreased along with the length of storage time. This is caused by during storage the evaporation of water can still take place. Drying the cob in an oven lowering the water content in the seed.²⁵ When compared with at harvest, and cob weight at air dried, the cob weight after oven dried getting were decreased. Water content is the amount of water contained in the material expressed in percent (%).²⁶ Cob water content at harvest average is 19%. This is not in line with the previous result that stated that the

average water content of grains such as sorghum and corn are 20-30%.²⁷ However, the water content is influenced by environmental conditions when harvest and also growth environmental condition. If the harvest was done in the dry season and environmental conditions too dry, then the seed water content can range between 17-20%.² Weight of cobs were measured on a 12% of water content. This is the balanced or equilibrium condition for the storage of corn grain.^{28,29} The cob length shows that cultivar with the highest cob length was Deep Yellow local cultivar, while the lowest cob length was Red Blood local cultivar. The length of cob size is related to the amount or composition of seed rows on the cob. The amount or composition of seed rows on the cob is closely linked to the success of pollination. In case of drought, little or no viable pollen were produced. If there are slightly fertile or viable pollen that formed, the succes of seed formation will also reduced, and this can affect the position of seed or seed row arrangement on the cob. Cultivars with highest cob diameter was Deep Yellow local cultivar (Table 1). Cob diameter is one of agronomic traits that usually related to the size of seed. Cob diameter also affects the crop yield components. If the seed has length size, the cob diameter tend to larger. Also, the length and diameter of the cob is closely related to the results of a varieties. If the average cob length of one varieties is longer, this varieties are likely to have a higher yield.

Drought occurred in the flowering stage, unviable pollen is potentially to produce and this can leads a lower production, and decrease the number of seeds.³⁰ The number of seeds per cob related to the value of anthesis-silking interval because between male and female flowers there must be a synchronization to ensure succesful fertilization, wich in turn affect the formation of seeds. This is in accordance with other fundings that under

Results and Discussion

Table 1. Proline content and yield components of corn from Kisar Island Maluku (Indonesia).

Variable tested	Corn cultivars						
	Rubby brown cob	Red blood	Waxy	Early maturing yellow	Deep yellow	White	Srikandi
Proline content (µmole/gFW)	13.8±3.1 ^b	17.0±4.6 ^b	17.3±2.9 ^b	18.4±1.4 ^b	27.4±4.6 ^a	14.2±2.9 ^b	18.7±2.5 ^b
Cob weight when harvest (g)	73.4±4.7 ^b	46.7±3.7 ^c	67.1±9.0 ^{bc}	85.6±6.7 ^b	128.0±24.0 ^a	88.3±7.3 ^b	69.6±14.7 ^b
Cob weight after air dry (g)	70.3±4.7 ^b	44.5±4.9 ^c	64.1±7.6 ^{bc}	80.7±6.4 ^b	122.5±23.2 ^a	85.5±7.2 ^b	66.5±18.6 ^{bc}
Cob weight after oven dried (g)	59.5±4.1 ^b	38.15±3.34 ^c	50.9±8.6 ^{bc}	68.6±5.1 ^b	104.1±20.5 ^a	70.9±4.9 ^b	56.0±11.8 ^{bc}
Cob water content when harvest (%)	19.4±0.4 ^a	19.4±0.7 ^a	19.4±0.8 ^a	19.7±0.2 ^a	19.5±0.8 ^a	19.6±1.1 ^a	19.4±0.8 ^a
Cob weight at the 12% of water content (g)	67.3±4.6 ^b	42.6±3.6 ^c	61.4±8.2 ^{bc}	77.4±6.2 ^b	117.0±21.6 ^a	80.6±5.6 ^b	62.3±16.4 ^{bc}
Cob yield at the 12% of water content (ton/ha)	0.3±0.02 ^b	0.1±0.02 ^c	0.2±0.04 ^b	0.3±0.02 ^b	0.5±0.09 ^a	0.3±0.03 ^b	0.2±0.06 ^b
Cob length (mm)	86.8±0.8 ^{cd}	73.4±1.05 ^d	94.3±8.5 ^{bc}	110.02±2.8 ^{ab}	116.1±2.6 ^a	103.6±10.9 ^{abc}	98.7±8.8 ^{abc}
Cob diameter (mm)	31.00±4.1 ^c	30.1±1.8 ^c	31.7±1.1 ^{bc}	34.8±3.2 ^b	38.0±1.8 ^a	35.4±0.6 ^{ab}	33.2±1.1 ^{bc}
Number of seed per cob (seed)	242.3±44.7 ^b	185.5±16.2 ^b	205.0±16.3 ^b	243.5±50.2 ^b	341.5±37.6 ^a	247.6±23.7 ^b	203.4±46.7 ^b
Number of seed row per cob (row)	10.8±0.1 ^b	10.6±0.8 ^b	11.1±0.5 ^b	10.3±0.5 ^b	14.1±0.6 ^a	11.6±0.3 ^b	10.7±1.0 ^b

Number followed with same letters in the same rows means no significant different at α 0.05 according to DMRT.

drought conditions, the length time of male and female flower induction, will extend the length of anthesis-silking interval and will affect the corn yield, especially the number of seeds on the cob.³¹

The results showed that the highest yield of cob at the 12% of water content was obtained by Deep Yellow local cultivar (0.56 tonnes/ha, and the lowest one in the Red Blood local cultivar (0.23 ton/ha). In general, the cob yield of all cultivars is very low. This is related to the environmental conditions. Drought that occurred at the flowering stage, is potentially decrease the corn yield,³² while if drought was occurred during grain filling, this can leads the decrease of corn yields as much as 30-60%.³³

The proline content is associated with the yield component of corn. This means that genotype with high proline content tended to be high in the yield components (as found in the Deep Yellow local cultivar). Among six local corn cultivars and reference variety, the highest value of proline content and yield components (except for cob water content after air dry) was showed by Deep Yellow cultivar. *Srikandi* variety that was recommended by the Research Institute of Cereal as a drought tolerant variety did not show better result on all variables observed compared with Deep Yellow local cultivar. Another researcher was stated that if a superior variety did not show a high result,³⁴ this was caused by the superior variety was gained by some selected optimum procedure and the observation of superior variety was done under optimum condition. Therefore the superiority of this variety under optimum condition does not always expressed under sub optimum condition.

Regarding to the tolerance to drought, it was predicted that Deep Yellow cultivar was the most tolerant cultivar that can adapt to the environment of Kisar Island as it's natural habitat compare with other local cultivar and reference variety. This result was strong supported by statement of,³⁴ that if the observed value of one traits from one cultivar were highest than the observed value of one traits from a reference variety (tolerance to drought), the genotype was more tolerant to drought. This suggests that based on the proline content and yield components, the Deep Yellow local corn cultivar are effective to measure the adaptation of corn cultivars, and can be recommended for further cultivation.

Conclusions

The highest proline content and yield components (except for cob water content) was obtained in Deep Yellow cultivar. The lowest proline content was obtained by Rubby Brown Cob cultivar. The lowest corn yield components

(except for cob water content when harvest) was obtained by Red Blood local cultivar. Deep Yellow cultivar can be proposed as superior drought tolerance variety, and can be recommended for further wide cultivation in Maluku province.

References

- Safriel U, Adeel Z. Dryland systems. In: Hassan R, Scholes R, Ash N, eds. Ecosystems and human well-being: current state and trends: findings of the condition and trends working group. Washington: Island Press; 2005. pp 623-662.
- Murtalaksono K, Anwar S. Potency, challenge, and strategy in the use of dryland and acid dryland for agricultural (rice, corn, soybean), veterinary, and using useful technology and location specific. Proc Natl Sem Suboptimal Land, 2014 Sept 26-27, Palembang, Indonesia. pp 1-15. [Article in Indonesian]
- Susanto AN, Sirappa MP. Future and strategies for corn development in supporting Food availability in Maluku. Res Dev Agric J 2005;24:70-9. [Article in Indonesian].
- Central Agency of Statistics of South West Maluku Regency. Maluku: Statistic of Southwest Maluku Regency; 2011. [Book in Indonesian].
- Pesireron M, Senewe RE. Performance of 10 composite corn varieties and hybrid on the dry land agroecosystem in Maluku. J Agric Cult 2011;7:53-8. [Article in Indonesian].
- Sirappa MP, Pesireron M, Dahamarudin L. Yield potential of some local corn in South West Maluku District with integrated plant management. Proceeding of National Seminars on Cereals, 2013 March 26-27, Banjar Baru, South Kalimantan, Indonesia. pp 220-230. [Article in Indonesian].
- Mohammadkhari N, Heidari R. Effects of drought stress on soluble proteins in two maize varieties. Turk J Biol 2008;32:23-7
- Barnaby JY, Kim M, Bauchan G, et al. Drought responses of foliar metabolites in three maize hybrids differing in water stress tolerance. PLoS One 2013;8:24-1
- Moaveni P. Effect of water deficit stress on some physiological traits of wheat (*Triticum aestivum*). Agric Sci Res 2011;1:64-4
- Liu C, Liu Y, Guo K, et al. Effect of drought on pigments, osmotic adjustment, and antioxidant enzymes in six woody plant species in Karst of Southwestern China. Env Exp Bot 2011;71:174-9
- Rahayu ES, Guhardja E, Ilyas S, Sudarsono. Polyethylene glycol in in-vitro media leading the drought stress to inhibit peanut (*Arachis hypogaea* L.) shoot. Periodic Biol Res 2005;11:39-7. [Article in Indonesian].
- Nazarli H, Faraji F. Response of proline, soluble sugars and antioxidant enzymes in wheat (*Triticum aestivum* L.) to different irrigation regimes in greenhouse condition. Cercetări Agronomice în Moldova XLIV 2011;4:28-5.
- Tohari S, Shiddiq D. Effect of drought stress on proline accumulation in patchouli (*Pogostemon cablin* Benth.). Agric Sci 2012;15:85-14. [Article in Indonesian].
- Effendi R. Response of tolerance and sensitive corn genotype toward drought stress at the germination stage: Proceeding of National Seminar on Cereals, 2009 June 21-26, Jakarta, Indonesia. 2009. pp 82-91. [Article in Indonesian].
- Efendi R, Suwardi, Isnaini M. Method in determine character for corn genotype selection on drought at the early vegetative phase. Proceeding of National Seminar on Cereals, 2010 July 26-30, Jakarta, Indonesia. 2010. pp 230-240. [Article in Indonesian].
- Sultan K, Atilla LT. The investigation on accumulation levels of proline and stress parameters of the maize (*Zea mays* L.) plants under salt and water stress. Act Physiol Plant 2010;32:541-8.
- Badami K, Amzeri A. Identification of somaclonal varian tolerance to drought on the corn population derived from in-vitro selection using polyethylene glycol. Agrovigor 2011;4:7-6. [Article in Indonesian].
- Soltani A, Waismoradi A, Heidari M, Rahmati H. Effect of water deficit stress and nitrogen on yield and compatibility metabolites on two medium maturity corn cultivars. Int J Agri Crop Sci 2013;5:737-3.
- Naghavi MR, Aboughadareh AP, Khalili M. Evaluation of drought tolerance indices for screening some of corn (*Zea mays* L.) cultivars under environmental conditions. Not Sci Biol 2013;5:388-5.
- Shaddad MAK, Abd El-Samad MH, Mohammed HT. Interactive effects of drought stress and phytohormones or polyamines on growth and yield of two maize (*Zea mays* L.) genotypes. Am J of Plant Sci 2011;2:790-17.
- Bates LS, Walderen RM, Teare ID. Rapid determination of free proline for water-stress studies. Plant Soil 1973;39:205-2.
- Claussen W. Proline as a measure of stress in tomato plants. Plant Sci 2005;168:241-8.
- Rachmawati D, Daryono BS, Sukma KPW. Yield potential of hybrid corn, derived from

- the crossing between varietas Guluk-Guluk variety and Yellow Srikandi-1. *Periodic Biol Res Special Edition* 2011;5A:153–5. [Article in Indonesian].
24. Mafakheri A, Siosemardeh A, Bahramnejad B, et al. Effect of drought stress on yield, proline and chlorophyll contents in three chickpea cultivars. *Aus J Crop Sci* 2010;4:580-5.
 25. Innocent COA, Gumbe LO, Gitau AN. Dewatering and drying characteristics of water hyacinth (*Eichhornia Crassipes*) petiole. Part II. Drying characteristic. *Agric Eng Int* 2008;7:11-1.
 26. Safrizal R. Material water content. Post harvest technique. Thesisi dissertation. Departement of Agricultural Technique. Faculty of Agriculture Syah Kuala University; 2010. [Article in Indonesian].
 27. Susila BA. Excellence quality nutrition and functional properties of Sorghum (*Sorghum vulgare*). Proceeding of National Seminar on Inovative Post Harvest for the Industrial Development Based on Agriculture, 2010 Nov 30-Dec 1, Bogor, Indonesia: Center for Post Harvest Research and Development; 2010. pp 132-9. [Article in Indonesian].
 28. Mwithiga G, Sifuna MM. Effect of moisture content on the physical properties of three varieties of shorgum seeds. *J Food Eng* 2006;75:486-80.
 29. Sedyowati YT. Drying corn is good support achieving sustained self-sufficiency. Ministry of Agriculture. Jakarta: Research Center and Development of Human Resources in Agriculture; 2011. [Article in Indonesian]
 30. Spitko T, Nagy Z, Zsubori ZT, et al. Effect of drought on yield components of maize hybrids (*Zea mays L.*). *Maydica* 2014;59:161-9.
 31. Ali Q, Elahi M, Hussain B, et al. Genetic improvement of maize (*Zea mays L.*) against drought stress: an overview. *Agric Sci Res J* 2011;10:228-37.
 32. Magorokosho C, Pixley KV, Tonggoona P. Selection for drought tolerance in two tropical maize populations. *Afr Crop Sci J* 2003;3:151-61.
 33. Efendi R, Suwarti. Anticipate climate changes with drought tolerant maize varieties and flooding. Proceeding of National Seminar on Inovation Technology of Agriculture, 2013 March 26-27, Banjar Baru, South Kalimantan: 2013. pp 133-142. [Article in Indonesian].
 34. Ceccareli S. Specific adaptation and breeding for marginal condition. *Euphytica* 1994;77:205-4.

Characterizing the dynamical accumulation of nuclear DNA in the sperm cells of *Lycium barbarum* L.

Hua Deng,¹ Pierre Nouvellet,² David Waxman¹

¹Centre for Computational Systems Biology, Fudan University, Shanghai, China; ²Medical Research Council Centre for Outbreak Analysis and Modelling, Department of Infectious Disease Epidemiology, Imperial College London, UK

Abstract

When sperm cells of the plant *Lycium barbarum* L. (*L. barbarum*) form in a style they begin to synthesize nuclear DNA (nDNA), which monotonically increases over time. To characterize the dynamics of nDNA accumulation, we present two new dynamical/statistical models. We applied these models to the accumulation of the nDNA content of sperm cells in *L. barbarum* between 16 to 32 hours after pollination in a style. A statistical analysis of experimental data, involving Markov chain Monte Carlo methods, allowed estimation of parameters of the models. We conclude that the model with no variation in the rate of nDNA accumulation adequately summarizes the data. This is the first work where the dynamics of nDNA accumulation has been quantitatively modeled and analyzed.

Introduction

Plant embryology includes studies of the nuclear DNA (nDNA) of male and female gametes.¹ Most of the previous research on this subject, for example, in the plants *Arabidopsis* and *Nicotiana tabacum* investigated the nDNA content of the gametes.^{2,3} By contrast, in the present work, we present mathematical modeling and analysis of the dynamics of nDNA accumulation. In particular, we analyzed data collected on the plant *Lycium barbarum* and studied the dynamics of nDNA accumulation in sperm cells. We introduced and employed two statistical models for this purpose. We used these models to determine the intrinsic rate of accumulation of nDNA content in *L. barbarum*. This plant is in the same family as *Nicotiana tabacum*, namely *Solanaceae*. The plant *L. barbarum* is economically important because it is a fruit producer.

It also has applications in Traditional Chinese Medicine.⁴⁻⁶ During the initial stages of fertilization, a pollen grain is transferred to a plant's stigma by the process of pollination. The plant *L. barbarum* falls under the class of plants that produce bicellular pollen grains (*i.e.*, containing one generative cell and one vegetative cell). Under appropriate conditions, a pollen grain germinates a pollen tube on a stigma, in which case the pollen tube elongates, and grows into the transmitting tissue in the style. For pollen of a bicellular type, a generative cell (which is linked to a vegetative cell) divides to form two sperm cells, some time after pollination, during pollen tube elongation. In previous experiments on *L. barbarum*,⁷ the styles were examined every 4 hours from the time of pollination and sperm cells were observed (under a microscope) only at 16 or more hours after pollination. Hence it is plausible that individual sperm cells formed between 12 and 16 hours after pollination. During the process of sperm cell development, good quality pollen tubes (*i.e.*, those which are potentially successful at achieving fertilization), contain sperm cells in the vicinity of the tip, and these are transported along, with the growth of the pollen tube.⁷⁻⁹ Sperm cells, once formed initiate nDNA content synthesis (their nuclei begin to accumulate DNA). Experimental techniques allow the measurement of the nDNA content of sperm cells at different times after their formation, at different stages of development. The analysis carried in the present work was used to *quantitatively* test a new dynamical hypothesis concerning DNA accumulation of the sperm cells (see below). A qualitative analysis of the data has been reported elsewhere,¹⁰ and relevant details of the experiments are given in this previous work; the primary focus of the present work is modeling and data analysis.

Hypothesis

The work presented here is based on the hypothesis that accumulation of nDNA content in plant sperm cells occurs *linearly* over time. This hypothesis is original to this paper and has not, to the best of our knowledge, been made elsewhere. This linear behavior is assumed to apply for the experiments on *L. barbarum* from the time of first observation of sperm cells, namely 16 hours after pollination, to the longest time that sperm cells were observed after pollination (32 hours). In principle, if measurements had been made over longer times than the longest times adopted (32 hours), then it is possible that some sort of saturation effect in the nDNA content of sperm cells could set in, prior to zygote formation, with the nDNA content/time curve leveling off at long times. We saw no evidence of this in the data collected up to 32 hours after pollination (Table 1), hence models with a linear

Correspondence: David Waxman, Centre for Computational Systems Biology, Fudan University, 220 Handan Road, Shanghai 200433, China.
Tel.: +86.021.5566.5547.
E-mail: davidwaxman@fudan.edu.cn

Key words: Statistical analysis; pollen grains; mathematical model.

Contributions: the authors contributed equally.

Conflict of interest: the authors declare no potential conflict of interest.

Received for publication: 7 May 2015.
Revision received: 5 July 2015.
Accepted for publication: 5 July 2015.

This work is licensed under a Creative Commons Attribution-NonCommercial 3.0 International License (CC BY-NC 3.0).

©Copyright H. Deng et al., 2015
Licensee PAGEPress srl, Italy
International Journal of Plant Biology 2015; 6:5996
doi:10.4081/pb.2015.5996

increase appear adequate, but a natural extension of this work could involve nDNA increase according to a saturating function of time. We thus introduced two models with linear accumulation of nDNA content over time. The virtue of the models is that they have only a few parameters, which can be estimated from the experimental data. Any non-linear model will generally involve more parameters than a linear model, and make greater demands on the data. However, extensions of the models are possible.

We assume the nDNA content of sperm cells have variability from *two* different sources. The first is an aspect of the fluorescence technique employed, which leads to errors in the measured nDNA content at any time. In principle, there is a second source of variability: the nDNA content of the sperm cells arises from intrinsic variation in the rate of accumulation of nDNA of different sperm cells. That is, different sperm cells may have different rates of DNA accumulation.

Materials and Methods

nDNA content determination

We determined the nDNA content of sperm cells using microscopy and fluorescence techniques. With a Leica DMR fluorescence microscope, we observed and photomicrographed sperm cells. The software associated with the microscope (Simple PCI) was used in the

analysis of the data. All parameters of the software were set in advance and the only parameter requiring adjustment was the exposure time. To analyze the data, we selected a cell in a photomicrograph, and by manually circling the cell, the software calculated the fluorescence value. The fluorescence value was not influenced by the exposure time, when below the saturation level, because the measured fluorescence was relative to the background fluorescence, and the difference, to good accuracy, is independent of the exposure time.

Statistical analysis

We used MCMC with the Metropolis-Hastings algorithm to sample the likelihood.¹¹ See the Models Section for a derivation of the likelihood functions.

Models

We introduce two dynamical models that incorporate the hypothesis that accumulation of nDNA content in the plant sperm cells occur linearly with time. We assume that at t hours after pollination, the nDNA content of plant sperm cells given by

$$D = A + Rt + \varepsilon \quad \text{Eq. (1)}$$

where:

D is the nDNA content (measured in units of C , where, by definition, a diploid cell has an nDNA content of $2C$) of a sperm cell at time t ; A is a constant; R is the rate of accumulation of

nDNA content of a sperm cell; ε is the error in the measured nDNA content of a sperm cell that is introduced by the fluorescence technique; we assume ε is an intrinsic property of the fluorescence technique.

We model the fluorescence error, ε , as a random variable that varies from sperm cell to sperm cell. We make the simplest assumptions that the fluorescence errors are independent for different sperm cells and unbiased - hence ε has an expected value of zero.

In the experiments, the nDNA content of sperm cells are measured at given times, with the measurement destroying the sperm cells, so they cannot be re-measured, hence different measurements are on different sperm cells.

Two models, within the framework of Eq. (1) suggest themselves.

Model 0

All sperm cells have an identical rate of DNA accumulation. Thus the parameter R in Eq. (1) is a constant that can be estimated from the data.

Model 1

A slightly more sophisticated model assumes that different sperm cells have different rates of DNA accumulation, so a randomly picked sperm cell will have a value of its rate of nDNA content accumulation, R , that is drawn from a continuous distribution. We model R as a normal random variable that for different

sperm cells are statistically independent and identically distributed. We also assume statistically independent fluorescence errors (ε). Because we model R as a normal random variable, we have a characterization of the rate of nDNA accumulation in terms of the median value of R and its variance, which we write as μ_R and σ_R^2 , respectively.

Statistical analysis of the models

We took the nDNA content of sperm cell i (with $i = 1, 2, 3, \dots$) at time t , which we denote by $D_{i,t}$, as $D_{i,t} = A + R_i t + \varepsilon$. In this formula, A is common to all sperm cells, R_i is the rate of nDNA content accumulation of the i 'th sperm cell at time t , and ε is the corresponding random error arising from the fluorescence measurement technique.

We next summarize the statistical analysis; fuller details are given in the Methods.

Model 0

In the first model we assumed no random effect in nDNA accumulation rate, and the model is summarized by $D_{i,t} = A + \mu_R t + \varepsilon$ where that fluorescence errors (ε) follow a normal distribution with mean zero and variance σ_ε^2 , while the R_i 's take only a single value, which we write as μ_R . The distribution of nDNA content is thus a normal distribution with mean $A + \mu_R t$ and variance σ_ε^2 . This corresponds to a classical linear regression and we estimate the parameters using a MCMC procedure with the Metropolis-Hastings algo-

Table 1. Nuclear DNA content of sperm cells at different times.

Description	No. measurements	RFU \pm SD	DNA level/C
Fluorescence value of bare slide (background value)	20	1.4 \pm 0.7	
Somatic cell in style (control)	240	131 \pm 19	2
Sperm cells after 16h of pollination in style	10	91 \pm 10	1.4
Sperm cells after 20h of pollination in style	28	112 \pm 11	1.72
Sperm cells after 24h of pollination in style	38	112 \pm 9	1.72
Sperm cells after 28h of pollination in style	55	120 \pm 12	1.83
Sperm cells after 32h of pollination in style	11	122 \pm 15	1.87

RFU, relative fluorescence units; SD, standard deviation; C, nuclear DNA content a diploid cells has, by definition, an nDNA content of $2C$. This table describes the nDNA content of sperm cells at different times after pollination in the style. The table summarizes how many sperm cell samples were tested. As an approximate guide, 100 relative fluorescence units (RFU) represent 1C of DNA. The calculation of DNA level of a sperm cell is given by: DNA level = [(RFU of a sperm cell - RFU of background (paraffin) - RFU of a slide) / (RFU of a somatic cell - RFU of background (paraffin) - RFU of a slide)] $\times 2C$, where the background fluorescence level is calculated for an area of paraffin identical to the area of the image of the sperm cell's nucleus.

Table 2. Summary of statistical results for the two models.

	Model parameters, means (95%CI)				DIC (effective No. parameters)
	A	μ_R	σ_R^2	σ_ε^2	
Model 0 (R constant)	1.16 (0.97-1.32)	0.024 (0.017-0.031)		0.032 (0.026-0.041)	-84.7 (2.3)
Model 1 (R random effect)	1.14 (0.96-1.30)	0.025 (0.018-0.032)	1.40×10^{-5} (0.08×10^{-5} - 4.12×10^{-5})	0.024 (0.009-0.036)	-83.8 (2.9)

This table gives all of the parameters estimated for Model 0 and Model 1 from the data. The median values of the parameter A are 1.16 and 1.14 respectively. These values are both close to one another (<2% different), suggesting that this parameter is not particularly sensitive to variability of in the nDNA rates. We note that the estimated constant rate of nDNA content accumulation of Model 0 is 0.024/hour and the median value of Model 1, of 0.025/hour, are close to one another, suggesting, again, insensitivity to the assumption of variability of different sperm cells. The Deviance Information Criterion supports this; Model 0 is marginally superior, according to this criterion. Thus it appears completely sufficient to adopt Model 0 for the analysis and interpretation.

rithm,¹¹ since this method can also accommodate Model 1 (which allows variation in the DNA accumulation rate). We shall compare the fit of both models using the Deviance Information Criterion (DIC)¹² - where a smaller value of DIC suggests a better fit.

Model 1

In a second, slightly more sophisticated model, we assumed that the rate of nDNA accumulation exhibits variation, from sperm cell to sperm cell, and hence the nDNA accumulation rate of a sperm cell is a random variable. We make the simplest assumption, that the R_i 's follow a normal distribution with mean μ_R and variance σ_R^2 . Each measurement of the nDNA content of a sperm cell exhibits randomness because of the R_i variation, and also because the fluorescence errors (the ϵ) follow a normal distribution with mean zero and variance σ_ϵ^2 . The distribution of the measured nDNA content at time t is thus a normal distribution with mean $A + \mu_R t$ and variance $\sigma_\epsilon^2 + \sigma_R^2 t^2$. The analysis is more complicated since different numbers of sperm cells were collected (and hence measured) at different times after pollination.

We give detailed results for Model 1, which includes variation in the rate of nDNA accumulation. Under the assumptions of this model, the parameters are: a constant, A , which is common to all sperm cells (see Eq. (1)); the median rate of nDNA accumulation of sperm cells, μ_R ; the variance of the rate of nDNA accumulation of sperm cells, σ_R^2 ; the variance of the error in a sperm cell's nDNA from the fluorescence technique, σ_ϵ^2 . We reported the median of the posterior distribution, as this quantity is known to be more stable than the mean to changes in sample size, and is more representative of a central tendency (especially for distributions which are asymmetric). Given the data D , the log likelihood is given by

$$\log [\text{Prob}(D|A, \mu_R, \sigma_R^2, \sigma_\epsilon^2)] = -\frac{1}{2} \sum_{i,t} \log(2\pi(\sigma_\epsilon^2 + \sigma_R^2 t^2)) - \frac{1}{2} \sum_{i,t} \frac{(D_{i,t} - A - \mu_R t)^2}{2\pi(\sigma_\epsilon^2 + \sigma_R^2 t^2)}$$

Eq. (2)

According Bayes' theorem

$$\begin{aligned} \text{Prob}(A, \mu_R, \sigma_\epsilon^2, \sigma_R^2|D) &= \text{Prob}(D|A, \mu_R, \sigma_\epsilon^2, \sigma_R^2) \\ &\text{Prob}(A, \mu_R, \sigma_\epsilon^2, \sigma_R^2) / \text{Prob}(D) \\ &\propto \text{Prob}(D|A, \mu_R, \sigma_\epsilon^2, \sigma_R^2) \text{Prob}(A, \mu_R, \sigma_\epsilon^2, \sigma_R^2). \end{aligned}$$

Eq. (3)

Using a flat prior, corresponding to no previous information on the parameters, we have

$$\begin{aligned} &\text{Prob}(A, \mu_R, \sigma_\epsilon^2, \sigma_R^2|D) \\ &\propto \text{Prob}(D|A, \mu_R, \sigma_\epsilon^2, \sigma_R^2) \end{aligned}$$

Eq. (4)

The results of the statistical analysis of the models, based on Eqs. (2), (3) and (4), are summarized in Table 2.

Results

The nDNA content of sperm cells of *L. barbarum*, estimated from experimental data, was given in terms of relative fluorescence units. These were converted to C value units (where the nDNA content of diploid cells have, by definition, an nDNA content of $2C$). Vegetative nuclei should, optimally, be treated as the control in this experiment because they are connected to the sperm cells and have an nDNA content of $2C$. However, during the experiments, vegetative cells were not seen, and somatic cells (which are diploid) were adopted as controls. We determined that these cells

were all in the same stage of development, by testing their fluorescence level (we chose a window of fluorescence levels of width 20 RFU around the mean value, as an indication of the stage of the development). It follows that in the experiments, the relative fluorescence of style somatic cells was used as the standard by which the sperm cells were compared and hence calibrated. Subtracting the background fluorescence of both the cytoplasm and the embedding medium allowed the nDNA content of the sperm cells to be estimated.

In Figure 1 we illustrate the data, in the form of frequency histograms, at different times after pollination. This illustrates the variability of the measured value of the nDNA content of a sperm cell.

The results of the statistical analysis of this data are summarized in Table 2.

For both Model 0 and Model 1, we obtained the joint posterior distribution of the parameters (Eq. (3), and its analogue for Model 0) by using MCMC methods.¹¹ The MCMC procedure was iterated 10^5 times, and we tuned the proposal variances to achieve good mixing of the different posterior distributions (*i.e.*, around 20% acceptance probability). Reported param-

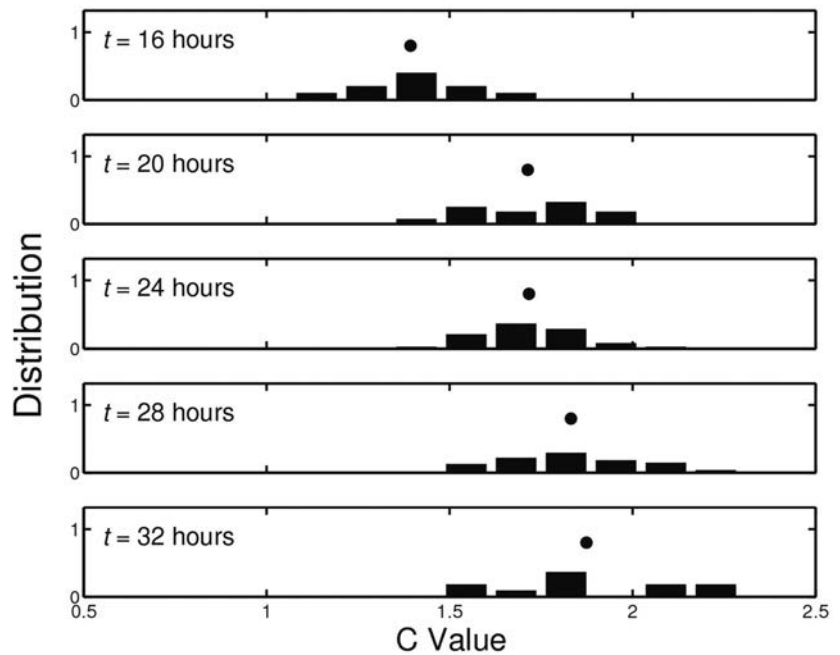


Figure 1. Distribution of nuclear DNA content of sperm cells at different times after pollination. In this figure, we show the empirical distribution of the nDNA content of sperm cells at different times after pollination. For example, the final histogram, labeled $t=32$ hours, is the empirical distribution of the sperm cell's nDNA content, when measured in C units, at 32 hours after pollination. The black dots in the figure represent the mean value of the nDNA content of a sperm cell, at a given time, as calculated from the data. The figure shows that the distribution of the nDNA content of sperm cells, at different times after pollination, has an increasing trend. Note that the measured nDNA content of some sperm cells exceeds the $2C$ which is the maximum level. This is assumed to be a consequence of the fluorescence technique, which effectively adds a random component to the actual nDNA content, and thereby extends the measured range.

eters and distributions were computed once convergence to stable distributions was achieved. Given the computational simplicity of the two models, we used a fixed burn-in period of 10^4 iterations for both models. Visual inspection of the likelihood traces indicate that this burn-in period is very conservative; for both models, convergence was achieved well before this number of iterations. Figure 2 shows the posterior distributions of the statistical analysis for Model 1.

To show differences of the two models, in Figure 3 we have plotted the *best straight lines* through the data, according to the parameters in Table 2. Additionally, we have averaged the data values collected at each time after pollination, and also plotted these in Figure 3. At different times after pollination, different numbers of sperm cells were collected, and the resulting data make different contributions to the parameters in Table 1. These differences were incorporated into the statistical analyses carried out.

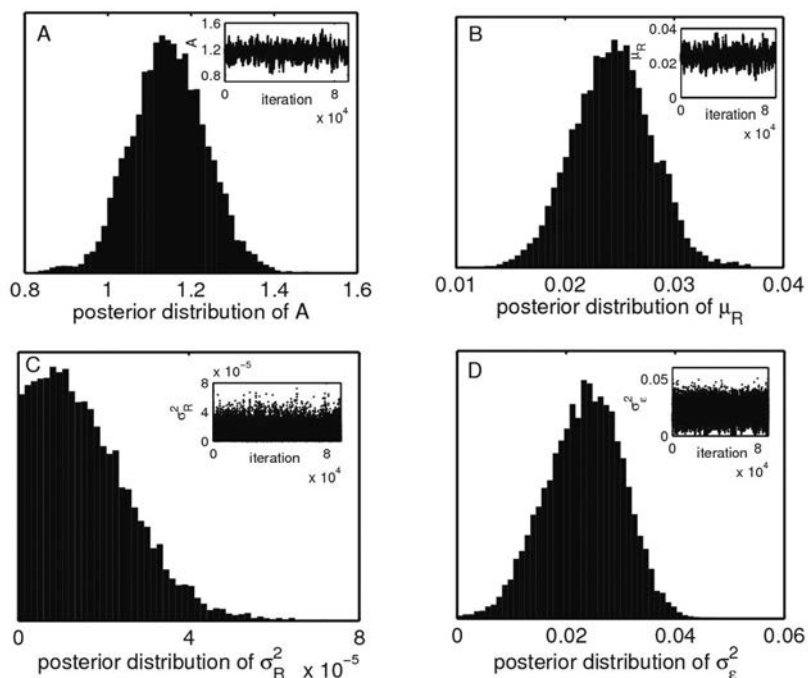


Figure 2. Posterior distributions of the statistical analysis. In this figure we give posterior distributions for Model 1 of: the initial nDNA content of a sperm cell, A , (Panel A); the rate of nDNA accumulation, μ_R , (Panel B); the variance in the rate of nDNA accumulation, σ_R^2 , (Panel C); the variance in measurement error, σ_ϵ^2 (Panel D). In each of the panels, we also plot, in inset, the parameter trajectories after the burn-in period, confirming that convergence and good mixing was achieved.

Discussion and Conclusions

Measurements of the nDNA content of sperm cells in plants, have, previously, had the objective of determining the nDNA content. In the present work we have analyzed the experimentally measured nDNA content of sperm cells of a plant at different times after pollination and focused on the dynamical aspect of nDNA synthesis. We have used the experimental data to investigate the rate at which nDNA content synthesis (or nDNA accumulation) occurs in sperm cells. We carried out a statistical analysis where two different dynamical models were fitted to the data. In both models, we made the dynamical assumption that for a given sperm cell, the accumulation of nDNA content occurs *linearly* with time. However, in our first model (Model 0) we assumed the rate of accumulation of nDNA content of different sperm cells was identical. We thus assumed that there was no variation in the rate of nDNA accumulation of different sperm cells. In Model 1 we allowed the possibility that there was variability in the rate of nDNA accumulation of

different sperm cells.

Eq. (1) describes the nDNA content of the plant sperm cells and has been fitted to data covering 16 to 32 hours after pollination. It is not meaningful to apply this equation for times where the sperm cells do not have an independent existence. We do not have a direct measure of this time, but the microscopy observations suggest that no sperm cells exist up to 12 hours after pollination, but only later than this time. However, if we nonetheless apply Eq. (1) from the time of pollination (time 0) onwards, not just from 16 hours after pollination, then the parameter A would have the plausible interpretation as the nDNA content of *half* of a generative cell (which is the direct precursor of a sperm cell). This would suggest a value of A that is close to unity, since all generative cells have an nDNA content of $2C$.³ Remarkably, the statistical analysis leads, in both models, to values of A within 16% of unity. This makes it plausible that the structure which develops into a sperm cell, from the time of pollination, accumulates nDNA near *linearly* over time, but we have no direct evidence of this. Let us now consider the factors influenc-

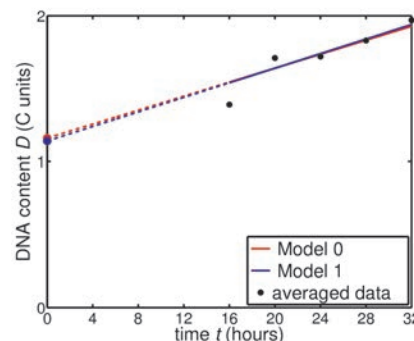


Figure 3. Plot of the best straight lines from the models. In this figure, we have plotted the two *best straight lines* that can be derived from the two models, namely $D=A+\mu_R t$. These lines cover the range 16 hours to 32 hours after pollination and are indicated by solid colored lines. They illustrate the small level of difference of the two models. The black dots mark the average of the measured values of the nDNA content of the sperm cells, at different times after pollination. In addition, we have plotted an extrapolation of the fitted lines to the range of times 0 to 16 hours after pollination (indicated by colored dashed lines). According to observations from microscopy, sperm cells do not have an independent existence during most of the extrapolated time interval, and hence the lines cannot directly refer to the nDNA content of sperm cells. However, the intercepts of the lines (indicated by colored dots) occur at the values 1.16C and 1.14C which are both close to 1C, i.e., close to the haploid C content of one half a generative cell, which is a precursor of a sperm cell.

ing the statistical results. We note that generally, the value of the nDNA content of sperm cells after pollination is likely to be influenced by the validity of two assumptions. The first assumption is that the measured nDNA errors, that arose from the fluorescence technique, were *unbiased*. That is, we assumed the distribution of the fluorescence errors were symmetrically distributed around zero.

The second assumption is that the value of the nDNA content of sperm cells, for a range of times after pollination, increases *linearly* with time. This assumption is the simplest that can be made, and is likely to break down at sufficiently long times, and lead to a *saturation effect*, since once an nDNA content of $2C$ has been achieved in a sperm cell, no further change in the sperm cell will be observed, prior to zygote formation.

The statistical analysis of both models (see the Statistical Analysis of the models section) allows their comparison, using the Deviance Information Criterion, which is known to combine goodness of fit with a penalty associated with the number of parameters contained in a model.¹² It appears that on the basis of the experimental data, there is no benefit in adopting the more complex model (Model 1) to summarize the data. Certainly, the variance in the rate of nDNA accumulation, for Model 1, is small: from Table 2, we have $\sigma^2_R = 1.40 \times 10^{-5}$. For different data sets, however, Model 1 may

be a more appropriate and more useful description.

References

1. Hu Sh Y. Reproductive biology of angiosperms. Beijing: Higher Education Press; 2005.
2. Friedman WE. Expression of the cell cycle in sperm of Arabidopsis: implications for understanding patterns of gametogenesis and fertilization in plants and other eukaryotes. *Development* 1999;126:1065-75.
3. Tian HQ, Yuan T, Russell SD. Relationship between double fertilization and the cell cycle in male and female gametes of tobacco. *Sex Plant Reprod* 2005;17:243-52.
4. Tian M, Wang M. Studies on extraction, isolation, and composition of Lycium barbarum polysaccharides. *J Trad Chin Herb Drugs* 2006;31:1603-7.
5. Zheng GQ. The Studies on the Relationship between the structure, development and sugar accumulation in fruits of Lycium barbarum L. Degree Dissertation. Northwestern University of China, China; 2011.
6. Tang WC, Eisenbrand G. Lycium barbarum L. and L. chinensis Mill. In: Tang WD, Eisenbrand G, eds. Chinese drugs of plant origin: chemistry, pharmacology, and use in traditional and modern medicine. 1st ed. Berlin: Springer; 1992. pp 633-638.
7. Deng H, Wang YY, Zhu XY, Tian HQ. Generative and sperm cell isolation in *Bauhinia blakeana* (Fabaceae). *Ann Bot Fennici* 2012;49:1-6.
8. Ge LL, Gou XP, Yuan T, et al. Migration of sperm cells during pollen tube elongation in *Arabidopsis thaliana*: behavior during transport, maturation and upon dissociation of male germ unit associations. *Planta* 2011;233:325-32.
9. Qiu YL, Yang YH, Zhang SQ, Tian HQ. Isolation of two populations of sperm cells from the pollen tube of Tobacco. *Acta Botanica Sinica* 2004;46:719-23.
10. Deng H, Song YX, Qin K, Tian HQ. DNA content and cell cycle changes of male and female gametes of *Lycium barbarum* L. *Plant Physiol J* 2012;48:869-73.
11. Chib S, Greenberg E. Understanding the Metropolis-Hastings algorithm. *Am Stat Assoc* 1995;49:327-35.
12. Spiegelhalter DJ, Best NG, Carlin BP, van der Linde A. Bayesian measures of model complexity and fit. *J R Stat Soc, B* 2002;64: 583-639.

Intrinsically disordered proteins: controlled chaos or random walk

T.C. Howton,¹ Yingqian Ada Zhan,² Yali Sun,¹ M. Shahid Mukhtar^{1,3}

¹Department of Biology, University of Alabama at Birmingham, AL; ²Institute for Bioinformatics and Evolutionary Studies, University of Idaho, Moscow, ID; ³Nutrition Obesity Research Center, University of Alabama at Birmingham, AL, USA

Abstract

Traditional conventions that a protein's sequence dictates its definitive, tertiary structure, and that this fixed structure provides the protein with the ability to carry out its designated role(s) are still correct but not for all proteins. Research over the past decade discovered that several key proteins possess intrinsically disordered regions (IDRs) that are crucial to their ability to perform specific functions and are observed clustered together within important classes of proteins. In this review, we aim to demonstrate how free energy landscapes, molecular dynamics simulations, and homology modeling are helpful in understanding key conformational dynamics of intrinsically disordered proteins (IDPs). Additionally, we use a list of predicted IDPs found in *Arabidopsis* to identify chromatin organizers and transcriptional regulators as being highly enriched in IDPs. Furthermore, we focus our attention to specific proteins within these families such as HAC5, EFS, ANAC019, ANAC013, and ANAC046. Future studies are needed to experimentally identify additional IDPs and their binding mechanisms.

Introduction

Over the past two decades, the world of proteomics has undergone a significant paradigm shift. The classical approach to the study of proteins depended on the adherence to the protein structure-function model, where each protein was composed of an amino acid sequence that lead to a static structure and function. With the discovery of intrinsically disordered regions (IDRs), researchers have developed new approaches and methodologies to better understand the unstructured and dynamic world of intrinsically disordered proteins (IDPs).¹ Although all domains of life con-

tain IDPs, eukaryotic proteins tend to show a significant level of enrichment. It has been demonstrated that approximately 33% of eukaryotic proteins contain at least one long stretch of residues (30 or more) that code for an intrinsically disordered region,² and greater than 30% of eukaryotic proteins have 50 or more consecutive disordered residues.³ Proteome-wide analyses of multiple plants have shown that roughly 30% of a plant's proteome is comprised of proteins containing at least one region with 50 or more disordered residues. It has been suggested that the pronounced occurrence of IDPs in plant genomes might be advantageous for them to mount effective cellular responses under varied biotic and abiotic environmental conditions. This increased frequency of IDPs in plants could also lead to a high level of phenotypic plasticity.⁴ Intrinsically disordered proteins are found in nearly every class of proteins within the eukaryotic proteome, including transcription factors, signaling proteins, and proteins involved in chromatin remodeling.

The intrinsically disordered regions of unstructured proteins serve multiple purposes under different environmental conditions. Given that proteins generally form macromolecular complexes to execute diverse cellular functions, proteins with unstructured regions can have a wide-range of binding partners and might participate in multiple biological processes.⁵ In addition, it was also demonstrated that the speed of a protein's ability to bind to its partner(s) increased drastically in proteins with intrinsically disordered regions when compared to their structured, globular counterparts.⁶ Intrinsically disordered regions known as *linker* regions can hold two globular portions of a protein in close proximity with each other, while still allowing a large amount of flexibility in their spatial relationship with one another.⁷ This perhaps allows a protein with IDRs to bind with several binding partners simultaneously under changing cellular states.

Researchers have created several tools in order to better understand IDPs and their functions. Computational analyses of free energy landscapes (mapping all possible conformations of an entity) are vital to experimentally defining an IDP. Typically, proteins fold into their stable state at a distinct trough of the free energy landscape. However, IDPs show multiple shallow troughs due the increased number of conformational states. Free energy landscapes, along with molecular dynamics studies and homology modeling, allow predicting the conformational dynamics of IDPs. In this review, we aim to highlight computational tools that are helpful in understanding key conformational dynamics of IDPs. Distinctively, we will focus on intrinsically disordered proteins within the plant *Arabidopsis*

Correspondence: Shahid M. Mukhtar, Department of Biology, The University of Alabama at Birmingham, Campbell Hall 369, 1300 University Blvd., Birmingham, AL 35294-1170, USA.
Tel.: +1.205.934.8335 - Fax: +1.205.975.6097.
E-mail: smukhtar@uab.edu

Key words: Intrinsically disordered regions; *Arabidopsis*; chromatin organizers; transcriptional regulators.

Acknowledgments: the authors would like to acknowledge Mr. Derek Moates for his valuable comments and suggestions on this manuscript. We acknowledge funding from UAB, College of Arts and Science graduate fellowship to YS and NSF (IOS-1557796) to MSM. The authors apologize to all authors whose work was not included within this review due to space restrictions. M. S. Mukhtar was supported through funds from the Department of Biology, The University of Alabama at Birmingham.

Contributions: all authors participated in developing the ideas presented in this manuscript, researching the literature, and writing parts of the text.

Conflict of interest: the authors declare no conflict of interest.

Received for publication: 10 September 2015.

Revision received: 12 September 2015.

Accepted for publication: 12 September 2015.

This work is licensed under a Creative Commons Attribution-NonCommercial 3.0 International License (CC BY-NC 3.0).

©Copyright T.C. Howton et al., 2015
Licensee PAGEPress srl, Italy
International Journal of Plant Biology 2015; 6:6191
doi:10.4081/pb.2015.6191

thaliana (*Arabidopsis*). Our Gene Ontology (GO) enrichment analysis determines that proteins families belonging to chromatin remodeling and transcriptional regulation are statistically enriched in IDPs. We will discuss the potential roles of these classes of proteins in diverse biological processes with specific examples.

Free energy landscape of intrinsically disordered proteins

Due to thermal fluctuation, proteins can exhibit various conformations. The occurrence of each conformation is presented by the topography of the free energy landscape. Natively structured proteins usually fold into a native structure at the bottom of a free energy

landscape (Figure 1A). On the other hand, IDPs have no well-defined structure in the unbound state and have multiple shallow dips for weakly bound states, which makes a rugged free energy landscape (Figure 1B). Consequently, IDPs have a broad range of conformational dynamics and constantly move between different conformations.⁸⁻¹⁰ This property makes it challenging to map an IDP's structures and dynamics to its function. In the past decade, IDPs have been found prevalent among living organisms where they play essential roles in many biological processes.^{1,11-13} Although difficult, it is very important to characterize the free energy landscape of IDPs which will help us better understand how a primary sequence encodes the diverse mechanisms and links to the functions in these proteins. Furthermore, a better understanding of IDPs conformations may lead to the development of new therapeutics based on structural drug design.¹⁴⁻¹⁶

Molecular dynamic simulations and homology modeling

Intrinsically disordered proteins exhibit high levels of flexibility and span multiple different conformations. Molecular dynamics (MD) simulations provide a tool to computationally explore the conformational space and examine the dynamics of a protein over time. Although computer simulations rely on a series of cumulative approximations that can be erroneous, it has become a necessary tool in the research involving IDPs.

Combined with experimental studies, typically NMR spectroscopy, the structural ensemble of the free energy landscape of IDPs can be constructed using computer simulations. Ensemble restrained MD simulations constitute a useful and important tool for modeling IDPs.¹⁷⁻¹⁹ Constructing an ensemble based on a pre-determined structural library represents another way of completing the task. ENSEMBLE,²⁰ Select (SAS),²¹ ASTEROIDS,²² and BEGR,²³ are pieces of software falling into this category.

IDPs are considered to have high specificity and low affinity when interacting with binding, partner molecules. Mutations may harm this interaction. MD simulations can be used to study an array of mutations to predict the consequences and provide mechanistic explanations without performing experiments. Using computational alanine scanning, Massova *et al.*²⁴ suggested an approach to probe protein-protein interactions and evaluated binding free energies. In their case, they applied the method to p53 and MDM2 binding system where p53 is intrinsically disordered, and their results show excellent agreement with experi-

mental data.²⁴ Homology modeling is a useful tool to predict and study the structure of a protein from a homologue protein, where the structure of the protein in question has not been solved experimentally and the structure of its homologue protein is known. In the Arabidopsis genome, the *COR15A* gene is paired with *COR15B*.²⁵ Proteins encoded by these two genes are homologous with 70% identity in their amino acid sequences. Overexpression of the *COR15A* gene in Arabidopsis produces excess mature COR15A protein in the chloroplast stroma,²⁶ leading to enhanced freezing tolerance of chloroplasts of intact leaves and of isolated protoplasts frozen and thawed *in vitro*.^{26,27} In contrast, functional or structural information has been reported for COR15B protein. Both proteins show homology

to the Pfam LEA_4 family of LEA proteins and both were predicted to be IDPs.²⁸ Thalhammer *et al.*²⁹ showed the structural modeling of these two proteins known LEA homologues and demonstrated the interactions between MGDC and the COR15 proteins that may help keep the cell integrity through freezing stress.

Arabidopsis protein families enriched in intrinsically disordered proteins

A recent genome-wide analysis was performed to predict IDRs in Arabidopsis and compare them with the human proteome.

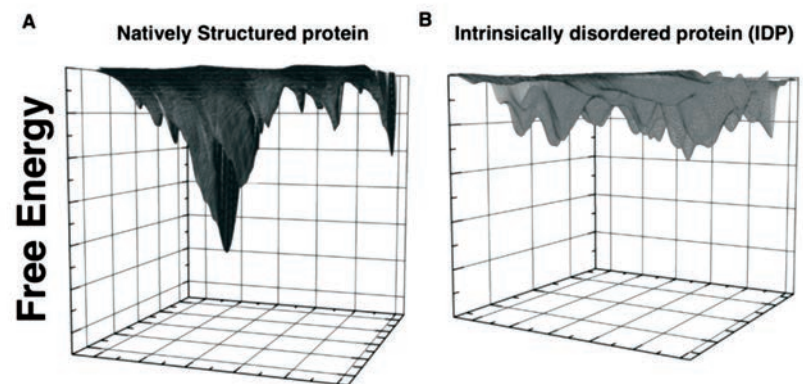


Figure 1. The free energy landscape of a natively structured protein. A natively structured protein (A) exhibits a well-defined minimum energy state corresponding to the folded conformation. In comparison, the energy landscape of an IDP (B) lacks a deep energy minimum.

Table 1. Identification of protein families enriched in intrinsically disordered regions.

	Count	P_Value	Benjamini
Annotation cluster 1 (enrichment score: 15.42)			
Chromosome organization	28	2.60E-18	1.50E-15
Chromatin modification	22	7.40E-18	2.10E-15
Chromatin organization	25	8.00E-17	2.10E-14
Chromatin regulator	15	1.40E-11	1.30E-09
Annotation cluster 2 (enrichment score: 7.94)			
DNA binding	85	1.90E-20	3.30E-18
Regulation of transcription	57	2.20E-10	3.10E-08
Nucleus	58	4.10E-09	2.00E-07
Transcription regulator activity	54	1.20E-08	6.90E-07
Transcription	40	4.20E-08	3.40E-06
Regulation of transcription, DNA-dependent	35	1.20E-07	6.90E-06
Regulation of RNA metabolic process	35	1.40E-07	7.20E-06
Transcription regulation	37	5.10E-07	1.60E-05
Transcription	37	8.30E-07	2.00E-05
Activator	17	2.70E-06	5.20E-05
Transcription factor activity	44	3.50E-06	1.00E-04
DNA binding	38	8.80E-06	1.20E-04

Intriguingly, it was discovered that specific functional classes are enriched with IDRs in *Arabidopsis*.³⁰ These functional groups include *post-translational protein modification* and *response to red or far red light*. While these broad functional classes provided insightful clues on the essential roles of these IDPs/IDRs in *Arabidopsis*, here we reevaluated these data to specifically predict protein families enriched with IDRs. To achieve this, we compiled a list of IDPs containing at least five long disordered regions (>30 residues). We subjected these IDPs to functional annotation tool, DAVID (the Database for Annotation, Visualization and Integrated Discovery)³¹ to predict the statistically enriched GO categories as well as enriched groups of different protein families (Supplementary Table S1: Functional Annotation of Predicted IDPs). DAVID employs a novel agglomeration algorithm to assemble a list of genes or associated biological terms into organized classes of related genes. Subsequently, we used the PANTHER (Protein ANalysis THrough Evolutionary Relationships)^{32,33} classification tool to organize the lists by molecular function (Figure 2). We identified the two most enriched groups contain chromatin organizers (Enrichment Score: 15.42) and transcription regulators (Enrichment Score: 7.94) (Table 1). We hypothesized that these two molecular groups play widespread roles in the downstream regulation of a vast majority of *Arabidopsis* genes under diverse cellular conditions. In the following sections of the review, we will discuss specific examples from these two groups and highlight key findings pertaining to their roles in conjunction with IDRs.

Chromatin remodeling

Even though cells within most eukaryotic organisms specialize in both structure and function, each contains the same genomic DNA of the organism. Therefore, the uniqueness of each cell is derived not by the DNA sequence but instead by the availability of portions of the DNA within that particular cell.³⁴ The accessibility of genes is regulated not only through the prevalence of transcription factors and enhancers, but also through the structure of the DNA itself. The DNA of eukaryotes is associated with histone octamers that sequester approximately 147 base pairs of DNA in a nucleosome complex. Histone octamers are eight-protein complexes consisting of two copies of four subunits (H2A, H2B, H3, and H4). The DNA that is associated with histone proteins is not accessible to the cellular machinery responsible for transcription, chromatin assembly, DNA repair, and a variety of other processes.³⁵ The tightness of this associ-

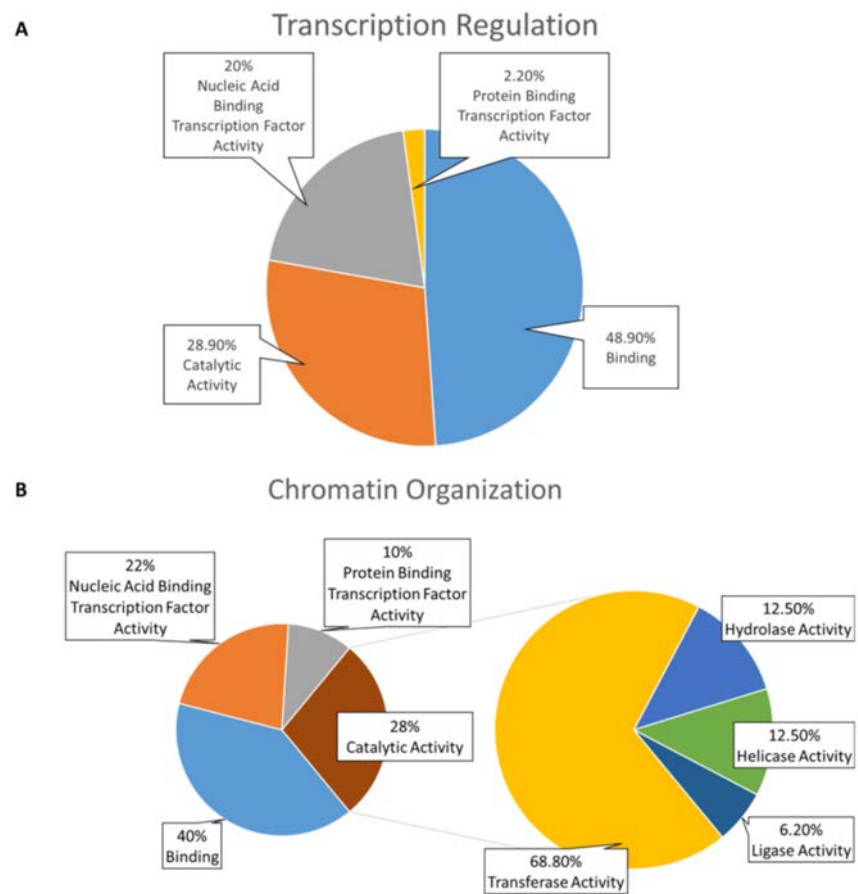


Figure 2. Classification of enrichment groups by molecular function. The two enriched groups, Transcription Regulation (A) and Chromatin Organization (B), are organized by their molecular function using the PANTHER classification tool.

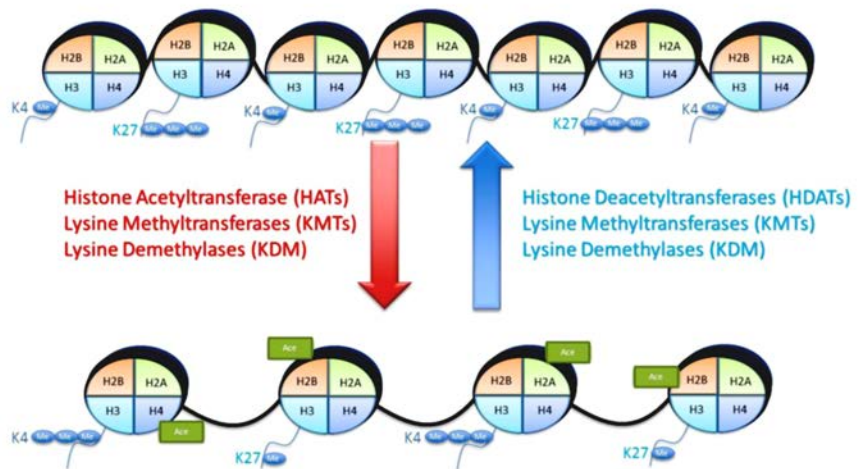


Figure 3. Chromatin organization through transferases. The transition between euchromatin and heterochromatin can be facilitated by various transferases. Acetylation of histones leads to the relaxation of chromatin structure. Histone methylation is more complex and depends on the location and extent of methylation

ation can create two different types of chromatin, heterochromatin and euchromatin. Heterochromatin occurs when the histone proteins are close together and undergo higher-ordered arrangements. This type of chromatin structure generally causes the genes associated with it to become silenced because the RNA polymerase is unable to bind to the promoter regions of the sequestered genes. Euchromatin occurs when the histone proteins disassociate with the DNA completely or spread apart, decreasing the amount of DNA directly associated with histones.

The structure of chromatin can be dynamic, and it is regulated by a group of proteins and complexes known as chromatin remodelers. These chromatin remodelers can modify the histone octamers in a variety of ways including acetylation, ubiquitination, phosphorylation, methylation, and sumoylation. The histone modifications either relax or tighten the structure of the localized DNA thereby permitting or restricting the transcription of nearby genes. Histone acetylation causes the relaxation of chromatin, thereby permitting an increase in the localized amount of transcription.³⁶ The acetylation of the N-terminal tails of histones removes the overall positive charge. When the histone's tail loses its positive charge, it loses its attraction to the negatively charged phosphate backbone of DNA as well as its attraction to other histones. Histone acetylation generally involves the transfer of an acetyl group from a molecule (such as acetyl coenzyme A) to a lysine amino acid residue on the tail of a histone octamer. Two opposing enzymes, histone acetyltransferases (HAT) and histone deacetyltransferases (HDAT), regulate the histone acetylation state (Figure 3).

One HAT with a predicted IDR is Histone Acetyltransferase of the CBP Family (HAC5) (Supplementary Table S1: Functional Annotation of Predicted IDPs). The HAT protein family of Arabidopsis consists of five CREB-binding proteins including HAC5.³⁷ The HAC family of proteins is implemented in a variety of cellular processes including cell differentiation, growth and homeostasis.³⁸ HAC5, in conjunction with HAC1, has been shown to be significant in the ethylene-signaling pathway. Interestingly, *hac1hac5* double mutants are hypersensitive in their ethylene signaling response in both dark and light conditions.³⁹ HAC5 has also implemented in a diverse group of developmental functions including flowering.^{40,41}

Histone methylation is not as straightforward as histone acetylation. Histone methyltransferases (HMT) can methylate lysine (K) and arginine (R) amino acid residues on both the H3 and H4 subunits of the histone complex. Additionally, histone methylation can lead to either transcriptional activation or repression, depending on the location of the

methylation and its surroundings. Nonetheless, histone methylation is an important key in epigenetic regulation of transcription. H3K4me3 is a key indicator of active transcription that is conserved in all eukaryotes.^{42,43} Early flowering in short days (EFS) is a well-studied SET-domain containing histone-lysine N-methyltransferase with predicted intrinsically disordered regions. EFS regulates flowering by actively promoting the flowering inhibitor *Flowering locus C* (FLC) via trimethylation of the localized histones at the H3K4 location.⁴⁴

Transcription factors

Transcription factors are modular proteins that contain one or more DNA-binding domains, recognize and bind to specific DNA sequences, therefore regulating the rate of transcription of genetic information from DNA to RNA. Generally, a prototypical transcription factor contains a DNA-binding domain (DBS), signal-sensing domain (SSD), and a transactivation domain (TAD). And the two processes involved in transcriptional regulations: protein-protein interaction and protein-nucleotide interaction have been reported to be accompanied often by a local folding in a protein molecule,⁴⁵ which may adjust the transcription factor flexibility correspondingly.

Seventy-eight different families of transcription factors contain different numbers of IDRs, according to our analysis. The first 10 enriched transcription factor families are MYB, AP2-EREBP, bHLH, MADS, C2H2, NAC, HB, WRKY, bZIP and C3H.

Four features of ID regions are very important for molecular recognition, including the combination of high specificity and low affinity in their interactions with functional partners, intrinsic plasticity, formation of large interaction surfaces and rapid turnover and reduced lifetime.⁴⁶ Besides, analysis of the distribution of disorder on transcription factors reflected the requirement of disorder regions for their flexibility and efficiency. It has been found in eukaryotes that the AT-hooks and basic regions of transcription factor DNA-binding domains are highly disordered, the degree of disorder in transcription factor activation regions is much higher than that in DNA-binding domains, and the level of -MoRFs (molecular recognition feature) prediction is much higher in transcription factors. MoRF is a specific structural element functioning in the recognition of protein or nucleic acid partners.

Long hypocotyl 5 (HY5) is a basic leucine zipper (bZIP) transcription factor family, involved in light-regulated transcriptional activation of G-box-containing promoters. It acts downstream of the light receptor network and directly affects transcription of light-induced genes, specifically involved in the blue light

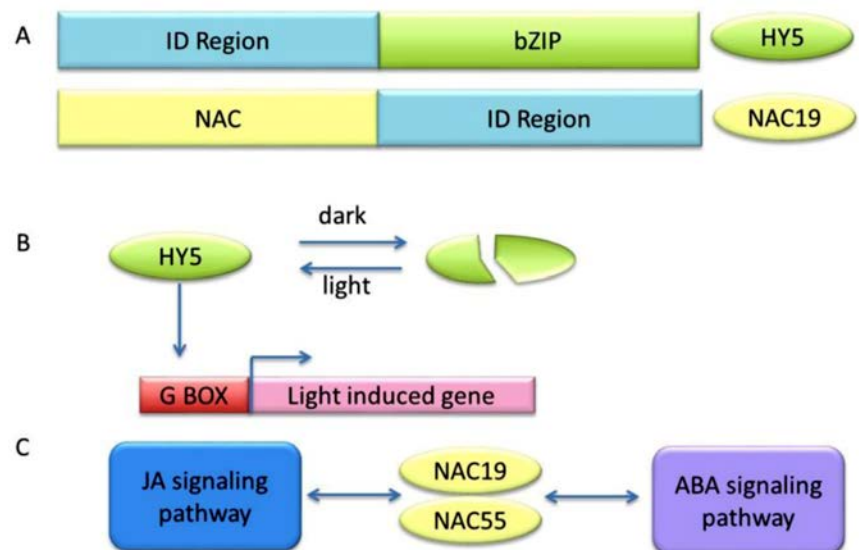


Figure 4. Model of the function of NAC and bZIP transcription factors. (A) Schematic organization of HY5 and NAC19 transcription factors. The ID regions are in blue, bZIP region is in green, NAC region is in yellow. (B) Model of the function of HY5. In darkness, the degradation of HY5 inhibits the activation of light-induced genes. After illumination, the accumulation of HY5 activates G-Box containing promoters and directly affects transcription of light-induced genes. (C) Role of NAC19 and NAC55 in the crosstalk between ABA and JA signaling pathway.

pathway, suggesting that it may participate in the transmission of cryptochromes (CRY1 and CRY2) signals. In darkness, the degradation of HY5 inhibits the activation of light-induced genes. It has been reported that HY5 is negatively regulated by COP1, a light-inactivable repressor of photomorphogenic development interacting directly and specifically with HY5.⁴⁷ Interestingly, the plant hormone cytokinin also induces similar phenotypes as the cryptochrome flavin-type photoreceptors. *hy5* mutants show a reduced induction of anthocyanin accumulation in blue light by cytokinins. It has been shown that cytokinins can increase the levels of HY5 protein accumulation, hinting that cytokinin could play a role in stabilizing HY5 protein, and that the regulation of HY5 stability could act at intersection of cytokinin signaling pathway and cryptochrome pathways.⁴⁸ Abscisic acid (ABA), another phytohormone, regulates seed germination and seedling development as light. It was found that HY5 binds to the promoter of the transcription factor ABI5, which is significantly enhanced by ABA, while overexpression of ABI5 led to increased light response.⁴⁹

NAC (NAM, ATAF, CUC) transcription factors share an N-terminal NAC domain and regulate stress perception and developmental programs. The crystal structure of the ANAC019 NAC domain consists of twisted β -sheet packing against a α -helix on both sides.^{50,51} The NAC transcription regulatory domains (TRDs) contain group-specific sequence motifs and have a high degree of intrinsic disorder.⁵² Both full-length and truncated ANAC019 are able to induce the expression of stress-responsive marker genes [COR47 (cold-responsive 47), RD29b (responsive-to-desiccation 29b) and ERD11 (early-responsive-to-dehydration11)]. Replacing the NAC domain of ANAC019 with the analogous regions from other NAC transcription factors still keeps the ability to regulate ABA signaling, while replacing the ANAC019 TRD with other TRDs loses the ABA signaling regulation ability.⁵² Further it has been shown that ANAC019 interacts with the RING-finger H2-type E3 ubiquitin-protein ligase RHA2a.⁵³ ANAC019 may play a dual role in regulating ABA and jasmonate response with the other RHA2a-interacting protein ANAC055. These two signaling pathways are involved in the activation of defense responses to both biotic and abiotic stresses, and ANAC019 and ANAC055 could serve as players linking the crosstalk between these two signaling pathways (Figure 4).⁵³ Additionally, two other ANAC proteins, ANAC046 and ANAC013, have recently been experimentally identified as IDPs. It has been shown that both of these aforementioned ANAC transcription factors are capable of interacting with the small hub protein known as Radical-induced Cell Death 1 (RCD1), at least partially due to their intrinsi-

cally disordered region. Both proteins are involved in plant senescence. Interestingly, the interaction between the two TFs and RCD1 does not appear to be dependent on a disorder-to-order transition.⁵⁴ Future research could focus on determining if ANAC019 interacts with its binding partners in a similar way.

Conclusions

The discovery of intrinsically disordered proteins created a novel area of proteomics. Specifically, the increased knowledge of protein folding dynamics may lead to a better understanding of plants' phenotypic plasticity. Because plants are fixed in soil and unable to move, they create complex mechanisms for coping with biotic and abiotic environmental stresses. The concept of flexible proteins, which are able to change their interaction profile based on cellular conditions, leads to a new way of thinking about plant plasticity. We have highlighted tools that are useful for characterizing IDPs' conformational dynamics. Additionally, we have demonstrated that Arabidopsis contains two highly enriched groups of IDPs; both of which are key components in the transcriptional regulation landscape. Further studies need to focus on experimentally verifying proteins as IDPs, and describing the advantages and disadvantages of intrinsically disordered regions over their more structured counterparts. Furthermore, IDPs have been recent targets for therapeutic strategies for mammalian diseases such as Parkinson's disease.⁵⁵ Similarly, IDPs found in plants could be targets for decreasing crops' susceptibility to disease or increasing overall yield. Additional research could focus on identifying key IDP targets for both therapeutics and plant resistance.

References

- 1 Tompa P. Intrinsically unstructured proteins. *Trends Biochem Sci* 2002;27:527-3.
- 2 Ward JJ, Sodhi JS, McGuffin LJ, et al. Prediction and functional analysis of native disorder in proteins from the three kingdoms of life. *J Mol Biol* 2004;337:635-45.
- 3 Dunker AK, Lawson JD, Brown CJ, et al. Intrinsically disordered protein. *J Mol Graph Model* 2001;19:26-59.
- 4 Marin M, Ott T. Intrinsic disorder in plant proteins and phytopathogenic bacterial effectors. *Chem Rev* 2014;114:6912-32.
- 5 Wright PE, Dyson HJ. Intrinsically unstructured proteins: re-assessing the protein structure-function paradigm. *J Mol Biol*

1999;293:321-31.

- 6 Huang Y, Liu Z. Kinetic advantage of intrinsically disordered proteins in coupled folding-binding process: a critical assessment of the fly-casting mechanism. *J Mol Biol* 2009;393:1143-59.
- 7 Tantos A, Han KH, Tompa P. Intrinsic disorder in cell signaling and gene transcription. *Mol Cell Endocrinol* 2012;348:457-65.
- 8 Dunker AK, Oldfield CJ, Meng J, et al. The unfoldomics decade: an update on intrinsically disordered proteins. *BMC Genomics* 2008;9:S1.
- 9 Higo J, Umezawa K. Free-energy landscape of intrinsically disordered proteins investigated by all-atom multicanonical molecular dynamics. *Adv Exp Med Biol* 2014;805:331-51.
- 10 Jensen MR, Zweckstetter M, Huang JR, Blackledge M. Exploring free-energy landscapes of intrinsically disordered proteins at atomic resolution using NMR spectroscopy. *Chem Rev* 2014;114:6632-60.
- 11 Uversky VN. Natively unfolded proteins: a point where biology waits for physics. *Protein Sci* 2002;11:739-56.
- 12 Dyson HJ, Wright PE. Intrinsically unstructured proteins and their functions. *Nat Rev Mol Cell Biol* 2005;6:197-208.
- 13 Uversky VN, Dunker AK. Understanding protein non-folding. *Biochim Biophys Acta* 2010;1804:1231-64.
- 14 Metallo SJ. Intrinsically disordered proteins are potential drug targets. *Curr Opin Chem Biol* 2010;14:481-8.
- 15 Uversky VN. Targeting intrinsically disordered proteins in neurodegenerative and protein dysfunction diseases: another illustration of the D(2) concept. *Expert Rev Proteomics* 2010;7:543-64.
- 16 Wang J, Cao Z, Zhao L, Li S. Novel strategies for drug discovery based on intrinsically disordered proteins (IDPs). *Int J Mol Sci* 2011;12:3205-19.
- 17 Ganguly D, Chen J. Structural interpretation of paramagnetic relaxation enhancement-derived distances for disordered protein states. *J Mol Biol* 2009;390:467-77.
- 18 Allison JR, Varnai P, Dobson CM, Vendruscolo M. Determination of the free energy landscape of alpha-synuclein using spin label nuclear magnetic resonance measurements. *J Am Chem Soc* 2009;131:18314-26.
- 19 Lindorff-Larsen K, Best RB, Depristo MA, et al. Simultaneous determination of protein structure and dynamics. *Nature* 2005;433:128-32.
- 20 Krzeminski M, Marsh JA, Neale C, et al. Characterization of disordered proteins with ENSEMBLE. *Bioinformatics* 2013;29:398-9.
- 21 Chen Y, Campbell SL, Dokholyan NV. Deciphering protein dynamics from NMR

- data using explicit structure sampling and selection. *Biophys J* 2007;93:2300-6.
- 22 Nodet G, Salmon L, Ozenne V, et al. Quantitative description of backbone conformational sampling of unfolded proteins at amino acid resolution from NMR residual dipolar couplings. *J Am Chem Soc* 2009;131:17908-18.
- 23 Daughdrill GW, Kashtanov S, Stancik A, et al. Understanding the structural ensembles of a highly extended disordered protein. *Mol Biosyst* 2012;8:308-19.
- 24 Massova I, Kollman P. Computational alanine scanning to probe protein-protein interactions: a binding free energies. *J Am Chem Soc* 1999;121:10.
- 25 Wilhelm KS, Thomashow MF. *Arabidopsis thaliana* cor15b, an apparent homologue of cor15a, is strongly responsive to cold and ABA, but not drought. *Plant Mol Biol* 1993;23:1073-7.
- 26 Artus NN, Uemura M, Steponkus PL, et al. Constitutive expression of the cold-regulated *Arabidopsis thaliana* COR15a gene affects both chloroplast and protoplast freezing tolerance. *Proc Natl Acad Sci USA* 1996;93:13404-9.
- 27 Steponkus PL, Uemura M, Joseph RA, et al. Mode of action of the COR15a gene on the freezing tolerance of *Arabidopsis thaliana*. *Proc Natl Acad Sci USA* 1998;95:14570-5.
- 28 Hundertmark M, Hinch DK. LEA (late embryogenesis abundant) proteins and their encoding genes in *Arabidopsis thaliana*. *BMC Genomics* 2008;9:118.
- 29 Thalhammer A, Hundertmark M, Popova AV, et al. Interaction of two intrinsically disordered plant stress proteins (COR15A and COR15B) with lipid membranes in the dry state. *Biochim Biophys Acta* 2010;1798:1812-20.
- 30 Pietrosevoli N, Garcia-Martin JA, Solano R, Pazos F. Genome-wide analysis of protein disorder in *Arabidopsis thaliana*: implications for plant environmental adaptation. *PLoS One* 2013;8:e55524.
- 31 Huang da W, Sherman BT, Lempicki RA. Bioinformatics enrichment tools: paths toward the comprehensive functional analysis of large gene lists. *Nucleic Acids Res* 2009;37:1-13.
- 32 Mi H, Muruganujan A, Thomas PD. PANTHER in 2013: modeling the evolution of gene function, and other gene attributes, in the context of phylogenetic trees. *Nucleic Acids Res* 2013;41:D377-86.
- 33 Mi H, Muruganujan A, Casagrande JT, Thomas PD. Large-scale gene function analysis with the PANTHER classification system. *Nat Protoc* 2013;8:1551-66.
- 34 Zhou Y, Kim J, Yuan X, Braun T. Epigenetic modifications of stem cells: a paradigm for the control of cardiac progenitor cells. *Circ Res* 2011;109:1067-81.
- 35 Marino-Ramirez L, Kann MG, Shoemaker BA, Landsman D. Histone structure and nucleosome stability. *Expert Rev Proteomics* 2005;2:719-29.
- 36 Gorisch SM, Wachsmuth M, Toth KF, et al. Histone acetylation increases chromatin accessibility. *J Cell Sci* 2005;118:5825-34.
- 37 Pandey R, Müller A, Napoli CA, et al. Analysis of histone acetyltransferase and histone deacetylase families of *Arabidopsis thaliana* suggests functional diversification of chromatin modification among multicellular eukaryotes. *Nucleic Acids Res* 2002;30:5036-55.
- 38 Bordoli L, Netsch M, Luthi U, et al. Plant orthologs of p300/CBP: conservation of a core domain in metazoan p300/CBP acetyltransferase-related proteins. *Nucleic Acids Res* 2001;29:589-97.
- 39 Li C, Xu J, Li J, et al. Involvement of *Arabidopsis* histone acetyltransferase HAC family genes in the ethylene signaling pathway. *Plant Cell Physiol* 2014;55:426-35.
- 40 Li C, Xu J, Li J, et al. Involvement of *Arabidopsis* HAC family genes in pleiotropic developmental processes. *Plant Signal Behav* 2014;9:e28173.
- 41 Han SK, Song JD, Noh YS, Noh B. Role of plant CBP/p300-like genes in the regulation of flowering time. *Plant J* 2007;49:103-14.
- 42 Berr A, Xu L, Gao J, et al. Set domain group25 encodes a histone methyltransferase and is involved in flowering locus C activation and repression of flowering. *Plant Physiol* 2009;151:1476-85.
- 43 Santos-Rosa H, Schneider R, Bannister AJ, et al. Active genes are tri-methylated at K4 of histone H3. *Nature* 2002;419:407-11.
- 44 Shafiq S, Berr A, Shen WH. Combinatorial functions of diverse histone methylations in *Arabidopsis thaliana* flowering time regulation. *New Phytol* 2014;201:312-22.
- 45 Spolar RS, Record MT, Jr. Coupling of local folding to site-specific binding of proteins to DNA. *Science* 1994;263:777-84.
- 46 Liu J, Perumal NB, Oldfield CJ, et al. Intrinsic disorder in transcription factors. *Biochemistry* 2006;45:6873-88.
- 47 Ang LH, Chattopadhyay S, Wei N, et al. Molecular interaction between COP1 and HY5 defines a regulatory switch for light control of *Arabidopsis* development. *Mol Cell* 1998;1:213-22.
- 48 Vandebussche F, Habricot Y, Condiff AS, et al. HY5 is a point of convergence between cryptochrome and cytokinin signalling pathways in *Arabidopsis thaliana*. *Plant J* 2007;49:428-41.
- 49 Chen H, Zhang J, Neff MM, et al. Integration of light and abscisic acid signaling during seed germination and early seedling development. *Proc Natl Acad Sci USA* 2008;105:4495-500.
- 50 Ernst HA, Olsen AN, Larsen S, Lo Leggio L. Structure of the conserved domain of ANAC, a member of the NAC family of transcription factors. *EMBO Rep* 2004;5:297-303.
- 51 Greve K, La Cour T, Jensen MK, et al. Interactions between plant RING-H2 and plant-specific NAC (NAM/ATAF1/2/CUC2) proteins: RING-H2 molecular specificity and cellular localization. *Biochem J* 2003;371:97-108.
- 52 Jensen MK, Kjaersgaard T, Nielsen MM, et al. The *Arabidopsis thaliana* NAC transcription factor family: structure-function relationships and determinants of ANAC019 stress signalling. *Biochem J* 2010;426:183-96.
- 53 Jiang H, Li H, Bu Q, Li C. The RHA2a-interacting proteins ANAC019 and ANAC055 may play a dual role in regulating ABA response and jasmonate response. *Plant Signal Behav* 2009;4:464-6.
- 54 O'Shea C, Kryger M, Stender EG, et al. Protein intrinsic disorder in *Arabidopsis* NAC transcription factors: transcriptional activation by ANAC013 and ANAC046 and their interactions with RCD1. *Biochem J* 2015;465:281-94.
- 55 Toth G, Gardai SJ, Zago W, et al. Targeting the intrinsically disordered structural ensemble of alpha-synuclein by small molecules as a potential therapeutic strategy for Parkinson's disease. *PLoS One* 2014;9:e87133.